Novel genetic tools for production strain development of *Corynebacterium glutamicum*

Jennifer Hochheim

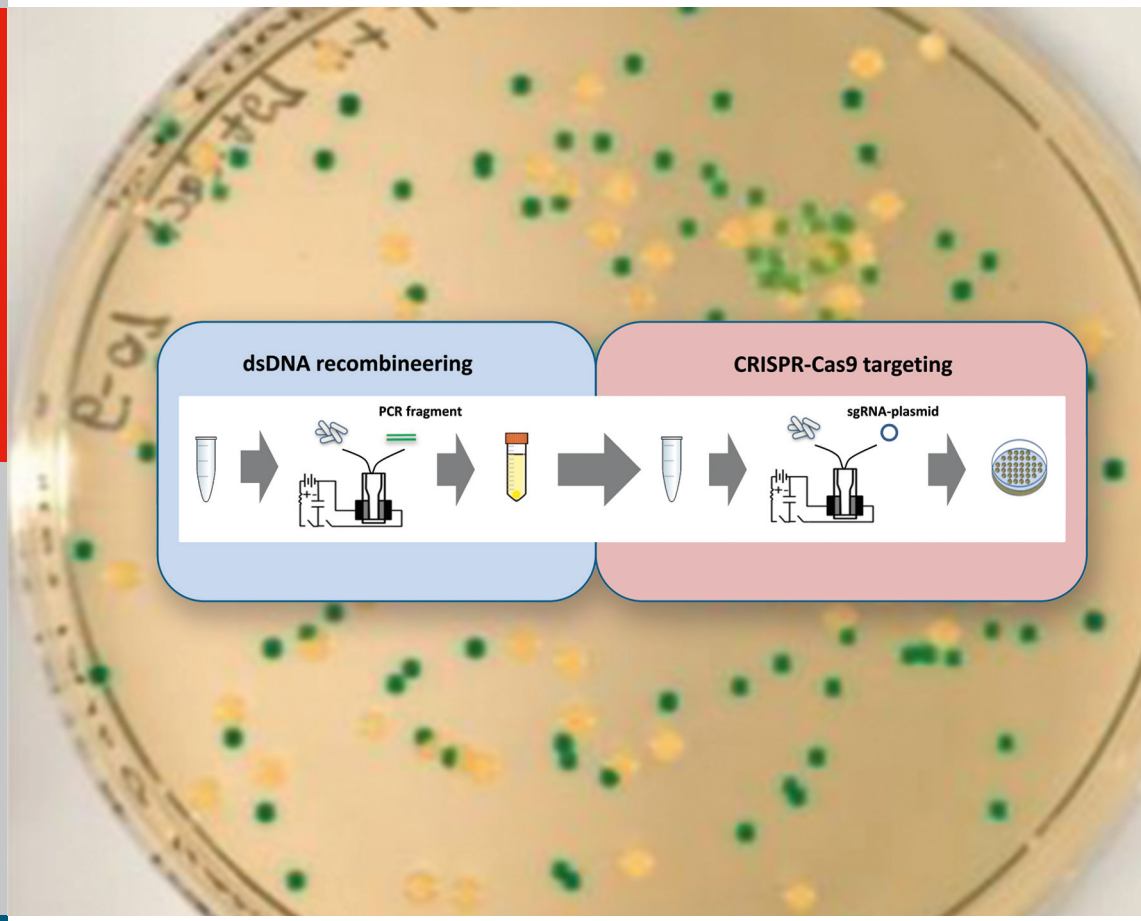

Gesundheit / Health
Band / Volume 83
ISBN 978-3-95806-212-2

JÜLICH
FORSCHUNGSZENTRUM

Schriften des Forschungszentrums Jülich
Reihe Gesundheit / Health Band / Volume 83

Forschungszentrum Jülich GmbH
Institute of Bio- and Geosciences
Biotechnology (IBG-1)

Novel genetic tools for production strain development of *Corynebacterium glutamicum*

Jennifer Hochheim

Schriften des Forschungszentrums Jülich
Reihe Gesundheit / Health

Band / Volume 83

ISSN 1866-1785

ISBN 978-3-95806-212-2

Bibliographic information published by the Deutsche Nationalbibliothek.
The Deutsche Nationalbibliothek lists this publication in the Deutsche
Nationalbibliografie; detailed bibliographic data are available in the
Internet at http://dnb.d-nb.de.

Publisher and Distributor: Forschungszentrum Jülich GmbH
Zentralbibliothek
52425 Jülich
Tel: +49 2461 61-5368
Fax: +49 2461 61-6103
Email: zb-publikation@fz-juelich.de
www.fz-juelich.de/zb

Cover Design: Grafische Medien, Forschungszentrum Jülich GmbH

Printer: Grafische Medien, Forschungszentrum Jülich GmbH

Schriften des Forschungszentrums Jülich
Reihe Gesundheit / Health, Band / Volume 83

D 61 (Diss. Düsseldorf, Univ., 2017)

ISSN 1866-1785
ISBN 978-3-95806-212-2

The complete volume is freely available on the Internet on the Jülicher Open Access Server (JuSER)
at www.fz-juelich.de/zb/openaccess.

Table of Content

Abstract

The development of new genetic tools plays a key role in the establishment of new and/or improved microbial production strains. Since *Corynebacterium glutamicum* belongs to the most important microorganisms in white biotechnology, the major task of this work was to establish new genome editing tools for this organism. To this end, the following results were obtained:

(1) dsDNA recombineering was established as a genome editing method using the RecET recombination system originating from the prophage Rac from *Escherichia coli*. Whereas single point mutations could be introduced with high frequencies, full-length genes were not integrated at the correct genomic target location. In-depth analyses revealed a correlation of DNA substrate length with DNA recombineering efficiency, allowing for only very low efficiencies of 9.8×10^2 recombinant cells per 10^{10} cells with fragments larger than 700 nt. With 5'-phosphorylated DNA fragments as template, dsDNA recombination efficiencies were enhanced by a factor of 10, whereas 5'-phosphorothioation decreased recombination efficiencies by a factor of 5.

(2) The CRISPR-Cas9 system was established in *C. glutamicum* allowing for the separation of different genotypes. In a mixture of the two *C. glutamicum* strains ATCC13032 and ATCC13032 with a point mutation resulting in MurE-G81E, all wild-type cells could be eliminated using an appropriate sgRNA. Since it was observed that the presence of Cas9 protein reduced living cell count, Cas9 toxicity was studied in more detail by analyzing various plasmid constructs and Cas9 variants. Exchanging the start codon of *cas9* from ATG to TTG led to highly reduced unspecific activity, whereas CRISPR-Cas9 targeting remained functional.

(3) Furthermore, pCLTON2, one of the expression plasmids used for *C. glutamicum,* was modified to establish a temperature-sensitive origin of replication. Whereas this plasmid was stably maintained during cultivation at 25 °C, cultivation at 34 °C led to immediate plasmid loss, rendering pCl2-OriTS a valuable tool for genome editing of this bacterium.

(4) With the aim to quantify the CRISPR-Cas9 genome editing efficiency, several test systems were evaluated. In the course of these experiments, the ß-galactosidase assay was identified as the most suitable test system for *C. glutamicum*, since recombinant cells can be distinguished from non-edited cells by visual differentiation in an easy time-efficient manner.

(5) The established β-galactosidase assay allowed for simulating the combination of genome editing by recombineering and targeted elimination of non-edited cells by CRISPR-Cas9. Depending on the plasmid carrying *cas9*, at best an enrichment factor of 5000 of the desired mutant was obtained. Assuming that dsDNA recombineering enables to obtain 1 recombinant per 100,000 cells means that theoretically only a low number of approximately 20 clones must be assayed to retrieve the desired mutant.

(6) Site-saturation mutagenesis of the UDP-N-acetylmuramoylalanyl-D-glutamate 2,6-diaminopimelate ligase (MurE) at position G81 allowed for the exchange of all amino acids possible in *C. glutamicum*. The characterization of the mutant strains revealed a systemic effect on L-lysine accumulation: Increased L-lysine accumulation is coupled to a reduced growth rate, which is most likely a cell response to limited meso-diaminopimelate availability, which is required for both L-lysine and cell wall synthesis.

In summary, two new genome editing techniques, dsDNA recombineering and CRISPR-Cas9 targeting, were established for *Corynebacterium glutamicum* enabling integration/deletion of small DNA fragments and separation of different genotypes.

Zusammenfassung

Die Etablierung neuer genetischer Methoden spielt eine wichtige Rolle in der Entwicklung und Optimierung von mikrobiellen Produktionsstämmen. *Corynebakterium glutamicum* zählt aufgrund seiner Fähigkeit zur effizienten industriellen Produktion diverser Aminosäuren zu den wichtigsten Mikroorganismen in der weißen Biotechnologie, weshalb in dieser Arbeit neue genetische Werkzeuge für diesen Mikroorganismus entwickelt werden sollten. Es wurden folgende Ergebnisse erzielt:

(1) Mit Hilfe des RecET-Rekombinationssystems des Prophagen Rac aus *Escherichia coli* konnte Doppelstrang-DNA (dsDNA)-Recombineering für *C. glutamicum* etabliert werden. Während Punktmutationen mit hoher Frequenz eingeführt werden konnten, war die Integration vollständiger Gene am gewünschten chromosomalen Zielort nicht möglich. Weitere Analysen ergaben eine Korrelation zwischen der Länge des DNA-Substrats und der Recombineering-Effizienz, sodass für Fragmente von mehr als 700 Basenpaaren nur sehr geringe Effizienzen von 9,8 x 10^2 rekombinanten Zellen bei einer Gesamtzellzahl von 10^{10} erreicht werden konnten. Mit Hilfe einer 5‘-Phosphorylierung des codogenen Stranges konnten die dsDNA-Recombineering Effizienzen um den Faktor 10 erhöht werden. 5-Phosphorothiolierung des codogenen Stranges hingegen führte zu einer Verringerung der Effizienzen um den Faktor 5.

(2) Das CRISPR-Cas9-System wurde in *C. glutamicum* etabliert, welches die Trennung verschiedener Genotypen ermöglicht. In einem Gemisch aus den beiden *C. glutamicum* Stämmen ATCC13032 und ATCC13032 mit einer Punktmutation im *murE*-Gen, wodurch MurE-G81E entstand, konnten mit der passenden sgRNA alle wildtypischen Zellen abgetötet werden. Aufgrund der Beobachtung, dass das Cas9-Protein die Lebendzellzahl reduziert, wurde die Toxizität von Cas9 genauer untersucht. Es wurden diverse Plasmidkonstrukte und Cas9-Varianten erstellt und analysiert, wobei sich der Austauch des Cas9-Startcodons von ATG zu TTG am vielversprechendsten erwies. Damit konnte eine sehr reduzierte unspezifische Cas9-Aktivität beobachtet werden, während das CRISPR-Cas9-Targeting in seiner Funktionalität nicht eingeschränkt wurde.

(3) Das *C. glutamicum* Expressionsplasmid pCLTON2 wurde mit einem temperatursensitiven Replikationsursprung versehen. Während das Plasmid bei einer Kultivierung bei 25 °C stabil in den Zellen gehalten wurde, führte die Erhöhung der Temperatur auf 34 °C zu einem fortschreitenden Plasmidverlust. Damit stellt das modifizierte Expressionsplasmid pCL2-OriTS ein wertvolles Werkzeug für die genetische Modifikation von *C. glutamicum*-Stämmen dar.

(4) Um die Effizienz des CRISPR-Cas9-*Targetings* quantifizieren zu können, wurden diverse Testsysteme evaluiert. Als am besten geeignet stellte sich das LacZ-System heraus, für welches zwei Stämme generiert wurden, in denen das *lacZ*-Gen unter Kontrolle eines starken konstitutiven Promotors ins Genom integriert wurde. In einem dieser beiden Stämme führte eine zusätzlich eingeführte Mutation im *lacZ*-Gen zur Inaktivierung der β-Galaktosidase.

(5) Mit Hilfe von verschiedenen Mischungsverhältnissen der beiden LacZ-Teststämme konnte dsDNA-Recombineering mit anschließendem CRISPR-Cas9-*Targeting* simuliert werden. Mit Hilfe des etablierten Systems konnte die Anzahl der Mutanten im Vergleich zum Wildtyp im besten Fall um den Faktor 5000 angereichert werden. Unter der Annahme, dass durch dsDNA-Recombineering eine rekombinante Zelle pro 100.000 Zellen erhalten wird, müssen nach CRISPR-Cas9-*Targeting* nur etwa 20 Zellen untersucht werden, um eine genetisch veränderte Zelle zu identifizieren.

(6) Mittels Sättigungsmutagenese der UDP-N-acetylmuramoylalanyl-D-glutamat 2,6-diaminopimelat-Ligase (MurE) konnte die Aminosäure Glycin an Position 81 in *C. glutamicum* durch jede andere vorkommende Aminosäure ersetzt werden. Die eingehendere Charakterisierung der mutierten Stämme konnte systemische Effekte bezüglich der L-Lysinanreicherung nachweisen: Eine erhöhte L-Lysinanreicherung ist an eine verringerte Wachstumsrate gekoppelt, was sich höchst wahrscheinlich aus der Antwort der Zelle auf eine limitierte Verfügbarkeit von Mesodiaminopimelat ableitet, welches sowohl für die L-Lysinproduktion, sowie für die Zellwandsynthese benötigt ist.

Zusammenfassend ist es in dieser Arbeit gelungen, die beiden genetischen Methoden dsDNA-Recombineering und das CRISPR-Cas9 System in *C. glutamicum* zu etablieren, welche die Integration und Deletion kleiner genomischer Fragmente, sowie die Trennung verschiedener Genotypen ermöglichen.

Abbreviations

Ω	Ohm
µ	micro (10^{-6})
A	ampere
ATc	anhydrotetracycline
ATP	adenosine triphosphate
BHI	*brain heart infusion*
bp	base pair
Cas	*CRISPR associated*
CFU	*colony forming units*
cm	chloramphenicol
CRISPR	*clustered regularly interspaced short palindromic repeats*
crRNA	CRISPR RNA
ctrl	control
d	*deactivated*
ds	double-stranded
e.g.	*exampli gratia* (latin: 'for example')
DNA	deoxyribonucleic acid
DSB	double-strand break
et al.	*et alii* (latin: 'and others')
F	Farad
FACS	*fluorescent activated cell sorting*
FOA	fluoroorotic acid
G	acceleration of gravity
GFP	*green fluorescent protein*
HDR	*homology-directed repair*
hyg	hygromycin
HPLC	*high performance liquid chromatography*
IPTG	isopropylthiogalactosidase
kb	kilo bases
kan	kanamycin
LB	*lysogeny broth*
M	molar
MIC	*minimal inhibitory concentration*
MNNG	N-methyl-N'-nitro-N-nitrosoguanidine
NHEJ	*non-homologous end joining*
n	nano (10^{-9})
nt	nucleotides
NT	*non-targeting*
OD	optical density
ORF	*open reading frame*
PAM	*protospacer adjacent motif*
PCR	*polymerase chain reaction*
PHO	phosphorylated

PTO	phosphorothioated
RFP	*red fluorescent protein*
RNA	ribonucleic acid
rpm	rounds per minute
SD	standard deviation
sgRNA	small guide RNA
SNP	*single nucelotide polymorphism*
SOB	*super optimal broth*
spc	spectinomycin
ss	single-stranded
tet	tetracycline
tracRNA	*transactivating CRISPR RNA*
U	units
V	Volt
WT	wild type
w/v	weight per volume
X-gal	5-Bromo-4-chloro-3-indoxyl-β-D-galactopyranoside

1 Introduction

1.1 *Corynebacterium glutamicum* as biotechnological platform organism

Corynebacterium glutamicum is a Gram-positive soil organism, which is immobile, exhibits relatively fast growth and biotin auxotrophy (Abe *et al.*, 1967; Gao and Gupta, 2012; Pascual *et al.*, 1995). Since the discovery as an L-glutamate producing organism in 1957 by Udaka and Kinoshita (Kinoshita *et al.*, 2004), *C. glutamicum* has become one of the most important microorganisms in white biotechnology (Eggeling and Sahm, 1999). Up to 2.5 million tons of L-glutamate and 2.2 million tons of L-lysine are produced annually with this organism (Eggeling and Bott, 2015; Vertes *et al.*, 2013). In addition to the production of amino acids, many strains have been engineered to produce other molecules, e.g. lactate (Okino *et al.*, 2008), cadaverine (Kind *et al.*, 2010), isobutanol (Smith *et al.*, 2010), succinate (Litsanov *et al.*, 2012), itaconate (Otten *et al.*, 2015), plant-derived polyphenols (Kallscheuer *et al.*, 2016) and other molecules (Wendisch *et al.*, 2016; Wieschalka *et al.*, 2013). Furthermore, *C. glutamicum* has been engineered to utilize carbon sources such as methanol (Witthoff *et al.*, 2015), various sugars such as lactose and galactose (Wendisch *et al.*, 2016) or lignocellulosic waste such as arabinose, xylose or cellubiose (Zahoor *et al.*, 2012). Due to the broad spectrum of biotechnological applications with genetically modified *C. glutamicum* strains, there is a rising interest in the fast and efficient engineering of production strains. This in turn requires the development of new tools for genome modification.

1.2 Genetic tools for strain improvement

Traditionally, production strains were constructed via multiple rounds of random mutagenesis and screening or selection (Demain, 2000; Ikeda, 2003). During this process, unspecific DNA mutations are introduced by exposure of cells to mutagens followed by a screening process that identifies strains with improved production levels. Most frequently used mutagens are N-methyl-N'-nitro-N-nitrosoguanidine (MNNG), hydroxyl amine, or ultraviolet light (Demain and Solomon, 1985). Even though, many different recombinant DNA techniques have emerged during the last years allowing for rational and precise genome modifications (Adrio and Demain, 2010), the traditional approach is still appreciated, as it also represents a valuable approach to gain new insights into the physiology of the host organism. Many recent examples demonstrate the power of random mutagenesis, e.g. construction of an L-threonine producing *Escherichia coli* strain (Zhang *et al.*, 2009) or a *Bacillus subtilis* strain, which accumulates riboflavin (Abbas and

Sibirny, 2011). Improved *C. glutamicum* production strains were generated amongst others for L-arginine (Park *et al.*, 2014) and L-lysine (Schrumpf *et al.*, 1992).

In contrast to the classical approach of mutagenesis and screening, the rational approach has become more frequently used due to the availability of many recombinant DNA techniques. Furthermore, with the sequencing of the whole genome of *C. glutamicum* (Ikeda, 2003; Kalinowski *et al.*, 2003; Tauch *et al.*, 2002) new methods such as proteomics, metabolomics and transcriptome analyses were established that have led to a variety of approaches in metabolic engineering to rationally construct/improve production strains. To obtain high-level producer strains both methods, the undirected approach as well as the directed approach, are closely linked and frequently used together, as evident from the fact that the mutations discovered in the undirected approach are transferred via metabolic engineering approaches (Binder *et al.*, 2013; Bott, 2015).

1.2.1 Genome modification with non-replicative integration vectors

Stable maintenance of expression plasmids is unfavorable in industrial production strains because antibiotics have to be supplied to the cultivation media. Consequently, heterologous genes are integrated or native genes are deleted in the genome of the respective organism. The insertion, deletion or substitution of genes in *C. glutamicum* is usually performed by homologous recombination using non-replicative integration vectors (Schwarzer and Pühler, 1991) and genome modification can be achieved via two rounds of positive selection (Schäfer *et al.*, 1994).

The non-replicative plasmid pK19mobsacB consists of three parts: i) a Tn*5*-derived kanamycin resistance cassette, ii) flanking sequences of about 500 nt homologous to chromosomal sequences up- and downstream of the DNA sequence to be exchanged and iii) a *sacB* gene encoding levansucrase that catalyzes cleavage of sucrose to glucose and fructose and furthermore converts fructose to the oligomeric levan. This compound kills *C. glutamicum* cells when they are grown in presence of sucrose (Jäger *et al.*, 1992). Since the pK19mobsacB plasmid is unable to replicate in *C. glutamicum*, only cells carrying the chromosomally integrated plasmid are selected after electroporation, because kanamycin resistance can be established. After cultivation, recombinant cells are selected for loss of vector sequences via a second homologous recombination event by spreading cells on plates containing sucrose.

Even though this has been the method of choice for genetic engineering of *C. glutamicum* for many years, it has the disadvantages of being time-consuming and inefficient due to the rare events of genomic integration of the plasmid or the high number of wild type cells after the second recombination step.

Next to the pK19mobsacB system, targeted genome modification in *C. glutamicum* can also be performed via conjugation by using *E. coli* vectors carrying manipulated *C. glutamicum* DNA fragments (Schwarzer and Pühler, 1991) or with the help of the Cre/loxP recombination system (Suzuki and Inui, 2013). Recently, an alternative method was established, allowing the fast substitution of single nucleotides in the genome by single-stranded (ss)-DNA recombineering (Binder *et al.*, 2013).

1.2.2 Homologous recombination by genetic engineering ('Recombineering')

Over the last years, recombineering has become a powerful technique for the precise genome editing of many organisms such as *E. coli* (Sharan *et al.*, 2009), *Pseudomonas syringae* (Bao *et al.*, 2012) or *Mycobacterium spc.* (van Kessel and Hatfull, 2007). Insertions, deletions or substitutions can be performed, only requiring homology regions of as little as 35-50 nt up- and downstream of the desired target position on the chromosome (Sharan *et al.*, 2009). Since the method is also based on homologous recombination, it neither depends on restriction sites nor does it rely on any plasmid, which integrates into the genome.

First established as genome editing tool in *E. coli*, the recombineering events are catalyzed by either the Red proteins from phage λ (Murphy, 1998; Murphy *et al.*, 2000) or the RecET system from the Rac prophage (Datta *et al.*, 2008; Zhang *et al.*, 1998). The λ Red system consists of three phage recombination genes: a 5'-3' double-stranded (ds) DNA-degrading exonuclease (*exo)*, a ssDNA annealing protein (*bet)* and the inhibitor Gam (*gam)*, preventing the RecBCD nuclease of *E. coli* from degrading linear DNA fragments (Murphy, 1998). In contrast, the RecET system only contains the adjacent genes *recE* and *recT*, but no *gam* homologue (Zhang *et al.*, 2009). Recombineering functions for two sorts of DNA substrates: ssDNA (oligonucleotides) and dsDNA (PCR fragments). For ssDNA recombineering, the ssDNA annealing protein RecT binds to the oligonucleotide, pairs it to complementary ssDNA (Hall and Kolodner, 1994; Karakousis *et al.*, 1998; Li *et al.*, 1998) and promotes homologous recombination at the genomic target location, during which the oligonucleotide is integrated as an Okazaki fragment (Figure 1, left) (Mosberg *et al.*, 2010). For dsDNA recombineering, an additional enzymatic step is required, which is carried out by the 5'-3' DNA exonculease RecE (Figure 1, right).

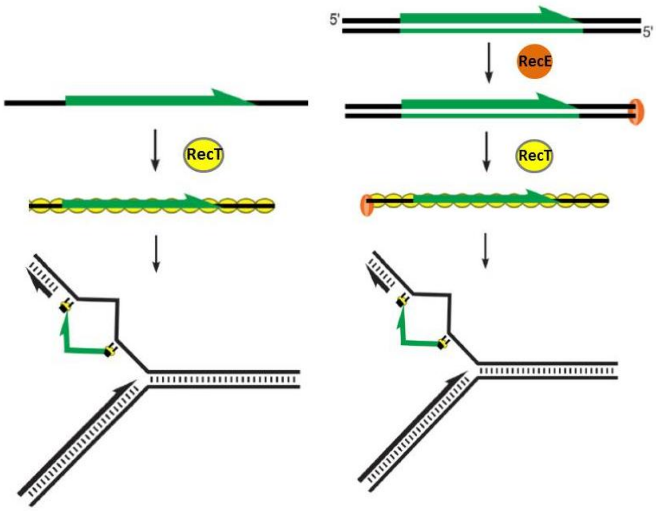

Fig. 1: Overview on RecET mediated recombineering, modified from *Mosberg et al.*, (2010). Left: ssDNA recombineering with oligonucleotides, right: dsDNA recombineering with PCR fragments. 5'-3' exonuclease RecE degrades PCR fragment into ssDNA intermediate, RecT binds ssDNA and pairs it to complementary single strand gaps at replication fork generating recombinant DNA. For ssDNA recombineering RecE activity is not needed.

Early models proposed that during dsDNA recombineering RecE turns the dsDNA fragment into a dsDNA fragment with ssDNA overhangs. These single-stranded regions of the DNA fragment are annealed to complementary single-stranded gaps arising at the replication fork during replication via the ssDNA annealing protein (Court *et al.*, 2002). However, Mosberg *et al.*, recently demonstrated the generation of a full-length ssDNA intermediate, which is then further treated as an oligonucleotide during ssDNA recombineering and is annealed to the lagging strand of the replication fork (Mosberg *et al.*, 2010).

For *C. glutamicum* ssDNA recombineering was established using RecT and recombineering was directly combined with a biosensor-based FACS screening approach for a fast generation and isolation of new production strains (Binder *et al.*, 2013). Recently, it has been reported that recombineering occurs in *C. glutamicum* without the expression of any heterologous recombinases (Krylov *et al.*, 2014). However, this could not be verified for the *C. glutamicum* strains used in this study.

1.2.3 Genome editing with CRISPR-Cas9

During the last decade another novel genome editing tool has shown its huge potential, because it allows the efficient and precise modification of genomes, especially in eukaryotes. The *clustered regularly interspaced short palindromic repeats* (CRISPR) – *CRISPR associated* (Cas) system allows a successful genetic targeting in a large number of organisms and cell lines, e.g. in human (Mali *et al.*, 2013), mouse (Mashiko *et al.*, 2014), yeast (DiCarlo *et al.*, 2013), fruit fly (Gratz *et al.*, 2014), zebrafish (Hwang *et al.*, 2013), plants (Feng *et al.*, 2013) and other organisms.

As a bacterial RNA-guided adaptive immune system that provides sequence-specific protection against invading viruses (Barrangou *et al.*, 2007; Brouns *et al.*, 2008) CRISPR-Cas systems can be found in 46 % of bacteria and 84 % of archaea (Grissa *et al.*, 2007). Three variations of CRISPR-Cas systems have currently been described, named type I, type II and type III depending on their signature genes and their individual mechanisms by which the immune response is generated (Makarova *et al.*, 2011). One of the simplest and most commonly used systems is the type II CRISPR-Cas9 system from *Streptococcus pyogenes* (Doudna and Charpentier, 2014). It consists of three main components: the mature CRISPR RNA (crRNA), a transactivating crRNA (tracRNA) and the endonuclease Cas9 (Jinek *et al.*, 2012). The genome of *S. pyogenes* harbors a set of Cas proteins as well as a CRISPR locus containing an array of repeat-spacer sequences (Figure 2)(Qi *et al.*, 2013). Whereas the repeats are identical, the spacer exhibit individual sequences complementary to foreign target DNA sequences. After infection of the cell, the CRISPR array is transcribed into a long precursor transcript, which is then cleaved into smaller fragments by tracRNA and host RNase III (Deltcheva *et al.*, 2011). After cleavage, the endonuclease Cas9 binds to the fragments assembling the crRNA complex, which then scans the DNA molecule. According to the current model, the Cas9-RNA complex engages the protospacer adjacent motif (PAM) GG dinucleotide using two arginine residues of Cas9 (Anders *et al.*, 2014). The target DNA duplex is positioned to allow for interaction of the +1 phosphate with the phosphate lock loop, which results in local strand separation immediately upstream of the PAM. Subsequently, base-pairing between the seed region of the guide RNA and the displaced target DNA is established and the nuclease activity of Cas9 introduces the formation of double-stranded DNA breaks (DSB). This allows the removal of cognate DNA molecules and leads to immunity against foreign DNA.

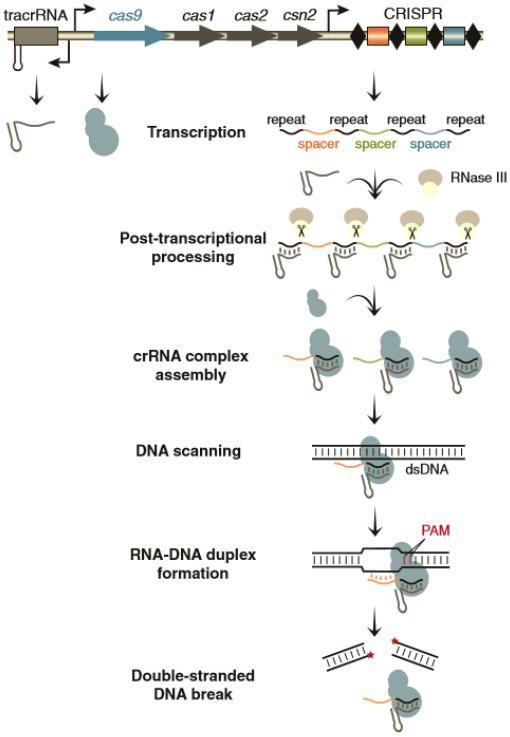

Fig. 2: Principle of CRISPR-Cas9 system in *S. pyogenes* (Qi *et al.*, 2013). After infection, the CRISPR array is transcribed into a longer precursor transcript, which is cleaved into smaller fragments by tracRNA and host RNase III. After cleavage, endonuclease Cas9 binds to small fragments and establishes crRNA complex. Cas9 guides crRNA to DNA and scans the DNA molecule. At the target location, the complex is stabilized by base pairing between the crRNA and DNA target and Cas9 induces double strand breaks (DSB).

Whereas the mechanism was first only regarded as a biological phenomenon, it was turned into a genetic engineering tool with huge potential when Jinek *et al.* described the reprogramming of the target DNA sequence by exchanging 20 nt in the crRNA and reduced the system to two components by constructing a chimeric small guide RNA (sgRNA) (Jinek *et al.*, 2012). This RNA combines the targeting specificity of the crRNA with the structural characteristics of the tracrRNA. Due to this, only the expression of Cas9 and the construction of an sgRNA with a 20 nt protospacer sequence complementary to the target DNA suffices for precise genome targeting. With the help of endogenous repair systems like homology directed repair (HDR) (Liang *et al.*, 1998) or non-homologous end joining (NHEJ) (Pfeiffer *et al.*, 1994) the DSB introduced by Cas9 can be repaired leading to wild-type or recombinant cells.

Without a heterologous template, in eukaryotic cells, the DSB introduced by Cas9 can be repaired by the erroneous NHEJ recombination system, most likely resulting in a mutation at the target site (Altenbuchner, 2016). During this process compatible DNA ends resulting from the DSB are combined in an error-prone manner by the protein Ku and the ligase LigD, which frequently results in the generation of insertions or deletions. NHEJ occurs at low frequency and is not present in most bacteria (Bowater and Doherty, 2006). For a precise genome editing, DSBs may be repaired by homologous recombination using an appropriate template with sufficient

homology. The latter process is more efficient in prokaryotes than in eukaryotes. Use of the CRISPR-Cas9 system has brought genome editing to a new level, because target site specific modifications can be easily performed (Doudna and Charpentier, 2014).

For some bacteria e.g. *B. subtilis* (Altenbuchner, 2016), *Streptomyces coelicolor* (Tong *et al.*, 2015) or clostridia (Wang *et al.*, 2015), successful CRISPR-Cas9 genome editing based on endogenous repair mechanisms similar to NHEJ or HDR was reported. Others, such as *E. coli*, *Lactococcus lactis*, *Lactobacillus reuteri* or *C. glutamicum* do not possess the ability to repair introduced DSB at high frequency, ultimately resulting in cell death. Hence, the CRISPR-Cas9 system cannot be used as an editing tool as described for eukaryotes, *B. subtilis*, *S. coelicolor* or clostridia. Instead, it was recently shown that the CRISPR-Cas9 system can be alternatively applied as a selection tool that allows the efficient targeting and killing of one genotype, whereas the corresponding mutant that harbors a different genotype at the genomic region of interest is not affected (Jiang *et al.*, 2015; Oh and van Pijkeren, 2014; Pyne *et al.*, 2015). By using DNA recombineering to edit cells followed by targeting of non-edited cells with the CRISPR-Cas9 system recombinant cells can be more easily detected, since the number of non-edited cells is drastically reduced. This method termed CRISPR-Cas9 recombineering already proved to significantly enhance genome editing frequencies in *E. coli* and *L. reuteri* (Jiang *et al.*, 2015; Oh and van Pijkeren, 2014; Pyne *et al.*, 2015).

However, the procedures of currently successfully established CRISPR-Cas9 recombineering vary substantially in different bacteria, showing the complexity of the system. Not only parameters like induction levels, plasmid backgrounds, or recombinases differ between the species, but also the number of transformation steps in one genome editing round varies as well as the templates supplied during electoporation (Jiang *et al.*, 2015; Li *et al.*, 2015; Pyne *et al.*, 2015). For example, in *E. coli* successful CRISPR-Cas9 recombineering could be established by transforming with the DNA substrate in form of PCR fragment or oligonucleotide and the plasmid containing the targeting sgRNA in one electroporation step (Li *et al.*, 2015; Pyne *et al.*, 2015). This method, however, was found not to be suitable for *L. reuteri*. In this organism two transformations had to be performed, first introducing the DNA substrate followed by the introduction of the targeting sgRNA in a subsequent electroporation (Oh and van Pijkeren, 2014). These results show the difficulties that arise during the approach to combine all requirements in the most efficient manner.

1.2.4 Expression plasmids with temperature-sensitive origins of replication

When production strains are constructed via metabolic engineering, the use of plasmids is indispensable. For DNA recombineering, the expression plasmid is stably maintained in the cell by supplementation of the respective antibiotic. Since industrial production strains should be

plasmid free, plasmids were developed harboring temperature-sensitive origins of replication for various organisms (Chen *et al.*, 2010; Hashimoto-Gotoh *et al.*, 2000; Silo-Suh *et al.*, 2009). By using hydroxylamine supplementation or error-prone PCR, plasmids were randomly mutated and transferred into the target organism. After several replica plating steps at different temperatures, mutated plasmids could be detected that allow cell growth at low temperatures, because replication is permitted. At higher temperatures, however, cells are not able to grow due to prohibited plasmid replication (Eichenlaub, 1979; Kim *et al.*, 2008). Using an expression plasmid with a temperature-sensitive origin is therefore advantageous, because the plasmid can be removed via cultivation at higher temperatures as soon as the respective gene expression is no longer needed. For *C. glutamicum* two temperature-sensitive cloning vectors based on the pBL1 and pCG1 replicons were established via the described principle. By substituting a single nucleotide (G2920A) in the Rep protein coding region of pBL1, Nakamura *et al*. first described the construction of the plasmid pSFKT2 that can be stably maintained at 25 °C, but is gradually lost at 34 °C (Nakamura *et al.*, 2006). They stated a plasmid loss of 99.96 % after 15 generations, when cultivated at 34 °C. At 25 °C, after 15 generations, 94 % of the cells were still stably maintaining the plasmid. These results were later supported by Okibe *et al*. that introduced the plasmid pCRD206, which contained two mutations G109D and E180K in the RepA protein coding region of pCG1 leading to growth at 25 °C, which was abolished at 37 °C (Okibe *et al.*, 2011).

1.3 The most suitable test system for the development of genetic methods

Prior to the application of new genetic methods they first have to be developed and characterized by using a simple and reliable test system. When appropriate, an easily selectable marker in form of an antibiotic resistance is used. In most cases the functionality of genome editing methods was verified by inserting an antibiotic resistance cassette into the genome (Bao *et al.*, 2012; Datta *et al.*, 2008; Swingle *et al.*, 2010) or by restoring an antibiotic resistance deficiency with a single nucleotide insertion/deletion (Binder *et al.*, 2013; Elgamal *et al.*, 2016). In other cases, one antibiotic resistance cassette was substituted by another to verify a functional gene exchange (Zhang *et al.*, 1998).

For alternative test systems the fluorescent protein GFP can be employed. In zebrafish, *gfp* was used to replace the first exon in *gata2* and edited cells were screened by fluorescence microscopy (Jessen *et al.*, 1998). In *Mycobacterium smegmatis* a linear DNA fragment encoding GFP and conferring hygromycin (*hyg*) resistance was introduced into the genome with later excision of the *gfp-hygr* cassette (Shenkerman *et al.*, 2014). Moreover, test systems that use

direct visual differentiation have been applied, for example the ß-galactosidase assay giving white/yellow cells a blue/green phenotype when spread on X-gal (Koenen *et al.*, 1982). Verification of successful edited cells is usually performed by PCR, restriction enzyme digestion, Southern blot analysis and/or sequencing.

For *C. glutamicum*, in addition to the traditional use of the antibiotics kanamycin, spectinomycin, tetracycline and choramphenicol, an alternative has been described. *C. glutamicum* strains harboring deletions in the alanine racemase encoding *alr* gene can be used for complementation of D-alanine auxotrophy with plasmids containing *alr* (Tauch *et al.*, 2002). Alanine racemase catalyzes the pyridoxal 5'-phosphate dependent reversible racemization between L- and D-alanine, which plays an important role in the biosynthesis of peptidoglycan of both Gram-positive and Gram-negative bacteria (Hayashi *et al.*, 1990). *alr* deletion strains therefore depend on the external addition of D-alanine to enable growth on minimal medium (Tauch *et al.*, 2002). Tauch *et al*. reported selection efficiencies similar to those observed by Tet^R selection (Tauch *et al.*, 2002).

1.4 Aims of this work

The establishment of new genetic tools plays a key role in the development of new and/or improved microbial production strains. The major task of this work was to establish and subsequently combine DNA recombineering and CRISPR-Cas9 editing for introducing mutations into the chromosome of *C. glutamicum* with an unprecedented precision and efficiency.

2 Material and Methods

2.1 Chemicals and enzymes

If not specifically mentioned otherwise, all chemicals and enzymes were supplied by Merck KGaA (Darmstadt, Germany), Roche Diagnostics GmbH (Mannheim, Germany), Thermo Fisher Scientific (Waltham, USA), Sigma-Aldrich Chemie (Deisenhofen, Germany) and VWR (Radnor, USA). Cultivation media were provided by BD (Franklin Lakes, USA).

2.2 Bacterial strains and plasmids

All bacterial strains used in this work are listed in table 1 and all plasmids can be viewed in table 2. The respective restriction maps are shown in the supplementary data.

Tab. 1: Used bacterial strains

Strain	Characteristics	Reference
E.coli		
DH5αMCR	F-*endA1 supE44 thi-λ- recA1 gyrA96relA1 deoR Δ (lacZYA-argF) U169Φ80dlacZM15 mcrA* Δ *(mrr-hsdRMS-mcrBC)*	(Grant *et al.*, 1990)
C. glutamicum		
ATCC13032	wild type (WT), biotin auxotroph	(Abe *et al.*, 1967)
MB001	Prophage-free variant of ATCC13032, genome reduced by 6 %	(Baumgart *et al.*, 2013)
DM1132	WT ATCC13032 from Evonik Industries AG stocks	Evonik Industries AG
DM1728	DM1132 with *pyc*P458S*, hom*V59A	(Georgi *et al.*, 2005)
DM1728kanR(+1)	DM1728 with integrated *aph(3´)-IIa* in lysOP7 region, additional nucleotide integrated at pos. 233 (+C)	(Binder *et al.* 2013)
DM1728kanR(-131)	DM1728 with partial *aph(3´)-IIa* in lysOP7 region, deletion of 131 nt (position 302-433)	This thesis
DM1728kanR(-766)	DM1728 with partial *aph(3´)-IIa* in lysOP7 region, deletion of 766 nt (position 334-432)	This thesis
ATCC13032::PH36lacZ	WT with integrated *lacZ* under control of PH36 promoter at lysOP7 region	This thesis
DM1132::PH36lacZ	DM1132 with integrated *lacZ* under control of PH36 promoter at lysOP7 region	This thesis
DM1132::PH36lacZ(+1)	DM1132 with partial *lacZ* under control of PH36 promoter at lysOP7 region, additional nucleotide integrated at pos. 1528 (+G)	This thesis
DM1728::PH36lacZ	DM1728 with integrated *lacZ* under control of PH36 promoter at lysOP7 region	This thesis
DM1728::PH36lacZ(+1)	DM1728 with partial *lacZ* under control of PH36 promoter at lysOP7 region, additional nucleotide integrated at pos. 1528 (+G)	This thesis
ATCC13032 ΔpyrF	WT with *in frame* deletion of *pyrF*	This thesis

ATCC13032::T7crim(+)	WT with integrated crimson under control of T7 promoter in lysOP7 region	This thesis
ATCC13032 MurE-G81E	WT with specific *murE* mutation	This thesis
ATCC13032 MurE-G81K	WT with specific *murE* mutation	This thesis
ATCC13032 MurE-G81S	WT with specific *murE* mutation	This thesis
ATCC13032 MurE-G81H	WT with specific *murE* mutation	This thesis
ATCC13032 MurE-G81T	WT with specific *murE* mutation	This thesis
ATCC13032 MurE-G81A	WT with specific *murE* mutation	This thesis
ATCC13032 MurE-G81Q	WT with specific *murE* mutation	This thesis
ATCC13032 MurE-G81F	WT with specific *murE* mutation	This thesis
ATCC13032 MurE-G81L	WT with specific *murE* mutation	This thesis
ATCC13032 MurE-G81W	WT with specific *murE* mutation	This thesis
ATCC13032 MurE-G81R	WT with specific *murE* mutation	This thesis
ATCC13032 MurE-G81N	WT with specific *murE* mutation	This thesis
ATCC13032 MurE-G81M	WT with specific *murE* mutation	This thesis
ATCC13032 MurE-G81P	WT with specific *murE* mutation	This thesis
ATCC13032 MurE-G81C	WT with specific *murE* mutation	This thesis
ATCC13032 MurE-G81E	WT with specific *murE* mutation	This thesis
ATCC13032 MurE-G81V	WT with specific *murE* mutation	This thesis
ATCC13032 MurE-G81I	WT with specific *murE* mutation	This thesis
ATCC13032 MurE-G81D	WT with specific *murE* mutation	This thesis

Tab. 2: Used plasmids

Plasmid	Characteristics	Reference
pEKEx3	*E. coli-C. glutamicum* shuttle vector for regulated gene expression, Spc^R, P_{tac}, $lacI^q$, $oriV_{Cg}$, $oriV_{Ec}$	(Hoffelder *et al.*, 2010)
pCLTON2	*E. coli-C. glutamicum* shuttle vector for regulated gene expression, Spc^R, P_{tet}, *tetR*, $oriV_{Cg}$, $oriV_{Ec}$	(Lausberg *et al.* 2012)
pVWEx2	*E. coli-C. glutamicum* shuttle vector for regulated gene expression, Tet^R, P_{tac}, $lacI^q$, $oriV_{Cg,}$ $oriV_{Ec}$	(Eikmanns *et al.*, 1991)
pCL2-OriTS	pCLTON2 with temperature sensitive $oriV_{Cg}$ (C4934T)	(Nakamura *et al.,* (2006
pCL2-recT	pCLTON2 with *recT* from prophage Rac from *E. coli*	(Binder *et al.,* 2013)
pEKEx3-recT	pEKEx3 with *recT* from prophage Rac from *E. coli*	(Binder *et al,.* 2013)
pVWEx2-recT	pVWEX2 with *recT* from prophage Rac from *E. coli*	This thesis
pCL2-recET	pCLTON2 with *recET* from prophage Rac from *E. coli*	This thesis
pCL2-recETCau	pCLTON2 with *recET* from *C. aurimucosum*	This thesis
pCL2-recE	pCLTON2 with *recE* from prophage Rac from *E. coli*	(Binder *et al,.* 2013)
pK18mobsacB	Integration vector, Kan^R, $oriV_{Ec}$, *oriT, sacB*, *mob*	(Schäfer *et al.,* 1994)
pK19mobsacB	Integration vector, Kan^R, $oriV_{Ec}$, *oriT, sacB*, *mob*	(Schäfer *et al,.* 1994)
pK18NCRkanR(+)	pK18mobsacB with *aph(3´)-IIa* and flanking regions of lysOP7 region	(Binder *et al.,* 2013)
pK18NCRkanR(-131)	pK18NCRkanR(+) with deletion of 131 nt in *aph(3´)-IIa*	This thesis
pK18NCRkanR(-752)	pK18NCRkanR(+) with deletion of 752 nt in *aph(3´)-IIa*	This thesis
pK19NCR_consensus	pK18mobsacB with 1000 nt of *lysOP7* region of *C. glutamicum* and MCS	This thesis
pK19mobsacBΔpyrF	pK19mobsacB with *in frame* deletion of *pyrF*	This thesis

pK18mobsacB_lysOP7_T7crim(+)	pK18mobsacB with *e2-crimson,* T7 RNA polymerase, and T7 control region and flanking regions of lysOP7 region	This thesis
pAN6-crimson	*E. coli-C. glutamicum* shuttle vector for regulated gene expression, Kan^R, P_{tac}, $lacI^q$, $oriV_{Cg}$, $oriV_{Ec}$, crimson	Supplied by Dr. G. Schaumann
PMJ806	pET-based custom vector with *cas9* from *S. pyogenes*	(Jinek *et al.,* 2012)
PMJ841	pET-based custom vector with *dcas9* from *S. pyogenes*	(Jinek *et al.,* 2012)
PMJ825	pET-based custom vector with *cas9n (D10A)* from *S. pyogenes*	(Jinek *et al,.* 2012)
PMJ826	pET-based custom vector with *cas9n (H840A)* from *S. pyogenes*	(Jinek *et al.*, 2012)
pEC309	pEC85Ω-Pcas9(Spy)-cas9(Spy)	Supplied by Dr. I. Fonfara
pEKEx3-cas9	pEKEx3 with *cas9* from *S. pyogenes*	This thesis
pCL2-recET-cas9	pCL2-recET with P_{tac}-cas9 from pEKEx3-cas9	This thesis
pCL2-recET-cas9(Pnat)	pCL2-recET with *cas9* under native *S. pyogenes* promoter	This thesis
pCL1(TS)-cas9	pCLTON1 with temperature sensitive origin and *cas9* under TetR expression control	Supplied by Dr. S. Matamouros
pCL1(TS)-cas9-Spc	pCL1(TS)-cas9, kanamycin resistance cassette was exchanged by spectinomycin resistance cassette	This thesis
pCL1(TS)-dcas9	pCLTON1 with temperature sensitive origin and *dcas9* under TetR expression control	Supplied by Dr. S. Matamouros
pCL1(TS)-dcas9-Spc	pCL1(TS)-cas9, kanamycin resistance cassette was exchanged by spectinomycin resistance cassette	This thesis
pEKEx3-cas9n(D10A)	pEKEx3 with nicked *cas9* (D10A) from *S. pyogenes*	This thesis
pEKEx3-cas9n(H840A)	pEKEx3 with nicked *cas9* (H840A) from *S. pyogenes*	This thesis
pCL1(TS)-ncas9	pCLTON1 with temperature sensitive origin and *ncas9* under TetR expression control	Supplied by Dr. S. Matamouros
pEKEx3-(recT)-Phil-ATGcas9	pEKEx3-recT with partially deleted LacIQ, ΔPtac, ΔrecT and *cas9* under TetR Expression control	This thesis
pEKEx3-(recT)-Phil-GTGcas9	pEKEx3-recT with partially deleted LacIQ, ΔPtac, ΔrecT and *cas9* (M1V) under TetR Expression control	This thesis
pEKEx3-(recT)-Phil-TTGcas9	pEKEx3-recT with partially deleted LacIQ, ΔPtac, ΔrecT and *cas9* (M1L) under TetR Expression control	This thesis
pEKEx3-(recT)-Phil-2xSTOPcas9	pEKEx3-recT with partially deleted LacIQ, ΔPtac, ΔrecT and *cas9* (L9*, D10*) under TetR Expression control	This thesis
pEKEx3-Phil-TTGcas9	pEKEx3 with *cas9* (M1L) under TetR Expression control	This thesis
pEKEx3-cas9-sgRNA:murE	pEKEx3-cas9 with sgRNA targeting *murE*	This thesis
pBHK18	*E. coli-C. glutamicum* shuttle vector, Kan^R, $oriV_{Cg}$, $oriV_{Ec}$	(Kirchner and Tauch, 2003)
pBHK18-sgRNA:murE	pBHK18 with sgRNA targeting *murE*	This thesis
pBHK18-sgrNA:ctrl	pBHK18 with sgRNA targeting *fapR* from *E. coli*	This thesis
pBHC18	*E. coli- C. glutamicum* shuttle vector, Cm^R, $oriV_{Cg}$, $oriV_{Ec}$	(Kirchner and Tauch, 2003)
pBHC18-sgRNA:kan(-131)	pBHC18 with sgRNA targeting *aph(3´)-IIa*	This thesis
pBHC18-sgRNA:ctrl	pBHC18 with sgRNA targeting *fapR* from *E. coli*	This thesis
pJC1	*E. coli-C. glutamicum* shuttle vector, Kan^R, $oriV_{Cg}$, $oriV_{Ec}$	(Kirchner and Tauch, 2003)
pJC1-sgRNA:murE	pJC1 with sgRNA targeting *murE*	This thesis
pJC1-sgRNA:ctrl	pJC1 with sgRNA targeting *fapR* from *E. coli*	This thesis
pBHK18-sgRNA:lacZ	pBHK18 with sgRNA targeting *lacZ*	This thesis
pBHK18-sgRNA:lacZ(+1)	pBHK18 with sgRNA targeting *lacZ*(+1)	This thesis

2.3 Oligonucleotides

All oligonucleotides used in this work were synthesized by Eurofins Genomics (Ebersberg, Germany). A detailed list can be found in the supplementary data.

2.4 Cultivation preparations and procedures

2.4.1 Cultivation media

All bacterial *E. coli* strains were cultivated in rich LB medium according to Sambrook *et al*. (Sambrook *et al.*, 1989). For the preparation of chemical competent *E. coli* cells SOB-Medium was used (Hanahan, 1983).

For cultivation of all *C. glutamicum* strains the rich BHI medium (Brain heart infusion, BD, Franklin Lakes, USA) was utilized. The cultivation for the preparation of competent cells and the regeneration after electroporation was performed in BHIS medium, which contains BHI medium supplemented with 0.5 M sorbitol. The cultivation of *C. glutamicum* strains with additional production titer analysis was performed in CGXII medium (Keilhauer *et al.*, 1993), which is supplemented with 4 % (w/v) glucose.

For the selection of recombinant *E. coli* strains the following antibiotics were added to the media:

Kanamycin	50 µg/ml (stock solution: 50 mg/ml in H_2O, sterile-filtered)
Spectinomycin	100 µg/ml (stock solution: 100 mg/ml in H_2O, sterile-filtered)
Tetracycline	5 µg/ml (stock solution: 5 mg/ml in H_2O, sterile-filtered)
Chloramphenicol	20 µg/ml (stock solution: 20 mg/ml in H_2O, sterile-filtered)

Recombinant *C. glutamicum* strains were selected by the addition of the following supplements to the media:

Spectinomycin	100 µg/ml (stock solution: 100 mg/ml in H_2O, sterile-filtered)
Kanamycin	25 µg/ml (to prevent plasmid loss, stock solution: 50 mg/ml in H_2O, sterile-filtered) 15 µg/ml (immediately after electroporation, stock solution: 50 mg/ml in H_2O, sterile-filtered)
Tetracycline	5 µg/ml (stock solution: 5 mg/ml in H_2O, sterile-filtered)
Chloramphenicol	7.5 µg/ml (stock solution: 20 mg/ml in H_2O, sterile-filtered)
X-gal	40 µg/ml (stock solution: 20 mg/ml in DMF)

For the induction of gene expression the cultures were induced with 0.5 mM IPTG if P_{tac} promoter was used and with 250 ng/ml anhydrotetracycline when genes were placed under control of the TetR expression system (Lausberg *et al.*, 2012).

The selection of *C. glutamicum* strains, where the integrative plasmid pK19mobsacB was excised from the genome, was performed on BHI medium with 10 % sucrose (w/v) (Schäfer *et al.*, 1994).

For the preparation of agar plates, BHI agar (BD, Franklin Lakes, USA) was used and complemented with 0.5 M sorbitol for BHIS plates. For all other agar plates, the media were supplemented with 1.5 % (w/v) agar (BD, Franklin Lakes, USA).

2.4.2 Cultivation of *E. coli* strains

E. coli strains were cultivated in 50-100 ml medium in 500 ml baffled Erlenmeyer shake flasks or in 4 ml medium in test tubes. The cultivation was performed at 37 °C and 120 rpm (170 rpm for test tubes).

2.4.3 Cultivation of *C. glutamicum* strains

The cultivation of *C. glutamicum* strains was performed in 50-200 ml medium in 500 ml baffled Erlenmeyer flasks or in 4 ml medium in test tubes. Strains were cultivated at 30 °C and 120 rpm, 170 rpm for test tubes. For the preparation of competent cells, precultures were cultivated overnight in 50 ml BHIS medium.

2.4.4 Cultivation of *C. glutamicum* strains in the BioLector

Strains were cultivated in the BioLector system (m2p-labs GmbH, Baesweiler, Germany) on microtiter scale to monitor growth and fluorescence online. Cultivation was performed in flower plates (m2p-labs GmbH, Baesweiler, Germany), which allow parallel cultivation and monitoring of 48 cultures. Due to its geometry, optimal mixing of each culture is provided. In each well, 750 µl minimal medium were inoculated with a cell suspension of the shake flask preculture. Cultivation was performed at 30 °C, 990 rpm, a throw of ø 3 mm and a relative air humidity of 80 %. To prevent evaporation, but to allow gas transfer, the flower plates were sealed with a self-adhesive foil. Growth was measured as backscatter.

2.4.5 Strain conservation of *C. glutamicum* strains

For long term storage of bacterial strains, glycerol stocks were prepared. Therefore, 700 µl of overnight cultures were mixed with 300 µl 87 % glycerol and transferred into sterile cryo tubes. For plasmid conservation, 1 µl of the necessary antibiotic was supplemented. The tubes were stored at -80 °C and used for inoculation of agar plates or precultures.

2.4.6 Determination of bacterial growth

The growth of bacterial cultures was determined by measuring the optical density (OD) at wavelength 600 nm in the Ultrospec 3300 pro spectrophotometer (Amersham Biosciences, Freiburg, Germany). A linear correlation is given up to an extinction of 0.5. Cell suspensions with higher extinction levels were therefore diluted in the respective medium.

2.5 Molecular biological methods

2.5.1 Isolation of DNA

Isolation of plasmid DNA

Starting from a 5 ml LB medium overnight culture, the plasmid DNA was isolated and purified from *E. coli* with the NucleoSpin Plasmid Kit (Macherey-Nagel GmbH & Co.KG, Düren, Germany). This method is based on the alkaline lysis principle (Bimboim and Doly, 1979). If higher amounts of plasmid DNA were needed, 50 ml LB medium were inoculated and the plasmid DNA was isolated and purified according to manufacturer's protocol (Qiagen, Hilden, Germany).

Purification of DNA

To purify DNA fragments from agarose gels or from enzymatic reactions, the NucleoSpin Gel and PCR Extraction Kit (Macherey-Nagel GmbH & Co.KG, Düren, Germany) was used according to manufacturer's protocol.

Determination of nucleic acid concentrations

For measurement of concentration and degree of purity of nucleic acids, the Nanodrop Spectrophotometer (Peqlab Biotechnologie GmbH, Erlangen, Germany) was used. The absorption of the aqueous nucleic acid solution was determined at 260 nm. An absorption rate of 1.0 equates to 50 µg/ml dsDNA in an aqueous solution. The degree of purity of the DNA was determined by the quotient $A_{260/280}$ or $A_{260/230}$, which lies in between 1.8 and 2.0. Lower values suggest contaminations of the DNA by proteins or polysaccharides.

2.5.2 Agarose gel electrophoresis

For the separation of DNA fragments agarose gel electrophoresis was performed. DNA fragments were separated according to size on 1 % (w/v) agarose gels in TAE buffer (40 mM Tris, 1 mM EDTA, pH was tuned to 8 with acetic acid) (Sambrook *et al.*, 1989). Samples were mixed with DNA loading dye (6x: 0.2 % bromphenol blue, 100 mM Na_2EDTA, 34 % (v/v) glycerol) before loading. As size marker, gene ruler 1 kb DNA ladder (Thermo Fisher Scientific, Waltham, USA) was used. The separation was performed at a voltage of 70-100 V for 1 h depending on gel size. After the electrophoretic separation, the gel was stained in an ethidium bromide solution (0.5

µg/ml). Ethidium bromide intercalates in double-stranded DNA and can be visualized by UV excitation, which was then analyzed by the gel documentation system Quantum (Peqlab Biotechnologie GmbH, Erlangen, Germany).

2.5.3 Recombinant DNA techniques

For the digestion of DNA, sequence specific restriction endonucleases were used according to manufacturer's protocol (Thermo Fisher Scientific, Waltham, USA). Reactions (50 µl for preparative reactions, 20 µl for analytical reactions) contained 200 ng - 1 µg of DNA and 5-15 U of the desired enzyme and were incubated at 37 °C for 1-2 h. The correct restriction was analyzed via agarose gel electrophoresis.

The dephosphorylation of the 5'-end of linear plasmid DNA is catalyzed by *Shrimp alkaline phosphatase* (Roche Diagnostics, Mannheim, Germany). Because the T4 DNA ligase is only able to combine 5'-phosphate ends with 3'-OH-ends, a recirculation of the linearized vector during ligation is prohibited. The reaction was performed according to manufacturer's protocol.

For the ligation reaction, the rapid ligation kit (Thermo Fisher Scientific, Waltham, USA) was used according to manufacturer's protocol.

2.5.4 Transformation techniques

Preparation and transformation of chemically competent E. coli cells

For the generation of chemically competent *E. coli* cells, the method of Hanahan was used where cells are treated with $RbCl_2$ (Hanahan, 1985). Cells were cultivated in 50 ml SOB medium until an OD_{600} of 0.15 was reached, harvested and treated according to protocol.

For transformation, 200 µl of competent cells were mixed with a ligation reaction or with plasmid DNA. After incubation on ice for 30 min., a heat-shock at 46 °C for 90 minutes was performed. Cells were then mixed with 800 µl of LB medium, regenerated at 37 °C and 800 rpm for 45 minutes and plates on LB agar plates with the respective antibiotic.

Preparation of transformation of electrocompetent C. glutamicum cells

Electrocompetent *C. glutamicum* cells were prepared and transformed by electroporation with an additional heat-shock as described by Tauch *et al*., (2002). For the preparation of competent cells, a 50 ml BHIS preculture was inoculated from a fresh agar plate or directly from the cryo tube and cultivated at 30 °C overnight. For strains harboring plasmids with antibiotic resistances, the respective antibiotic was added. The next day, 200 ml BHIS medium was inoculated with 4 ml of the preculture and cultivated at 30 °C and 100 Upm until an OD_{600} of 1.75 - 2.0 was reached, corresponding to approximately 2.3×10^{12} cells. Cells were harvested in four 50 ml Falcon tubes, placed on ice for 20 min. and centrifuged (4 °C, 20 min., 5000 g).

Subsequently, cells were washed twice with TG-buffer (1mM Tris, 10 % (v/v) glycerol, pH 7.5) and twice with 10 % (v/v) glycerol. Competent cells were then resuspended in 800 µl 10 % (v/v) glycerol and 150 µl aliquots were prepared that were stored at -80 °C.

The electroporation was performed in precooled electroporation cuvettes (Type Gene Pulser Cuvette, 0.2 cm, Biorad, Hercules, USA). Therefore one aliquot of competent cells was mixed with the plasmid DNA or the respective DNA substrate and transferred to the cuvette. Then 800 µl of 10 % (v/v) glycerol were carefully overlaid and the cuvette was transferred to the gene pulser XCell™ (Biorad, Hercules, USA). Cells were pulsed with a voltage of 2.5 kV, an impedance of 200 Ω and a condensator capacity of 25 µF. After the electrical pulse, cell suspensions were immediately transferred to 4 ml prewarmed BHIS medium (46 °C) and incubated for 6 min. After the heat-shock, cells were regenerated at 30 °C, 170 rpm for 1h and plated on BHIS agar plates containing the respective antibiotic.

2.5.5 Amplification of DNA fragments via polymerase chain reaction

DNA fragments were amplified for analytic and preparative purposes by polymerase chain reaction (PCR) (Mullis and Faloona, 1987). If not stated otherwise, analytic PCR's e.g. for the analysis of transformants or mutant strains were performed with Taq-DNA polymerase (DreamTaq™ PCR master mix, Thermo Fisher Scientific, Waltham, USA) in a T3000 Thermocycler (Biometra, Göttingen, Germany). Preparative samples were amplified with KOD Hot Start DNA polymerase (Merck, Darmstadt, Germany). All PCR conditions were performed according to manufacturer's protocol.

In vitro amplification of DNA fragments

For the amplification of DNA fragments *in vitro*, a total volume of 50 µl was used. Each reaction contained 0.1-1 µg of DNA template, 300 nM of each oligonucleotide, 0.02 U of KOD Hot Start Polymerase, 5 µl of 10x PCR buffer, 1.5 mM $MgSO_4$ and 200 µM each of dATP, dGTP, dTTP and dCTP. The PCR-Cycler program contained an initial heating step to 95 °C to allow a hot start reaction. After a single 2 min. step of denaturation at 95 °C, the DNA was denatured for 20 s at 95 °C. Annealing of the oligonucleotides was performed at 55 °C - 65 °C for 10 s and fragments were elongated at 70 °C for 20 s/kb with DNA polymerase. After the repetition of denaturing, annealing and elongation for further 30 cycles, a final elongation of 10 min. at 70 °C was performed. For the calculation of the annealing temperature for each pair of oligonucleotides, the melting temperature values (T_m) were subtracted by 5 °C. T_m can be calculated with the following formula: Tm [°C]: [(G+C) x 4] + [(A +T) x 2].

Colony PCR

For the analysis of correct *E. coli* transformants and *C. glutamicum* mutants a colony PCR was performed. In one reaction, 2x DreamTaq™ PCR master mix that already included buffer, dNTPs and $MgCl_2$, was mixed with 400 nM of oligonucleotides and water to a final volume of 20 µl. Single colonies were picked with a sterile pipette tip and resuspended in the reaction mixture. The PCR program contained an initial denaturation step of 10 min. at 95 °C to disrupt the cells. Moreover, 30 repeating cycles of DNA denaturation for 30 s at 95 °C, primer annealing for 10 s at 55 °C - 65 °C and primer elongation with DNA polymerase for 1 min/kb at 72 °C were performed. The last step contained a final elongation for 10 min. at 72 °C. All temperatures for primer annealing and elongation time were calculated as described in the previous paragraph.

2.5.6 Construction of *C. glutamicum* mutants

All *C. glutamicum* mutants were generated with help of the pK19mobsacB plasmid (Schäfer *et al.*, 1994). This plasmid contains a kanamycin resistance cassette, the levansucrose encoding gene *sacB* and the gene of interest flanked by two 500 bp fragments of the genomic target region, where the gene should be integrated. In this thesis, all genes were integrated in the intergenic region of *cg 1121-1122*. The pK19mobsacB vector is not replicated in *C. glutamicum*, but is instead integrated into the chromosome by homologous recombination. After transformation, kanamycin resistant clones that have integrated the plasmid were picked and cultivated in BHIS medium for 2 h at 30 °C and 170 rpm. By cultivation in rich medium without antibiotics a second homologous recombination event can occur. After 2 h, different dilutions of the cultivations were plated on BHIS agar plates containing 10 % (w/v) sucrose. The levansucrose encoding gene *sacB* on pK19mobsacB allows the cleavage of sucrose to glucose and fructose. Moreover it converts fructose to the oligomeric levan, which leads to mortality (Jäger *et al.*, 1992). Therefore, only clones will grow where a second recombination event took place, leading to the loss of the *sacB* gene. These kanamycin sensitive and sucrose resistant clones are checked for their genotype by PCR, because clones could either harbor the gene of interest or the wild type situation was restored.

2.5.7 DNA sequencing analysis

All DNA samples were sequenced by the chain termination method (Sanger *et al.*, 1977) by Eurofins MWG GmbH (Ebersberg, Germany). Received sequences were analyzed with *Clone Manager 9 Professional Edition* (Version 9.1 G, Scientific & Educational Software).

2.5.8 Genome editing methods

Recombineering

Electrocompetent cells carrying the respective recombineering plasmid were electroporated with 1 µg of the respective PCR fragment for dsDNA recombineering or 10 µg of the respective oligonucleotide for ssDNA recombineering. The 4 ml regeneration media additionally contained the antibiotic responsible for keeping the respective recombineering plasmid. After the 6 min. heat-shock at 46 °C, cells were regenerated for 5 h at 30 °C and 170 rpm. Finally either 100 µl were plated directly or all cells were harvested by centrifugation (10 min., 4800 g), the medium discarded and the cells resuspended in the remaining medium. Subsequently, the cell suspensions were spread on BHIS agar plates containing the respective antibiotics. For analysis, if not stated otherwise the number of colony forming units (CFU) corresponds to a total number of approximately 10^{10} cells.

CRISPR-Cas9 targeting

Electrocompetent cells carrying plasmids with *cas9* under control of various promoters were transformed with a second plasmid harboring the sgRNA as described in 2.5.4. After regeneration of 1-1.5 h 100 µl of the suspensions were spread on BHIS agar plates with the respective antibiotics. Moreover, the remaining cells were harvested by centrifugation and the resuspended pellet was additionally spread on agar plates.

2.6 Quantitative measurement of L-lysine titers by HPLC

L-lysine concentrations were quantified after *o*-phtaldialdehyde derivatisation by high-pressure liquid chromatography using an uHPLC 1290 Infinity system (Agilent, Santa Clara, USA), which was equipped with a Zorbax Eclipse AAA C18 3.5 micron 4.6 x 75 mm column and a fluorescence detector. A gradient of 0.01 M sodium borate buffer (pH 8.2) with increasing concentrations of methanol was used as eluent and the fluorescent isoindole derivatives were detected at λ_{ex} =230 nm and λ_{em}=450 nm.

3 Results

3.1 dsDNA recombineering

In the first part of this work it was the task to develop dsDNA recombineering as a genome editing tool for *C. glutamicum*. It could be previously shown that ssDNA recombineering is functional in *C. glutamicum* (Binder *et al.*, 2013), but only enables the insertion or deletion of SNPs. dsDNA recombineering could overcome this limitation. This method was already established for a variety of different bacteria, allowing the genomic integration of full-length genes (Yu *et al.*, 2000), very large DNA fragments (Kuhlman and Cox, 2010) or even full gene clusters (Alcazar-Fuoli *et al.*, 2014). Currently, in case of *C. glutamicum,* larger fragments are generally inserted or deleted using the time-consuming pK19mobsacB method (Schäfer *et al.*, 1994). Thus, in this work dsDNA recombineering was analyzed as a potential alternative for genome alteration in *C. glutamicum*.

3.1.1 Analysis of recombinases and variation of induction parameters

In order to establish dsDNA recombineering in *C. glutamicum*, a variety of different recombinases was tested for their functionality in this bacterium. As test system, the L-lysine producer strain *C. glutamicum* DM1728kanR(+1) was used (Binder *et al.*, 2013). This strain harbors a defective *aph(3´)-IIa* gene from the transposon Tn5 conferring kanamycin resistance (Santamaria *et al.*, 1984), which was inserted into the intergenic region of cg1121 and cg1122. The gene is inactive due to an inserted cytosine at position 234 of the kanamycin resistance cassette (Figure 3). The addition of this nucleotide shifted the open reading frame towards a non-functional gene. Furthermore the insertion created an additional *Eco*RI site for subsequent analysis purposes.

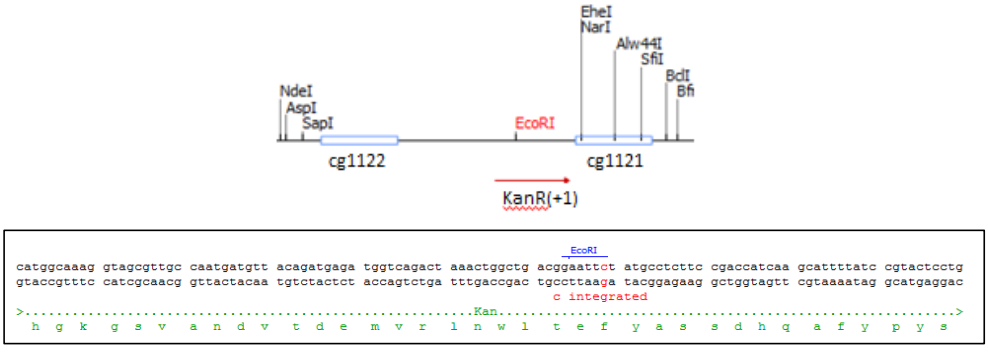

Fig. 3: Genomic region of L-lysine producer strain *C. glutamicum* DM1728kanR(+1) carrying the insertion. The defective *aph(3´)-IIa* gene is inserted in the intergenic region of cg1121-cg1122. Due to one additional nucleotide insertion at position 234 of the *aph(3´)-IIa* gene and the resulting shift of the open reading frame, the kanamycin conferring resistance gene is non-functional. Additionally, due to this point mutation an *Eco*RI restriction site is generated, which enables a diagnostic restriction analysis.

During initial experiments, the basic parameters for dsDNA recombineering were analyzed. Binder *et al.* reported for ssDNA recombineering highest functionality with RecT, whereas the recombinase Bet from the λ Red system did not lead to a significant number of recombinant colony forming units (CFU) (Binder *et al.*, 2013). Furthermore, ssDNA recombineering could also be performed using rCau, a gene 60 % identical to RecT, originating from *C. aurimucosum*. Based on this information and the fact that for dsDNA recombineering also RecE is required (Zhang *et al.*, 1998), the following two recombinase/exonuclease pairs were tested for dsDNA recombineering: a.) *recET* from the *E. coli* prophage Rac and b) orf-1962 and orf-1963 (further named recETCau) from *C. aurimucosum*. Both gene constructs were inserted into the expression plasmid pCLTON2 (pCL2), which harbors the tightly regulated TetR expression system that can be induced with anhydrotetracycline (ATc) (Lausberg *et al.*, 2012).
A standard dsDNA recombineering experiment was performed: competent cells of strain *C. glutamicum* DM1728kanR(+1)/pCL2-recET were prepared and *recET* expression was induced with 250 ng ATc during cultivation. Then, cells were electroporated with 1 µg of dsDNA substrate (PCR fragment), harboring 600 bp of the correct *aph(3´)-IIa* (further called *kan*) gene sequence centered around the mutation in the *kan(+1)* gene. After a 6 min. heat-shock at 46 °C, cells were regenerated for 5 h and plated on BHIS agar plates containing spectinomycin and kanamycin.

With RecET from prophage Rac a 2000-fold increase in kanamycin-resistant CFU could be obtained compared to using the RecET homologs from the closely related species *C. aurimucosum* (Figure 4). dsDNA recombineering with only RecT from the prophage Rac also led to recombinant CFU (5.0×10^3), which might be due to endogenous exonucleases present in *C. glutamicum* that convert the PCR fragment into the ssDNA intermediate that is used as substrate by RecT (Mosberg *et al.*, 2010). Furthermore, the induction parameters of the exonuclease/recombinase pair RecET were analyzed, because RecE might have toxic effects on the cell (Yang *et al.*, 2015) and the operon structure of *recET* could influence the level of induction. For *C. glutamicum* highest numbers of recombinant CFU (1.1×10^5 per µg DNA) were generated when the Tet promoter was fully induced with ATc (250 ng/ml). Shorter induction times during preparation of the competent cells as well as no induction led to decreased levels in kanamycin-resistant clones (Figure 4).

The obtained results indicate that repairing the defective kanamycin resistance gene of *C. glutamicum* strain DM1728kanR(+1) is a suitable test system for establishing dsDNA recombineering, since no spontaneous repair of the kanamycin resistance deficiency did occur when recombinases were absent in the cell. The sole presence of RecE led to 99 CFU, for recombineering with the empty plasmid pCL2 28 kanamycin-resistant colonies were obtained.

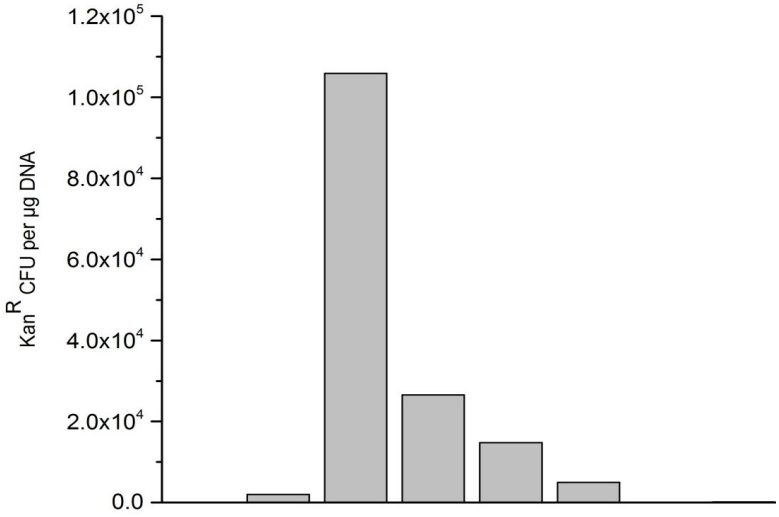

Kan^R CFU	**0.0**	**5.0 x 10^1**	**1.1 x 10^5**	**2.7 x 10^4**	**1.5 x 10^4**	**5.0 x 10^3**	**9.9 x 10^1**	**2.8 x 10^1**
PCR fragment 600nt	Kan (+)	Kan (+)	Kan (+)	Kan (+)	Kan (+)	Kan (+)	Kan (+)	Kan (+)
Recombinases	-	recET Cau	recET	recET	recET	recT	recE	pCL2
Induction time		4.5h	4h	0.5h	0h	4h	0.5h	4h

Fig. 4: Comparison of dsDNA recombineering efficiencies in strains *C. glutamicum* DM1728kanR(+1)/ pCL2-recET, DM1728kanR(+1)/pCL2-recETCau, DM1728kanR(+1)/pCL2-recE and DM1728kanR(+1)/pCL2-recT with different recombinases and different induction times. *C. glutamicum* strains were transformed with a 600 bp PCR fragment (Kan (+)) to repair the kanamycin resistance deficiency. Gene expression was induced with 250 ng/ml ATc and induction times were varied. As negative controls, the empty plasmid pCL2 was used and recombineering was performed without any recombinases. Best efficiencies could be obtained with full induction of *recET* from prophage Rac.

3.1.2 Possibilities and limitations of dsDNA recombineering

After the initial parameters were set for dsDNA recombineering, the method was tested for the integration of full genes via dsDNA recombineering. Therefore, the full-length *aph(3´)-IIa* gene conferring kanamycin resistance with various lengths of flanking regions was amplified by PCR from pK18NCRkanR(+) and used as DNA substrate to transform *C. glutamicum* WT/pCL2-recET. The flanking regions were homologous to the intergenic region of cg1121-cg1122, the *meso*-diaminopimelate dehydrogenase (*ddh)* gene (2,761,024-2,760,062) or the phosphoenolpyruvate carboxykinase (*pck)* gene (3,052,060-3,053,892). However, dsDNA recombineering with the full-length *aph(3´)-IIa* gene did not lead to correct genomic integration. A number of kanamycin-resistant colonies were obtained, though the integration locus in the chromosome could not be determined. In all three genomic loci tested, no correct integration could be verified.

To determine the maximum size of genetic alterations that can be 'repaired' via dsDNA recombineering and the necessary lengths of the flanking regions, two additional defective *C. glutamicum* DM1728kanR strains were constructed with deletions in the kanamycin resistance gene of 131 nt and 752 nt, respectively: DM1728kanR(-131) and DM1728kanR(-752). As DNA substrates, two different partial Kan fragments of 131 nt and 752 nt with flanking regions of 400 nt, 900 nt or 1500 nt respectively were amplified by PCR from the plasmid pK18NCRkanR(+). The kanamycin resistance could be efficiently restored in *C. glutamicum* strains DM1728kanR(+1) and DM1728kanR(-131), whereas only very few kanamycin-resistant CFU could be detected for strain DM1728kanR(-752) (Figure 5). When comparing all three strains, it could be observed that dsDNA recombineering efficiencies decreased as the length of the fragments to be integrated increased.

dsDNA recombineering can therefore be used in *C. glutamicum* in order to introduce mutated fragments around 131 nt with around $2x10^3$ recombinants per 10^9 cells. However, the integration of longer fragments (e.g. full-length genes or polycistronic operons) only leads to little or no CFU, which renders the method unsuitable for the integration of heterologous genes e.g. for metabolic engineering. Instead, dsDNA recombineering can only be applied for the integration of smaller DNA substrates, e.g. to mutate several genomic targets, which are located in close proximity in one experiment.

The experiments were performed numerous times to verify the results. Due to the observation, that between experiments several factors like electroporation efficiency and the competency of the cells vary strongly, a high standard deviation (SD) could be observed (Figure 5). However, within a single experiment the number of CFU was consistent, verifying the observed results. The exact numbers of CFU in each experiment are shown in supplementary Table 17.

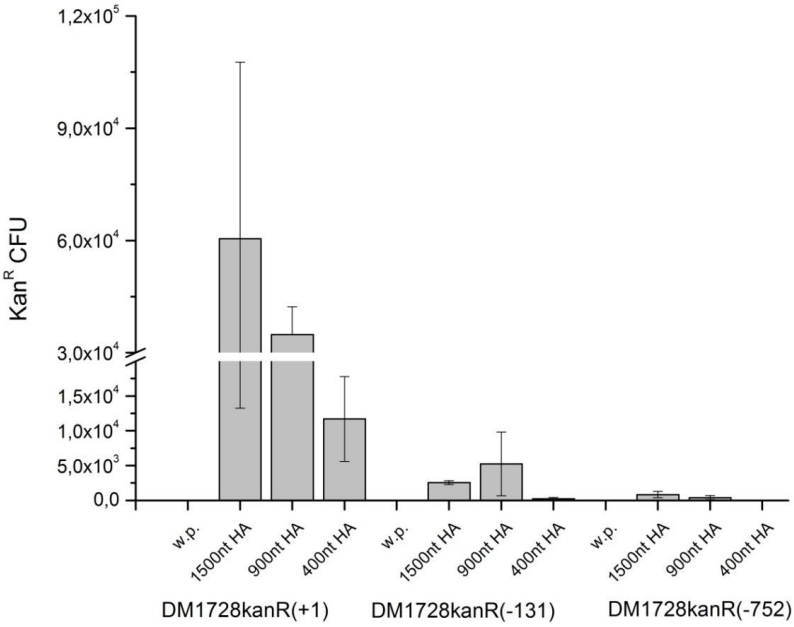

Fig. 5: Comparison of dsDNA recombineering efficiencies in three different *C. glutamicum* strains: DM1728kanR(+1)/pCL2-recET, DM1728kanR(-131)/pCL2-recET and DM1728kanR(-752)/pCL2-recET. PCR fragments with homology arms (HA) of 400 nt, 900 nt and 1500 nt were used as DNA substrates, w.p.: strain without plasmid. The number of kanamycin-resistant CFU per µg DNA decreases as the length of the deletion to be repaired increases.

3.1.3 5'-modifications of DNA substrate

In *C. glutamicum* genome editing via dsDNA recombineering only allows the integration of small fragments with low efficiencies. In order to increase recombinant CFU numbers, applicability of 5'-modified dsDNA substrates was tested. The exonuclease RecE degrades dsDNA in 5'-3' direction and prefers phosphorylated 5'-ends (Subramanian *et al.*, 2003), whereas phosphorothioated ends prevent enzymatic cleavage (Liu and Liu, 2010; Mosberg *et al.*, 2010). With protection of the 5'-end of the non-template strand and a modification of the 5'-end of the template strand that is preferred by the enzyme, more ssDNA intermediates might be generated, which would lead to an increase in recombinant CFU. Applicability of two types of modified dsDNA fragments were tested in comparison to the unmodified fragment. The modifications contained a phosphorothioated 5'-end (PTO) of the template strand with a phosphorylated 5'-end (PHO) of the non-template strand, or a phosphorylated 5'-end (PHO) of the template strand only. With the PCR product containing the phosphorylated 5'-end of the template strand a twofold increase in recombinant kanamycin-resistant CFU could be obtained (1.3×10^4) compared to the unmodified DNA substrate (5.4×10^3) (Figure 6). The 5'-phosphorothioation of the template strand of the PCR fragment reduced the number of kanamycin-resistant CFU by 50 % (2.9×10^3).

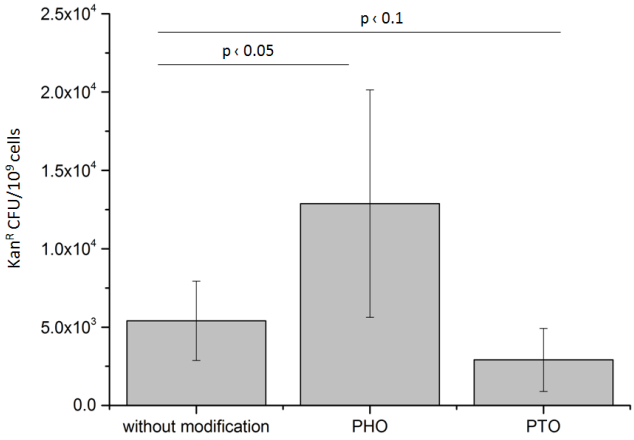

Fig. 6: dsDNA recombineering with strain *C. glutamicum* DM1728 kanR(-131)/pCL2-recET with different DNA substrate modifications. The strain was transformed with a 1931 nt kanamycin DNA fragment with 900 bp of flanking regions and different 5'-modifications: i.) no modification, ii.) 5'-phosphorylation of template strand (PHO) and iii.) phosphorothioation (PTO) of template strand (with 5'-phosphorylation of non-template strand). n = 7. Highest kanamycin-resistant CFU per 10^9 cells could be obtained with 5'- phosphorylation of the template strand.

3.1.4 Comparison of dsDNA recombineering and ssDNA recombineering

The editing tool of dsDNA recombineering allows at best the generation of up to 3 x 10^4 recombinants per µg DNA. According to Binder *et al.* with ssDNA recombineering recombinant numbers of 10^5 CFU per 10^8 cells could be generated (Binder *et al.*, 2013). In order to directly compare efficiency levels of both methods, two DNA substrates of the same length (100 bp) were generated. Strain *C. glutamicum* DM1728kanR(+1) was transformed with pEKEx3-recT or pCL2-recET and for both strains competent cells were prepared. Cells were transformed with the following fragments: For *C. glutamicum* DM1728kanR(+1)/pEKEx3-recT 10 µg of an 100 nt oligonucleotide were used and for *C. glutamicum* DM1728kanR(+1)/pCL2-recET 1.2 µg of a 100 bp PCR fragment was applied. With dsDNA recombineering higher numbers of recombinant CFU could be generated (3.19 x 10^5) than with ssDNA recombineering (9.85 x 10^4) (Table 3). The use of the oligonucleotide as DNA substrate when RecET was present decreased the efficiency (1.98 x 10^3) as compared to the presence of RecT only. This lower efficiency could be due to the presence of RecE or the use of a different plasmid background. As a control, the 600 bp fragment used in paragraph 3.1 was used, which led to fewer kanamycin-resistant colonies compared to the usage of the 100 bp fragment. Amongst others, this effect might result from a reduced transfer efficiency of the DNA fragment during electroporation into the cell, or an easier integration of a 100 nt ssDNA fragment into the genome as an Okazaki fragment as compared to a 600 nt ssDNA fragment.

However, when comparing efficiencies between ssDNA and dsDNA recombineering, it has to be considered that both methods were performed according to their established standard protocol. Therefore 1.2 µg of PCR fragment was used and 10 µg of oligonucleotides, which only allows for an indirect comparison.

Tab. 3: Comparison of DNA recombineering efficiencies with *C. glutamicum* strains DM1728kanR(+1)/pCL2-recET and DM1728kanR(+1)/pEKEx3-recT. 600 bp and 100 bp dsDNA fragments and 100 nt ssDNA fragments (Oligo) were used as DNA substrates.

Plasmid	DNA substrate	DNA amount	Total Kan^R CFU
pCL2-recET	PCR Kan 100 bp	1.2 µg	3.19×10^5
pCL2-recET	Oligo 100 nt	10 µg	1.98×10^3
pEKEx3-recT	Oligo 100 nt	10 µg	9.85×10^4
pCL2-recET	PCR Kan 600 bp	1.2 µg	8.8×10^4

When targeting single nucleotides, efficiencies of dsDNA recombineering are comparable or even better than ssDNA recombineering. In contrast to that, successful introduction or modification of larger DNA fragments could only be observed at very low efficiencies.

3.2 CRISPR-Cas9

As an alternative and/or potential addition to the genome editing tool of DNA recombineering, the CRISPR-Cas9 system should to be established in *C. glutamicum*. A functional CRISPR-Cas9 system in *C. glutamicum* would enable the differentiation between two different genotypes. Combined with DNA recombineering as an editing tool, the CRISPR-Cas9 system used as a targeting tool would enable the elimination of non-recombinant cells thus leading to enhanced efficiencies of genome modifications.

3.2.1 A functional nucleoprotein complex in *C. glutamicum*

First, in order to analyze whether a CRISPR-Cas9 method can be established in *C. glutamicum*, a functional nucleoprotein complex consisting of the large nuclease Cas9 (158 kDa) and the small sgRNA (192 nt) had to be expressed in *C. glutamicum*. Therefore, two expression plasmids were constructed: i) pEKEx3-cas9 and ii) pCL2-recET-cas9. The first contained the Cas9 nuclease encoding gene under control of the leaky *tac* promoter. For the second plasmid, the P_{tac}-*cas9* construct from pEKEx3-cas9 was integrated into the recombineering plasmid pCL2-recET. In general, the construction of plasmids containing genes encoding RecET, RecET together with Cas9, or even Cas9 only, generated many challenges. This was most likely due to toxic Cas9 activity, which can lead to the introduction of unspecific DSB. Several different construction designs were tested, but all failed and were therefore not described in this work.

For the functional CRISPR-Cas9 nucleoprotein complex, next to the Cas9 nuclease, a small guide RNA (sgRNA) had to be expressed that guides the nucleoprotein complex to the correct genomic target location. This sgRNA consists of three parts: i.) the 20 nt protospacer sequence

complementary to the genomic target region, ii.) the Cas9 handle for binding and iii.) a terminator from *S. pyogenes*.

For *C. glutamicum*, the sgRNA with a protospacer complementary to the genomic sequence of MurE at position G81 was synthesized and placed under the strong minimal synthetic promoter PJ23119 (Qi *et al.*, 2013). Behind the *S. pyogenes cas9* terminator an additional *E. coli* terminator was added (Figure 7, left) and the construct was integrated into the low copy number plasmid pBHK18 (pBHK18-sgRNA:murE). For a functional nucleoprotein complex, the protospacer sequence not only has to be complementary to the genomic sequence, but furthermore a PAM motif must be located in the genome adjacent to the protospacer sequence. In pBHK18-sgRNA:murE, the protospacer corresponded to MurE G81, which allowed a functional nucleoprotein complex targeting *C. glutamicum* WT MurE G81 (Figure 7, left). Coincidentally, in strain *C. glutamicum* ATCC13032 MurE-G81E, *murE* at position 243-245 was mutated from TGG to TGA. Since TGG represented the essential PAM sequence, a functional nucleoprotein complex could not be generated in *C. glutamicum* MurE-G81E and such cells were not targeted by the CRISPR-Cas9 system. This effect enabled the differentiation between *C. glutamicum* WT and *C. glutamicum* MurE-G81E.

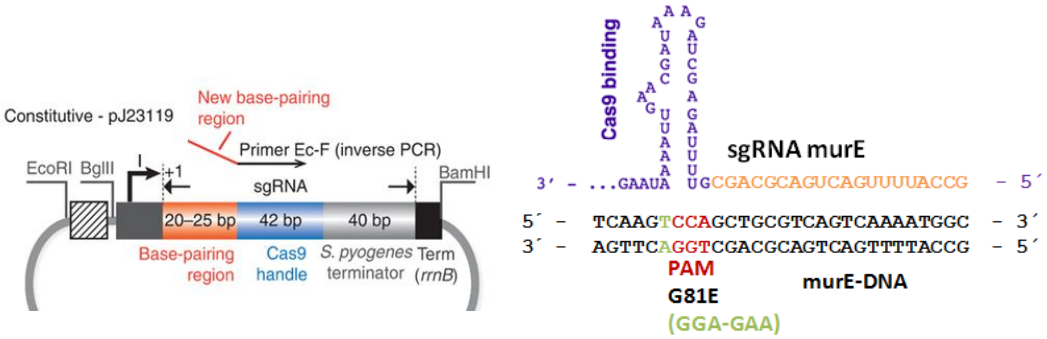

Fig. 7: Design of sgRNA plasmid targeting *C. glutamicum* WT MurE (G81).
Left figure: Schematic structure of sgRNA plasmid composition. The sgRNA consists of a Cas9 binding handle, a 20 nt base-pairing region (protospacer sequence) and a terminator originating from *S. pyogenes*. The plasmid furthermore contains the constitutive promoter PJ23119 and the additional *rrnB* terminator originating from *E. coli* (modified from Larson *et al.*, (2013)).
Right figure: sgRNA designed to specifically target *C. glutamicum* ATCC13032. The protospacer sequence (orange) is complementary to 3'-5' genomic sequence of *murE*. In the *murE* wild-type genomic sequence, the protospacer sequence is followed by a PAM motif (red), which is TGG, allowing for functional targeting. In case of the mutant strain MurE-G81E the PAM sequence is mutated to TGA, disabling the function of the nucleoprotein complex.

In the initial experiments, *C. glutamicum* ATCC13032 (WT), *C. glutamicum* ATCC13032 MurE-G81E (G81E) and *C. glutamicum* ATCC13032 MurE-G81K (G81K) mutants were used. For *C. glutamicum* strains WT/pEKEx3-cas9 and ATCC13032 MurE-G81E/pEKEx3-cas9 as well as

WT/pCL2-recET-cas9 and ATCC13032 MurE-G81K/pCL2-recET-cas9 competent cells were prepared and the expression of *cas9* under the control of the P_{tac} promoter was induced by the addition of 0.5 mM IPTG. Competent cells were electroporated with 100 ng of pBHK18_sgRNA:murE, regenerated for 1.5 h and plated on BHIS agar plates supplemented with spectinomycin and kanamycin.

In both strains the nucleoprotein complex of sgRNA:murE and Cas9 was formed, which scanned the DNA for the complementary sequence of the protospacer. In *C. glutamicum* WT cells the PAM motif (TGG) adjacent to the complementary protospacer sequence allowed a binding of the nucleoprotein complex, leading to the introduction of a site-specific double-strand break by the nuclease Cas9 resulting in cleaved DNA and no kanamycin-resistant CFU (Figure 8). In cells possessing the mutation in MurE-G81, an altered PAM motif was present (TGA for G81E, TAA for G81K) resulting in the inability of the RNA-Cas9 complex to bind and cut the DNA. As a result for *C. glutamicum* ATCC13032 MurE-G81E 15,500 kanamycin-resistant cells were able to survive (Figure 8, left). Comparable results could be obtained when the expression plasmid pCL2-recET-cas9 was used. The transformation of *C. glutamicum* strain ATCC13032 MurE-G81K/pCL2-recET-cas9 with pBHK18-sgRNA:murE resulted in 39,000 kanamycin-resistant cells, assuming that no targeting by the RNA-Cas9 complex could be established. In contrast to that, only 215 colonies survived for *C. glutamicum* WT/pCL2-recET-cas9 transformed with the sgRNA:murE providing plasmid (Figure 8, right). These results show the functionality and the specific targeting of the CRISPR-Cas9 nucleoprotein complex in *C. glutamicum* as provided by the plasmids used.

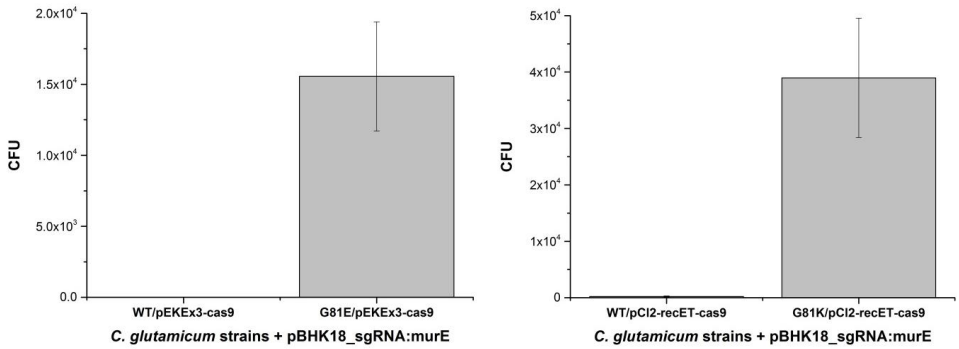

Fig. 8: Analysis of functional CRISPR-Cas9 targeting in *C. glutamicum* strains ATCC13032 (WT), ATCC13032 MurE-G81E (G81E) and ATCC13032 MurE-G81K (G81K). Strains containing expression plasmids pEKEx3-cas9 (left) and pCL2-recET-cas9 (right) are transformed with 100 ng pBHK18_sgRNA:murE.

Furthermore, it was analyzed whether mutated cells can be separated from wild-type cells by using CRISPR-Cas9 targeting. Competent cells of *C. glutamicum* strains WT/pEKEx3-cas9 and ATCC13032 MurE-G81E/pEKEx3-cas9 (the expression of *cas9* was induced with IPTG) were mixed in a 1:2 ratio and electroporation with pBHK18-sgRNA:murE was performed. As controls, both strains were also individually transformed with the targeting DNA. The mixture of *C. glutamicum* WT/pEKEx3-cas9 and *C. glutamicum* ATCC13032 MurE-G81E/pEKEx3-cas9 contained 4.17 x 10^3 cells, which is half of the amount of cells, in which only *C. glutamicum* ATCC13032 MurE-G81E/pEKEx3-cas9 cells were present (1.1 x 10^4) (Figure 9). For *C. glutamicum* WT/pEKEx3-cas9, all cells were targeted by CRISPR-Cas9 and were therefore not able to grow.

The grown colonies of this mixture were further analyzed by colony PCR and DNA restriction analysis (Figure 10). The PCR fragment amplified from strain *C. glutamicum* WT/pEKEx3-cas9 (Primer ds-murE-fw and ds-murE-rv) is cleaved by *Pvu*II into two fragments (289 bp + 311 bp), whereas the fragment from strain *C. glutamicum* ATCC13032 MurE-G81E/pEKEx3-cas9 will not be digested due to a silent mutation abolishing cleavage (600 bp). All colonies except one were exhibiting *C. glutamicum* MurE-G81E properties, showing that the two genotypes of *C. glutamicum* can be separated by CRISPR-Cas9 targeting. The observed single colony with the wild-type fragment, a so called 'escaper cell', is most likely due to spontaneous mutations/deletions of the plasmid encoded spacer or in the Cas9 machinery (Jiang *et al.*, 2013; Stern *et al.*, 2010).

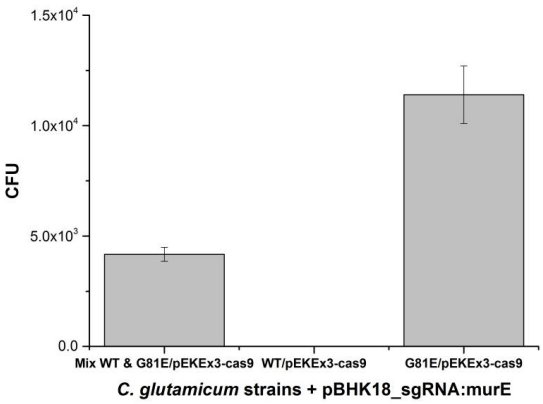

Fig. 9: Analysis of CRISPR-Cas9 targeting by separating *C. glutamicum* strains WT/pEKEx3-cas9 and ATCC13032 MurE-G81E/pEKEx3-cas9. Strains are transformed with 100 ng of pBHK18_sgRNA:murE. Left bar: 1:2 mix of WT and ATCC13032 MurE-G81E, middle bar: WT and right bar ATCC13032 MurE-G81E.

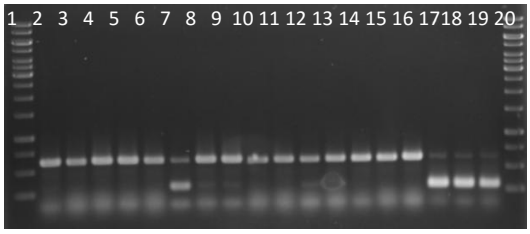

Fig. 10: Colony PCR of *murE* fragment with subsequent restriction analysis. 600 bp PCR fragments from *C. glutamicum* strain MurE-G81E are not digested by *Pvu*II (WT: 289 bp + 311 bp). From left to right: lane 1 and 20: 1kb ladder, 2-11: single cell colonies from mix WT + ATCC13032 MurE-G81E, lane 12-16: single cell colonies from ATCC13032 MurE G81E, 17-19: WT cells.

3.2.2 Toxicity of Cas9

According to literature and further supported by findings described in this work, strong toxic effects of Cas9 on cell viability could be observed (Bikard *et al.*, 2013; Jiang *et al.*, 2015). This effect is most likely due to the introduction of unspecific DSB into the genome even without an sgRNA being present. To assess Cas9 toxicity in *C. glutamicum,* WT cells were transformed with several constructs harboring *cas9* under the control of different promoters. After transformation, CFU numbers as well as size and homogeneity of cells were determined (Table 4). For plasmids harboring *cas9*, an up to 10-fold reduced transformation efficiency could be observed compared to standard transformation rates. Whereas with pEKEx3 1.03 x 10^5 transformants were obtained per µg DNA, *cas9* placed under the leaky P_{tac} promoter only led to 2.3 x 10^4 transformants. For *cas9* under control of the more tightly controlled promoter P_{tet} (Lausberg *et al.*, 2012) 9.75 x 10^3 CFU were detected after transformation. Interestingly, when *cas9* was controlled by the native promoter from *S. pyogenes* P_{nat}, which supposedly naturally prevents unspecific Cas9 toxicity, also reduced numbers of transformants were obtained (3.75 x 10^4). The comparison of transformation efficiencies between the two plasmids pEKEx3-cas9 and pCL2-recET-cas9, both originating from the original plasmid pBL1, shows that even though the plasmids exhibit strong differences in size (pEKEx3-cas9 with 12439 nt and pCL2-recET-cas9 with 17200 nt) transformation efficiencies are comparable (2.3 x 10^4 and 1.8 x 10^4).

Furthermore, two modified versions of Cas9, dead (dcas9) and nicked (ncas9) Cas9, were analyzed in terms of toxic effects on *C. glutamicum* cells. dCas9 is a deactivated version, where Cas9 lacks nuclease activity due to the presence of two point mutations in the RuvC and the HNH domain of Cas9 (H840A and D10A) (Qi *et al.*, 2013). The application of dCas9 has led to the downregulation of genes via a mechanism called CRISPR interference (CRISPRi) (Bikard *et al.*, 2013; Larson *et al.*, 2013). The nucleoprotein complex is formed and blocks transcription initiation or elongation, but does not introduce DSB. Furthermore, it is not irreversible, because no permanent DNA-encoded mutations are introduced (Gilbert *et al.*, 2013; Larson *et al.*, 2013). The other variant, nCas9, harbors either one of the two described point mutations. Due to the inactivation of one nickase domain, nCas9 only introduces single-strand breaks (SSB) (Gasiunas *et al.*, 2012; Jinek *et al.*, 2012; Sapranauskas *et al.*, 2011) resulting in improved on-site DSB specificity. By using two different sgRNAs simultaneously, nCas9 introduced two specific SSBs leading to the specific deletion of a genomic fragment (Mali *et al.*, 2013).

Both Cas9 variants were tested in terms of toxicity in *C. glutamicum*, because they offer potential alternatives in genome editing to the classical CRISPR-Cas9 system. *ncas9*, *dcas9* and *cas9* were placed on the temperature-sensitive plasmid pCL1-TS and transformation rates were compared after electroporation of *C. glutamicum* WT with the respective plasmids. Transformation with

plasmids carrying the dead and nicked versions of Cas9 exhibited higher numbers of transformants (6.5 x 10^4 and 2.6 x 10^4) compared to functional Cas9 (9.75 x 10^3), indicating that nCas9 and dCas9 proteins show less unspecific DSB activity than native Cas9. However, a reducing effect remains, because transformation rates similar to those observed with the empty expression plasmid pEKEx3 could not be obtained. This effect might result from the different plasmid sizes when *dcas9* or *ncas9* are present and the involving transformation efficiency. Yet, a remaining toxicity effect of dCas9 was also observed by Cleto *et al*. who faced difficulties in cloning and the expression of the *dcas9* gene in *C. glutamicum* (Cleto *et al.*, 2016).

In contrast to earlier reported findings where the presence of the sgRNA alone affected transformation rates (Jiang *et al.*, 2015), no reducing effect on living cell count could be detected for the sole presence of sgRNA in *C. glutamicum*. The somewhat smaller colony size observed with the sgRNA delivery plasmids was due to the plasmid pBHK18 as control experiments with the empty plasmid showed (data not shown).

Tab. 4: Influence of Cas9 on living cell count after electroporation of *C. glutamicum* ATCC13032 with 100 ng of the respective plasmid. After transformation cells were spread on BHIS medium with the respective antibiotic and incubated for 3 days at 25 °C.

Plasmid	Size (bp)	Copy number	Resistance	Characteristics	CFU Size	CFU per µg DNA
pEKEx3	8319	8-30**	Spectinomycin		3-4mm	1.03 x 10^5
pEKEx3-cas9	12439	8-30	Spectinomycin	*cas9* under P_{tac}	heterogenous many small CFU's	2.3 x 10^4
pCL2-recET	11502	8-30	Spectinomycin	Allows dsDNA recombineering	3-4 mm	2.0 x 10^5
pCL2-recET-cas9 (Ptac)	17200	8-30	Spectinomycin	*cas9*(P_{tac}) from pEKEx3-cas9	1-3 mm	1.8 x 10^4
pCL2-recET-cas9 (Pnat)	15792	8-30	Spectinomycin	*cas9* under native $P_{S. pyogenes}$	3 mm	3.75 x 10^4
pCL1(TS)-cas9-Spc*	13334	8-30	Spectinomycin	*cas9* (P_{tet}) in temperature sensitive vector	0.1-2 mm heterogenous, many small CFU's	9.75 x 10^3
pCL1(TS)-dcas9-Spc*	13334	8-30	Spectinomycin	Deactivated *cas9*, no nuclease activity	3 mm	6.5 x 10^4
pCL1(TS)-ncas9*	12211	8-30	Kanamycin	Nicked *cas9*, single nuclease activity	2 mm	2.6 x 10^4
pEKEx3-cas9-sgRNA	12618	8-30	Spectinomycin	*cas9*(P_{tac}) and sgRNA:murE (P_{J23119})	0.1-2mm heterogenous, many small CFU's	1.13 x 10^4
pBHK18-sgRNA:murE	3492	3-4***	Kanamycin	sgRNA targeting *murE* (P_{J23119})	2 mm	7.43 x 10^4
pBHK18-sgRNA:ctrl	3492	3-4	Kanamycin	sgRNA targeting *fapR* from *E. coli* (P_{J23119})	2 mm	3.0 x 10^5

*Original plasmid supplied by Dr. S. Matamouros, resistance cassette was exchanged

**estimated copy number for plasmids with pBL1 replicon according to (Santamaria *et al.,* 1984)

*** estimated copy number for pBHK18 according to (Handbook of Microbiology, 2nd edition)

The presence of Cas9 protein in *C. glutamicum* cells did not only result in reduced numbers of transformants, but also in the heterogeneity of the obtained colonies. Even when strain *C. glutamicum* WT was transformed with pEKEx3-cas9 without induction by IPTG or without the presence of a corresponding sgRNA, transformants grew to colonies of different size, emphasizing the toxic effect of the nuclease Cas9 in *C. glutamicum* (Figure 11).

Interestingly, when a single large clone carrying Cas9 was isolated and used for further studies, in subsequent transformations this heterogeneous effect was no longer visible. Though, when six small clones were isolated and spread on fresh agar plates, two colonies remained small, whereas the growth defect could be restored for all others. Thus, the original heterogeneity caused by the Cas9 constructs can be neglected during development of the CRISPR-Cas9 technique as long as Cas9 is active. The heterogeneity could be due to alterations in Cas9, in the plasmid backbone, or in the genome of the plasmid-carrying strain, but this was not further investigated.

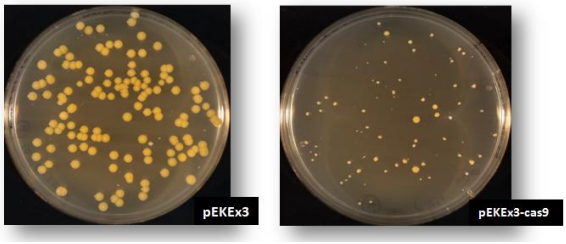

Fig. 11: Influence of Cas9 on heterogeneity of cells.
Transformation of *C. glutamicum* WT with 100 ng of plasmid DNA of pEKEx3 leads to normal sized homogenous colonies (left), whereas after transformation with 100 ng of pEKEx3-cas9 (right) heterogeneous colonies can be observed.

Effect of *cas9* start codon exchange on living cell count

As reported for other organisms e.g. *Chlamydomonas reinhardtii* (Jiang *et al.*, 2014) and also shown here for *C. glutamicum*, the nuclease Cas9 possesses negative effects on living cell count and drastically reduces cell count after transformation. Furthermore, the enzyme influences cell morphology, leading to heterogenous colony sizes.

Among the various approaches to reduce toxicity effects of Cas9 on *C. glutamicum*, a genetic construct with the aim to tightly regulate *cas9* expression was designed. Previously, it could be shown that gene expression in *C. glutamicum* can be tightly controlled when the Tet-Repressor based expression system is used (Lausberg *et al.*, 2012). The gene of interest is placed under the *B. subtilis* derived TetR-controllable promoter P_{tet} and expression is further regulated by the *tet* repressor which is under the control of the P_{gap} promoter (Figure 12).

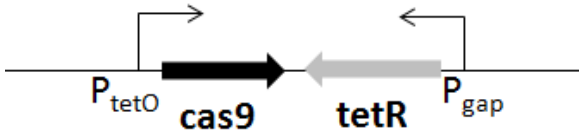

Fig. 12: Schematic drawing of TetR-Repressor expression system. *cas9* is under control of P_{tetO}, further regulated by the TetR repressor, whose gene is under control of the *gap* promoter.

In order to construct a CRISPR-Cas9 recombineering plasmid with less Cas9 toxicity, four *cas9* variants (ATG-cas9, GTG-cas9, TTG-cas9 and ATG-cas9 following 2xSTOP (further called 2xSTOPcas9)) under control of the TetR expression system were synthesized (by Dr. Philana van Summeren). All constructs were supposed to be inserted into the ssDNA recombineering plasmid pEKEx3-recT to generate pEKEx3-recT-Phil-ATGcas9, pEKEx3-recT-Phil-GTGcas9, pEKEx3-recT-Phil-TTGcas9 and pEKEx3-recT-Phil-2xSTOPcas9. The cloning was independently tried three times without success. A detailed DNA sequence analysis of all obtained constructs revealed that full length *recT* with the P_{tac} promoter as well as parts of the repressor gene *lacIq* where invariably lost (restriction maps of plasmid sequences are shown in supplementary data). This compares to the difficulties that have already occurred during the generation of Cas9 expression plasmids (Jiang *et al.*, 2015; Oh and van Pijkeren, 2014). Thus, in this work, plasmids harboring *cas9* with different start codons, but without RecT were available. Due to remaining partial sequences of the *recT* expression cassette, plasmids were named pEKEx3-(recT)-Phil-ATGcas9, pEKEx3-(recT)-Phil-GTGcas9, pEKEx3-(recT)-Phil-TTGcas9 and pEKEx3-(recT)-Phil-2xSTOPcas9 (later collectively described as pEKEx3-(recT)-Phil-NTGcas9).

To analyze if the constructed plasmids containing the *cas9* variants still led to reduced transformation rates, *C. glutamicum* WT was transformed with the four plasmids pEKEx3-(recT)-Phil-NTGcas9 (Figure 13). Using 100 ng of the respective plasmid DNA, the number of CFU increased with expected decreased translation initiation rates (ATG > TTG). Furthermore, the heterogeneity of the colonies decreased accordingly. Whereas with ATG-Cas9 73 ± 12 small-sized colonies were obtained, for TTG-Cas9 only normal sized colonies were detected. With pEKEx3-(recT)-Phil-2xSTOPcas9 small amounts of both sizes of transformants were obtained, possibly due to the absence of an intact replicon.

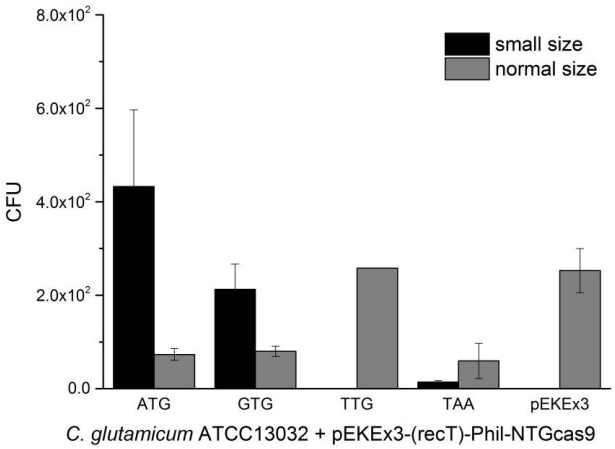

Start codon	Normal size CFU	Small size CFU
ATG	73 ± 12	432 ± 164
GTG	80 ± 11	106 ± 27
TTG	258*	0
TAA(ATG-TAA-TAG)	59 ± 38	14 ± 3
pEKEx3	253 ± 47	0

* For TTG only two values could be obtained

Fig. 13: Influence of start codon exchange of *cas9* in pEKEx3-(recT)-Phil-NTGcas9 on transformation efficiency. *C. glutamicum* WT was transformed with 100 ng DNA of the respective plasmid DNA. 100 µl of transformation suspension were spread on BHIS agar plates supplemented with spectinomycin. As a negative control, the empty expression plasmid pEKEx3 was used. Number of normal sized colonies is shown in grey bars, number of small sized colonies shown in black bars.

Effect of *cas9* start codon exchange on CRISPR-Cas9 targeting

Exchanging the start codon of *cas9* from ATG to TTG under control of the TetR expression system has most likely led to reduced expression levels of *cas9*, which resulted in higher numbers of living cells after electroporation. In the following experiment, it was analyzed if a functional CRISPR-Cas9 nucleoprotein complex can still be formed when TTG-*cas9* is expressed. Since CRISPR-Cas9 targeting could be successfully established targeting the WT sequence of *murE*, the already constructed plasmid pBHK18-sgRNA:murE was used to test for TTG-Cas9 functionality. As control, an sgRNA with a protospacer sequence complementary to *fapR* from *E. coli*, which is not complementary to any genomic region in *C. glutamicum*, was constructed (sgRNA:ctrl). Furthermore, to analyze potential effects of the plasmid backbone on targeting efficiencies, two standard expression plasmids harboring the sgRNA sequences were compared, the high-copy plasmid pJC1 and the low-copy plasmid pBHK18 (Table 5).

Because of previously observed high transformation rates (further analyzed in 3.5.2), *C. glutamicum* strain DM1728kanR(+1) was used as test strain. Since no spontaneous repair of the defective kanamycin resistance gene could be observed in earlier experiments (Fig. 4) and due to lack of other suitable antibiotic resistances, colonies were selected after electroporation based on kanamycin resistance to ensure uptake of the sgRNA plasmids encoding the kanamycin resistance gene.

The *cas9* variants with the three different start codons ATG, GTG or TTG all led to a functional Cas9 nucleoprotein complex by using the corresponding sgRNA:murE. The complex enabled

CRISPR-Cas9 targeting of all cells, with the exception of a few 'escaper cells'. With the construct 2xSTOP-Cas9 no functional CRISPR-Cas9 targeting could be observed, which is why it was not further analyzed. Interestingly, the choice of the plasmid backbone providing the sgRNA did not influence targeting efficiency, but led to different numbers of CFU when transformed with the control. With pBHK18-sgRNA:ctrl approximately 3000 CFU were obtained compared to 600 CFU generated with pJC1-sgRNA:murE. This was most likely due to different sizes of both plasmids (pJC1= 6108 bp and pBHK18 = 3337 bp) and consequentially their different transformation effiency.

Concluding from the observed reduced toxicity of TTG-Cas9 as well as the remaining ability to enable CRISPR-Cas9 targeting, the plasmid pEKEx3-(recT)-Phil-TTGcas9 could be used as a valuable tool during method development of CRISPR-Cas9 recombineering.

Tab. 5: CRISPR-Cas9 targeting using *cas9* with different start codons ATG, GTG and TTG.
C. glutamicum strains DM1728kanR(+1)/pEKEx3-(recT)-Phil-NTGcas9 were electroporated with 100 ng of sgRNA plasmid DNA to enable CRISPR-Cas9 targeting. 100 µl cell suspensions and the resuspended cell pellet were spread on BHIS agar plates supplemented with spectinomycin and kanamycin. n.t = not tested.

Plasmid	Transformation with plasmid DNA	CFU 100µl	Total CFU per 10^{10}cells
pEKEx3-(recT)-Phil-ATGcas9	pBHK18-sgRNA:murE	0	8
pEKEx3-(recT)-Phil-ATGcas9	pBHK18-sgRNA:ctrl	> 3000	> 100,000
pEKEx3-(recT)-Phil-ATGcas9	pJC1-sgRNA:murE	0	30
pEKEx3-(recT)-Phil-ATGcas9	pJC1-sgRNA:ctrl	606	Approx. 6000
pEKEx3-(recT)-Phil-GTGcas9	pBHK18-sgRNA:murE	0	2
pEKEx3-(recT)-Phil-GTGcas9	pBHK18-sgRNA:ctrl	> 3000	Bacterial layer
pEKEx3-(recT)-Phil-GTGcas9	pJC1-sgRNA:murE	0	20
pEKEx3-(recT)-Phil-GTGcas9	pJC1-sgRNA:ctrl	667	Approx. 6000
pEKEx3-(recT)-Phil-TTGcas9	pBHK18-sgRNA:murE	0	n.t.
pEKEx3-(recT)-Phil-TTGcas9	pBHK18-sgRNA:ctrl	> 6000	n.t
pEKEx3-(recT)-Phil-TTGcas9	pJC1-sgRNA:murE	3	n.t
pEKEx3-(recT)-Phil-TTGcas9	pJC1-sgRNA:ctrl	> 3000	n.t

3.2.3 Influence of Cas9 on dsDNA recombineering

As described in 3.2.1, a functional CRISPR-Cas9 nucleoprotein complex could be generated with both plasmids pEKEx3-cas9 and pCL2-recET-cas9 leading to efficient targeting and killing of cells. Because pCL2-recET-cas9 is currently the only construct where the editing and targeting function are combined on one plasmid, prior to a possible application this plasmid had to be further characterized.

A standard dsDNA recombineering experiment was performed with strain *C. glutamicum* DM1728kanR(+1)/pCL2-recET-cas9 (as described in 3.1.1), repairing the mutation in the *aph(3´)-IIa* gene with a 600 bp dsDNA fragment leading to kanamycin resistance. As a control, the original recombineering plasmid pCL2-recET without *cas9* was used (Figure 14). In addition

to the number of recombinant CFU, the total number of cells (recombinant and non-recombinant CFU) was determined to judge the relative recombineering efficiency.

The presence of *cas9* on pCL2-recET-cas9 (Fig. 14, bar 1) compared to the original plasmid pCL2-recET without *cas9* (bar 5) led to reduced numbers of recombinant kanamycin-resistant CFU. These numbers most likely result from basal *cas9* expression when gene expression was controlled by the *tac* promoter. When IPTG was added, *cas9* expression was strongly induced, which further decreased the number of recombinant kanamycin-resistant CFU (bar 3). To investigate the relative recombineering efficiencies, the ratio of recombinant cells (spectinomycin-resistant and kanamycin-resistant)/total number of cells (spectinomycin-resistant) after recombineering was analyzed. The decreased number of recombinant cells due to functional Cas9 correlates with the reduced number of total living cells (grey bars) after electroporation. These results indicate that recombineering efficiencies are not negatively influenced by *cas9* expression, but the total number of living cells is highly reduced, leading to fewer recombinant clones.

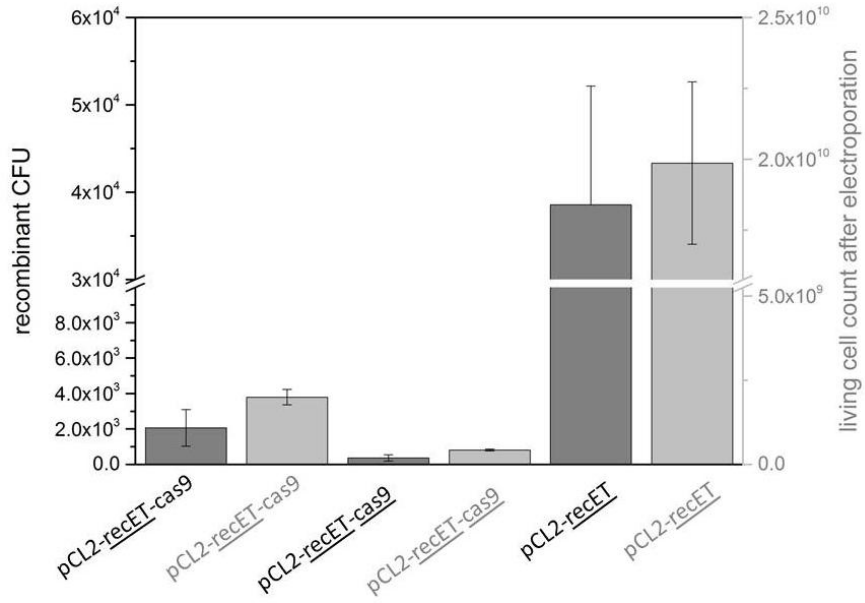

Fig. 14: dsDNA recombineering with *C. glutamicum* strains DM1728kanR(+1)/pCL2-recET-cas9 and DM1728kanR(+1)/pCL2-recET as negative control and a 600 bp dsDNA fragment. Recombinant spectinomycin-resistant and kanamycin-resistant cells shown in dark grey bars, total living cell count (spectinomycin-resistant cells) shown in light grey bars. For underlined genes the expression was induced during preparation of electrocompetent cells with ATc (250 ng for *recET*) or IPTG (0.5 mM for *cas9*).

3.3 Temperature-sensitive origins of replication

After genome editing using methods such as DNA recombineering or CRISPR-Cas9, the generated strains still harbor the necessary plasmids encoding the editing functions. However, these plasmids are no longer needed or might even prohibit additional metabolic engineering efforts to further modify the microbial strains. To generate favored plasmid-free strains, two research groups have developed plasmids for *C. glutamicum* with temperature-sensitive replicons that allow plasmid loss at higher cultivation temperatures (Nakamura *et al.*, 2006; Okibe *et al.*, 2011).

In order to test, whether the modification towards a temperature-sensitive origin of replication can be applied to plasmid pCL2-recET-cas9, the empty expression plasmid pCLTON2 (pCL2) harboring the pBL1 replicon and a spectinomycin resistance cassette was mutated via QuikChange PCR in the Rep protein coding region at position C5769A generating the plasmid pCL2-OriTS, harboring a temperature-sensitive origin of replication. Cultivations were performed without the supplementation of spectinomycin at 25 °C and 34 °C. After 5, 10 and 15 generations, cell suspensions were spread on BHIS plates with and without spectinomycin. When cultivated at 34 °C, a plasmid loss of 99.9 % could be observed after 15 generations (Figure 15). The number of generations needed to achieve a complete plasmid loss most likely resulted from the fact that pBL1 is present in several copies, which are estimated to be 8-30 (Pátek *et al.*, 1989; Trautwetter and Blanco, 1991). However, cultivations at 25 °C without antibiotics also led to plasmid loss of 74 %, emphasizing the necessity of supplementing antibiotics for plasmid stability.

Concluding from these results, the modified expression plasmid pCL2-OriTS can be used as a functional tool in genome editing, because after generation of genome-edited strains, the plasmid can be cured by cultivation at higher temperatures.

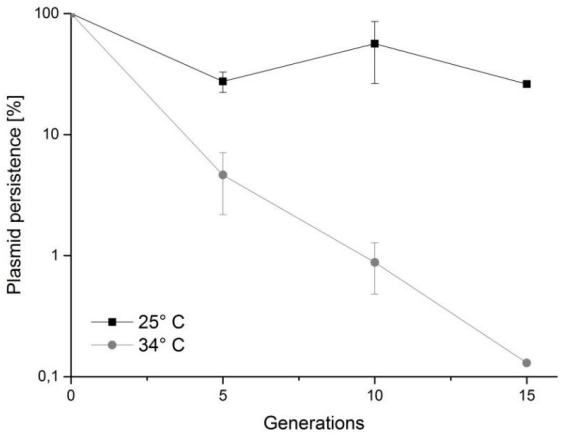

Fig. 15: Analysis of plasmid stability of expression plasmid pCL2-OriTS at 25 °C (black graph) and 34 °C (grey graph). Plasmid persistence is shown in percent after 5, 10 and 15 generations.

3.4. Finding the best-suited test system for establishing the combination of CRISPR-Cas9 and DNA recombineering

Prior to the application of new genetic editing methods, the initial characterization is preferably performed with a simple test system. In most cases either an antibiotic resistance is generated or abolished to select for edited cells (Huang *et al.*, 2015; Li *et al.*, 2015) or edited cells are indirectly detected by visual differentiation e.g. via GFP or RFP (Bikard *et al.*, 2013; Qi *et al.*, 2013). In this work, the aim was to enable the use of dsDNA recombineering in *C. glutamicum* and additionally allow selection for correct editing by targeting non-edited cells with the CRISPR-Cas9 nucleoprotein complex. In the course of experiments, several different test systems were evaluated to be subsequently used during method development. Most of the obtained results would only be confusing, when incorporated in the section describing all methods used in this work. Therefore the different approaches to assay for the best test system possible are described in this section.

3.4.1 Selection for kanamycin resistance

Binder *et al.* used strain DM1728kanR(+1) to establish ssDNA recombineering in *C. glutamicum* (Binder *et al.*, 2013). Therefore, the same principle of repairing the kanamyin resistance gene was used to assay for success of dsDNA recombineering. To assay whether restoring the kanamycin resistance cassette in the newly constructed *C. glutamicum* deletion strain DM1728kanR(-131) can be utilized for CRISPR-Cas9 recombineering, the two *C. glutamicum* strains DM1728kanR(+1) and DM1728kanR(-131) were targeted by CRISPR-Cas9. If successful, this would result in the killing of one genotype and the survival of the other. With a functional CRISPR-Cas9 targeting, the kanamycin deficiency could be first restored by DNA recombineering following by targeting of non-edited cells by CRISPR-Cas9. To test for efficient CRISPR-Cas9 targeting, *C. glutamicum* strains DM1728kanR(+1)/pCL2-recET-cas9(Pnat) and DM1728kanR(-131)/pCL2-recET-cas9 (Pnat) were transformed with an sgRNA (sgRNA:kan(-131)) targeting DM1728kanR(-131). The constructed sgRNA:kan(-131) placed on plasmid pBHC18 contains a protospacer sequence that is 100 % identical to the 5'-3' genomic sequence of strain DM1728kanR(-131), allowing for complete base-pairing of sgRNA with the 3'-5'-strand of the target DNA (Fig. 16). Because strain DM1728kanR(+1) does not contain the deletion of 131 nt in the kanamycin resistance gene, the genomic sequence at this position is different (Fig. 16, green letters). Since base-pairing between target DNA and sgRNA can therefore only be established for the first 8 nucleotides (Fig. 16, black letters), a functional CRISPR-Cas9 nucleoprotein complex should not be enabled.

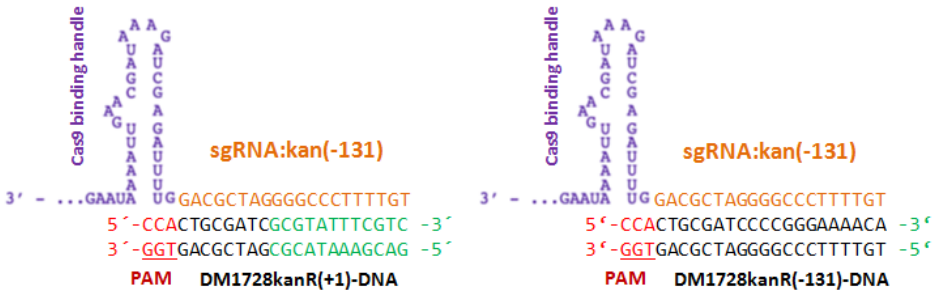

Fig. 16: CRISPR-Cas9 targeting with sgRNA:kan(-131) in *C. glutamicum* strains DM1728kanR(+1) and DM1728 kanR(-131). Red: PAM sequence TGG on NT strand, black: genomic sequence complementary to protospacer sequence, green: genomic sequence non-complementary to protospacer sequence. Left: The genomic sequence of strain DM1728kanR(+1) only allows base-pairing of the first eight nucleotides of the protospacer (black letters), which should not enable a functional nucleoprotein complex. Right: In strain DM1728kanR(-131) CRISPR-Cas9 is functional, because all nt of the protospacer are homologous to the genetic sequence.

However, both strains were targeted by the sgRNA:kan(-131) (Table 6). Whereas a typical protospacer sequence contains 20 nt for efficient targeting (Jinek *et al.*, 2012), it has been reported that only mutations in the 12 nucleotides immediately upstream of the PAM abrogated CRISPR-Cas9 targeting (Jiang *et al.*, 2013). However, the results in Table 6 indicate that a protospacer sequence of 8 homologous nucleotides seems to suffice for functional CRISPR-Cas9 targeting. Therefore, the use of the Kan^R deletion strains for CRISPR-Cas9 testing was limited, since non-edited cells (DM1728kanR(-131)) contained a sufficient identical amount of protospacer sequence elements as edited cells (DM1728kanR) thus turning the design of specific sequences targeting the non-edited cells into a challenge.

Tab. 6: Analysis of CRISPR-Cas9 targeting in *C. glutamicum* strains DM1728kanR(-131) and DM1728kanR(+1) strains by transformation with pBHC18-sgRNA:kan(-131) and pBHK18-sgRNA:ctrl. 100 µl of the suspension was spread on BHIS plates supplemented with spectinomycin (100 µg/ml) and chloramphenicol (7.5 µg/ml).

Strain	sgRNA	CFU per 100 µl
DM1728kanR(-131)/ pCL2-recET-cas9(Pnat)	pBHC18-sgRNA:kan(-131)	0
DM1728kanR(-131)/ pCL2-recET-cas9(Pnat)	pBHC18-sgRNA:ctrl	17 ± 9
DM1728kanR(+1)/ pCL2-recET-cas9(Pnat)	pBHC18-sgRNA:kan(-131)	1 ± 2
DM1728kanR(+1)/ pCL2-recET-cas9(Pnat)	pBHC18-sgRNA:ctrl	418 ± 139

3.4.2 Selection by restriction analysis

With the help of a genetically encoded biosensor Binder *et al.* were able to identify L-lysine producing strains harboring amongst others mutations in the *murE* gene encoding UDP-N-acetyl-muramoyl-L-alanyl-D-glutamate 2,6-diaminopimelate ligase (Binder *et al.,* 2013). Due to the nucleotide exchanges in *murE*, mutants do not harbor the PAM motif (TGG) at position 81 present in *C. glutamicum* WT. Therefore, *C. glutamicum* strains WT, ATCC13032 MurE-G81E and

ATCC13032 MurE-G81K were used in initial CRISPR-Cas9 experiments testing the functionality of the nucleoprotein complex. Furthermore, recombineering could be performed using *murE* as target, because recombineering with the oligonucleotide murE-G81E-fw (5'-AACAACGATGACTGGGCGGGTCTCTCCTGCTTCGTTGAGCACCTCAAGTTCAGCGGCGTCAGTCAAAAT GGCCACAGCTTTCGCAGCGTTATCCGTACCT-3') not only results in a G81E exchange, but also introduces one additional SNP, leading to an abolished *Pvu*II restriction site. Thus, recombinant strains can be identified via diagnostic digests of PCR products. However, since colonies of recombinant cells cannot be detected immediately by phenotype, using this method becomes laborious and unsuitable for the in-depth analysis of new genome editing methods.

3.4.3 Selection for streptomycin resistance

For *C. glutamicum* ATCC13032 the point mutation A128G in *rpsL* was reported to serve as a potential positive selection marker (Kim *et al.*, 2011). *rpsL* encodes the ribosomal protein S12 and the mutation confers streptomycin resistance to bacteria. Krylov *et al*. used this system to obtain oligonucleotide-dependent recombination in *C. glutamicum* ATCC13032 without the use of exogenous recombinases at a frequency of 6.7 $\times 10^{3}$ per assay (Krylov *et al.*, 2014). This system harbors the attractive advantage that Kan, Tet and Cm resistances are still available for the combination with different plasmids.

To test the applicability of this system for *C. glutamicum* ATCC13032, first the minimal inhibitory concentration (MIC) for streptomycin was determined to be 25 µg/ml for both *C. glutamicum* and *C. glutamicum*/pCL2-recET when spread on BHIS after electroporation and regeneration. Then, competent cells of strain *C. glutamicum*/pCL2-recET enabling ssDNA and dsDNA recombineering were prepared. Using the oligonucleotide rpsL_P6_fw (5'-AGCGTCGTGGCGTATGCACCCGTGTGTACACCACCACCCCGCGCAAGCCTAACTCTGCTCTTCGTAAGG TCGCTCGTGTGCGCCTTACCTCCGGCATCGA-3') a recombineering assay was performed. The oligonucleotide carries the A128G mutation (nucleotide underlined) causing the K43R exchange in the amino acid sequence of RpsL. After transformation, cells were spread on BHIS containing 25 µg/ml streptomycin. In several independent assays only 50-70 streptomycin-resistant CFU were obtained, which were also obtained with the control oligonucleotide harboring the WT sequence (rpsL_wt). Since recombineering to establish streptomycin resistance via the RpsL mutation was non-functional, this assay did not seem suitable for testing gene editing methods in our *C. glutamicum* strain ATCC13032. The different behavior of different wildtype strains of ATCC13032 was also experienced in the present work by determining the transformation efficiencies of strains. For example, with the wild type of Evonik, DM1132, an approximately fivefold higher transformation efficiency was obtained with the same plasmid than with our in-house *C. glutamicum* wild type (data not shown).

3.4.4 Selection for fluoroorotic acid resistance

Selections based on the resistance to the compound 5-fluoroorotic acid (FOA) have been used for many years, primarily in yeasts (Boeke *et al.*, 1984). FOA itself is non-toxic, but is converted to the toxic 5-fluoro-UMP by two genes encoding for an orotate phosphoribosyltransferase (*pyrE*) and orotidine 5-phosphate decarboxylase (*pyrF*). Inactivation of *pyrE*, *pyrF,* or both enable the cells to grow on rich medium supplemented with FOA, whereas wild-type cells will not grow. Thus, cells with inactive PyrE or PyrF require uracil, which is present in rich media.

Only recently, this selection system was successfully used in a variety of bacteria and archaea. In *Clostridium thermocellum* FOA-resistance was used to delete *pyrF* and to counterselect in the *pyrF* deleted strain for plasmid loss (Tripathi *et al.*, 2010). Similar approaches were successfully performed with *Thermococcus barophilus* (Thiel *et al.*, 2014), *Caldicellulosiruptor hydrothermalis* (Groom *et al.*, 2014), *Haloferax mediterranei* (Liu *et al.*, 2011), or *Staphylococcus aureus* (Redder and Linder, 2012). Since a number of mutations will inactivate *pyrE* and *pyrF*, an assay based on FOA-resistance would easily enable the testing of a variety of parameters, like deletions, insertions, length of homology arms and ssDNA or dsDNA as substrates.

To test the suitability of this system for *C. glutamicum*, first a *pyrF* deletion mutant was generated (*C. glutamicum* ΔpyrF). For both the deletion mutant and the wild type a loop of cells was spread on BHIS plates supplemented with 0.2 g/L FOA or 1.0 g/L FOA (similar plates also with 0.1 g/L uracil). Whereas *C. glutamicum* WT was not able to grow on both FOA-containing plates, the *pyrF* deletion mutant grew at both FOA concentrations. Supplementation of uracil (0.1 g/L) only marginally improved growth. However, a number of spontaneous FOA-resistant clones could be detected, when a large inoculum of *C. glutamicum* wild type was spread on the agar plate.

Next ssDNA recombineering was performed with the *C. glutamicum* WT carrying either pEKEx3-recT, pVWEx2-recT or pCL2-recET and the editing oligonucleotide pyrF-fw*PHO with a phosphorylated (PHO) 5'-end: 5'-PHO-TCAAGGCTTAAGCCCTATGACATTCGGCGAGAAGCTT CTGAACGCCGCCTACCCGTGGCAGGCTATGCGTGGGCATTGATCCCCACGAAAGCCTGCTGAC-3',
which introduces the deletion of two cysteine codons at position 34 and 35 of PyrF. Unexpectedly, in all cases approximately 300 CFU were growing on BHIS supplemented with FOA when 100 µl of the suspension was spread. Furthermore, this number was also observed for the control, in which *C. glutamicum* WT was transformed with water instead of an oligonucleotide as DNA substrate.

These results rendered FOA resistance unsuitable as test system for editing/targeting in *C. glutamicum*. The easy appearance of FOA-resistant cells is most likely due to spontaneous

mutations, since a number of mutations both in *pyrE* or *pyrF* would result in inactive enzymes. Furthermore, it is known that FOA can be incorporated into nucleic acid to act as an anticancer drug (Riviere *et al.*, 2011). This would cause an increase of the spontaneous mutation rate. In the experiments performed in this work, approx. 1.5×10^4 FOA-resistant cells per assay containing 3.7×10^9 viable cells were obtained, from which a mutant frequency of 4.05×10^{-6} can be derived.

3.4.5 Visual differentiation: Carotenoids

Opposed to selection, optical differentiation enables the direct analysis of edited cells and total cell count in one single assay. This test system is advantageous, since Cas9 negatively influences cell viability (Bikard *et al.*, 2013; Jiang *et al.*, 2015) and the total cell count is necessary for the determination of editing/targeting frequencies.

However, the system also harbors disadvantages, the large number of plates to analyze being difficult to handle. Furthermore, a strong coloration must be ensured to detect differences between edited/non-edited colonies. Another disadvantage is the existence of sister chromatides. A detailed study by Sawitzke *et al.* with *E. coli* observed segregation within one clone occurring on petri dishes (Sawitzke *et al.*, 2011). This is due to the fact that up to 4 or 8 copies of the chromosome are present requiring proper allele segregation. When one edited allele is present, selection allows the formation of one resistant colony, whereas in case of color differentiation the single edited allele might be outcompeted by the others, which results in a phenotype that cannot be differentiated from the wild type.

Due to their natural carotenoid synthesis, *C. glutamicum* colonies exhibit a yellowish color, whereas mutant colonies of *C. glutamicum* and *C. glutamicum* ssp. *flavum* devoid of carotenoids are uncolored (Krubasik *et al.*, 2001). Dr. S. Matamouros used dCas9 together with the sgRNA::catB to downregulate carotenoid synthesis (unpublished results). *C. glutamicum* strains SM28 and SM29 of Dr. S. Matamouros containing dCas9 were transformed with either sgRNA:catB or as control sgRNA:random and their color difference on BHIS in different mixtures and dilutions was inspected. Only during cultivation, not at the stage of colonies on plates, a slight difference in coloration could be observed. Therefore, a reduced or absent carotenoid synthesis was considered unsuitable to recognize edited cells of *C. glutamicum* among large numbers of unedited cells.

3.4.6 Visual differentiation: Crimson

According to Dr. S. Binder the E2-crimson gene integrated into the chromosome of *C. glutamicum* can be expected to result in red colored colonies. Therefore, together with scientists from the SenseUP GmbH (Forschungszentrum Jülich, Jülich, Germany), the plasmid

pK18mobsacB_lysOP7_T7crim(+) was designed and constructed. The plasmid encodes the T7 RNA polymerase gene under control of the *trc* promoter, the T7 promoter region, the red-fluorescence-protein E2-crimson and sequences to enable integration at the intergenic region of cg1121 and cg1122 of the *C. glutamicum* chromosome. A wild-type derivative containing these sequences was constructed but no coloring was visible. As a control *C. glutamicum* WT/pAN6-crimson obtained from Dr. G. Schaumann was used, which again showed no color. However, on IPTG-containing plates *C. glutamicum* WT/pAN6-crimson colonies exhibited slightly bluish coloring. Based on these findings, using this fluorescence protein was considered insufficient to serve as a basis for a reliable assay system.

3.4.7 Visual differentiation: β-Galactosidase activity

A promising alternative test system based on optical differentiation is the β-galactosidase assay, because LacZ activity can easily be recognized on petri dishes as used in assays for *E. coli* (Koenen *et al.*, 1982). Therefore *C. glutamicum* strain ATCC13032::PH36lacZ was constructed, that contains a genomically integrated *lacZ* gene in the intergenic region of cg1121 and cg1122. For a strong, constitutive *lacZ* expression the promoter PH36 encompassing a sequence of 70 nt was used (Yim *et al.*, 2013).

When spread on BHIS containing X-Gal (5-Bromo-4-chloro-3-indoxyl- β-D-galactopyranoside) in a concentration of 40 µg/mL, colonies from *C. glutamicum* ATCC13032::PH36lacZ exhibited a clear green/blue color as opposed to the yellow colonies of *C. glutamicum* wild type (Figure 17).

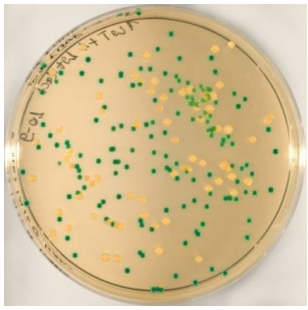

Fig. 17: Visual differentiation of a mixture of *C. glutamicum* ATCC13032 (yellow) and ATCC13032:: PH36lacZ (green) cells on BHIS plates supplemented with 40 µg/ mL X-Gal.

For CRISPR-Cas9 targeting, an additional variant of ATCC13032::PH36lacZ was generated by inserting an additional guanine-nucleotide at position 1526 of the *lacZ* gene resulting in strain ATCC13032::PH36lacZ(+1). This insertion not only inactivates the *lacZ* gene leading to a wild-type like phenotype, but also establishes a PAM motif for later CRISPR-Cas9 targeting. Due to observed differences in transformation efficiencies between some strains, both constructs were also integrated into *C. glutamicum* strains DM1132 and DM1728. Since a mixture of the two strains ATCC13032::PH36lacZ and ATCC13032::PH36lacZ(+1) plated on BHIS plates

supplemented with X-Gal showed similar results as observed for WT and ATCC13032::PH36lacZ, these strains will be used for the further work on CRISPR-Cas9 recombineering in *C. glutamicum*.

3.5 The way towards CRISPR-Cas9 recombineering

The CRISPR-Cas9 system proved to be a powerful method for genome editing in eukaryotes, which resulted in many success stories (Sander and Joung, 2014). However, whereas eukaryotes and few prokaryotes harbor endogenous repair systems like HDR or NHEJ (DiCarlo *et al.*, 2013; Jiang *et al.*, 2013; Tong *et al.*, 2015), most prokaryotes naturally do not possess mechanisms to repair introduced DSB. Therefore, CRISPR-Cas9 has been combined with DNA recombineering and used as a selection tool rather than a genome editing tool. The combination of both methods enables genome editing via DNA recombineering with the additional targeting of non-edited cells by CRISPR-Cas9 thus increasing the ratio of recombinant to non-recombinant cells (Jiang *et al.*, 2015; Oh and van Pijkeren, 2014). Even though DNA recombineering and CRISPR-Cas9 are successfully applied as genome editing tools individually, until now the combination of both was applied successfully only in a very limited number of prokaryotes (Jiang *et al.*, 2015; Li *et al.*, 2015; Oh and van Pijkeren, 2014; Pyne *et al.*, 2015).

Since the challenge to establish successful CRISPR-Cas9 recombineering in *C. glutamicum* is combining all components in a functional interplay, the experimental protocols of successfully developed CRISPR-Cas9 recombineering as shown for *L. reuteri* and *E. coli* were analyzed in more detail (Table 7). In both organisms the combined method was functional, when a strain harboring an expression plasmid for both *cas9* and the recombinase genes was transformed with sgRNA and the editing template. For *E. coli* a two-step procedure, introducing both the sgRNA and the editing template during the second electroporation, was identified as most suitable. In contrast to that, for *L. reuteri* more recombinant clones could be obtained with a three-step method, introducing the guide RNA in a separate second electroporation.

Tab. 7: Experimental protocol of CRISPR-Cas9 recombineering in *L. reuteri* and *E. coli*. Each step represents a transformation with the indicated plasmids (p) or templates (t).

Literature	(Oh and van Pijkeren, 2014)		(Jiang *et al.*, 2015)		(Li *et al.*, 2015)	(Pyne *et al.*, 2015)
Organism	***L. reuteri***	***L. reuteri***	***E. coli***	***E. coli***	***E. coli***	***E. coli***
Step 1	p1-Cas9-tracrRNA p2-RecT	p1- Cas9-tracrRNA p2-RecT	p1- Cas9-RecET	p1-Cas9-RecET	p1-Cas9-λRed	p1-Cas9 p2- λRed
Step 2	p3- crRNA t1- ssDNA	t1- ssDNA	p2-sgRNA-dsDNA	p2-sgRNA t1-dsDNA	p2-sgRNA t1-ssDNA	p3- crRNA t1-dsDNA
Step 3		p3- crRNA				

To assay for the applicability of one of these approaches in *C. glutamicum*, various combinations of the individual components were used to test for DNA recombineering and CRISPR-Cas9 selection in *C. glutamicum.* This included the transformation of dsDNA and sgRNA templates in one electorporation as shown for *E. coli* (Jiang *et al.*, 2015; Li *et al.*, 2015; Oh and van Pijkeren, 2014; Pyne *et al.*, 2015), as well as in two separate electroporations as reported for *L. reuteri* (Oh and van Pijkeren, 2014). Furthermore, the dsDNA template was initially placed on the Cas9-recET expression plasmid in order to allow only one electroporation with the targeting RNA. However, with all different approaches no recombinants could be obtained. Therefore, further studies were performed investigating various expression plasmids, different *C. glutamicum* strains and also different test systems in more detail (as described in 3.4).

3.5.1 Suitable strains for CRISPR-Cas9 recombineering

Since the establishment of CRISPR-Cas9 recombineering is dependent on a variety of factors, many different parameters have to be balanced to ensure successful genome editing. As described in 3.2.2 size and copy number of the plasmid can influence transformation efficiencies. To investigate if the strain background also shows an effect and if CRISPR-Cas9 targeting can be performed with similar efficiencies in different strains, four different *C. glutamicum* strains harboring pEKEX3-(recT)-Phil-TTGcas9 were transformed with sgRNA targeting *murE* and a control sgRNA (Table 8). Whereas *C. glutamicum* strain DM1728kanR(+1) enabled highly efficient CRISPR-Cas9 targeting with plasmid pEKEx3-(recT)-Phil-TTGcas9, in DM1728 and its ancestor strain DM1132 (WT of Evonik) very weak CRISPR-Cas9 activity could be detected. *C. glutamicum* WT/pEKEx3-(recT)-Phil-TTGcas9 exhibited the worst ratios of 'escaper' cells /cells transformed with control sgRNA.

Tab. 8: CRISPR-Cas9 targeting with various *C. glutamicum* strains. Strains expressing pEKEX3-(recT)-Phil-TTGcas9 were transformed with 100 ng pBHK18-sgRNA:murE/ctrl and spread on BHIS plates supplemented with spectinomycin and kanamycin.

Strain	Targeting RNA	CFU (200 µl)
DM1728kanR(+1)	pBHK18-sgRNA:murE	0
DM1728kanR(+1)	pBHK18-sgRNA:ctrl	6000
DM1728	pBHK18-sgRNA:murE	350
DM1728	pBHK18-sgRNA:ctrl	1760
DM1132	pBHK18-sgRNA:murE	89
DM1132	pBHK18-sgRNA:ctrl	656
ATCC13032	pBHK18-sgRNA:murE	17
ATCC13032	pBHK18-sgRNA:ctrl	55

Due to these results and further direct comparisons of transformation efficiencies (data not shown), strain DM1132, the wild-type *C. glutamicum* strain of Evonik, was further used for working on CRISPR-Cas9 recombineering in *C. glutamicum.*

3.5.2 CRISPR-Cas9 targeting with *C. glutamicum* strains DM1132::PH36lacZ and DM1132::PH36lacZ(+1)

As described, the β-galactosidase assay was determined to be the most suitable assay system for the establishment of CRISPR-Cas9 recombineering. After confirmation that visual differentiation between both *C. glutamicum* strains DM1132::PH36lacZ and DM1132::PH36lacZ(+1) was possible (see paragraph 3.4.7), strains were targeted by CRISPR-Cas9 and appropriate sgRNAs. Two sgRNAs were designed, sgRNA:lacZ(+1) and sgRNA:lacZ.

In strain DM1132::PH36lacZ(+1) a new PAM motif was generated through the additional nucleotide in the *lacZ* gene, which was not present in strain DM1132::PH36lacZ. This PAM motif allows for successful targeting with sgRNA:lacZ(+1) in strain DM1132::PH36lacZ(+1), whereas strain DM1132::PH36lacZ is not affected. The other constructed sgRNA (sgRNA:lacZ) targets both strains, because the protospacer sequence chosen is homologous to the corresponding genomic sequence in both strains. The results of CRISPR-Cas9 targeting in strains with the integrated *lacZ* gene are shown in Table 9. In both strains, a functional CRISPR-Cas9 nucleoproetin complex could be established with the corresponding sgRNA. Transformation with the control sgRNA led to similar CFU numbers observed in other test systems, e.g. when *murE* G81 was targeted.

Tab. 9: Analysis of CRISPR-Cas9 targeting in *C. glutamicum* strains DM1132::PH36lacZ(+1)/pEKEX3-cas9 and DM1132::PH36lacZ/pCL2-recET-cas9. Strains were transformed with either pBHK18-sgRNA:lacZ, pBHK18-sgRNA:lacZ(+1) or pBHK18-sgRNA:ctrl. 10 µl, 50 µl and 200 µl cell suspensions were spread on BHIS plates supplemented with spectinomycin and kanamycin and the mean value of CFU per µg DNA was calculated (MV).

Strain	Plasmid with sgRNA	10 µl	50 µl	200 µl	MV CFU/µg DNA
DM1132::PH36lacZ(+1)/ pEKEx3-cas9	pBHK18-sgRNA:lacZ(+1)	0	2	1	1.1×10^3
DM1132::PH36lacZ(+1)/ pEKEx3-cas9	pBHK18-sgRNA:lacZ	0	1	1	0.65×10^3
DM1132::PH36lacZ(+1)/ pEKEx3-cas9	pBHK18-sgRNA:ctrl	160	644	approx. 4000	7.2×10^5
DM1132::PH36lacZ/ pCL2-recET-cas9	pBHK18-sgRNA:lacZ	0	1	0	0.65×10^3
DM1132::PH36lacZ/ pCL2-recET-cas9	pBHK18-sgRNA:lacZ(+1)	155	721	approx. 4000	7.2×10^5
DM1132::PH36lacZ/ pCL2-recET-cas9	pBHK18-sgRNA:ctrl	220	875	approx. 4000	9.87×10^5

3.5.3 Simulation of CRISPR-Cas9 recombineering

After the determination that *C. glutamicum* strains DM1132::PH36lacZ/pCL2-recET-cas9 and DM1132::PH36lacZ(+1)/pCL2-recET-cas9 could be separated by CRISPR-Cas9 with sgRNA:lacZ(+1), cells of both strains were mixed in different ratios to characterize the efficiency of the targeting system and to determine the enrichment factor that can be achieved.

Two individual precultures were cultivated overnight and the main culture was inoculated with the respective mixture (1:2, 1:10, 1:100, 1:1000, 1:10.000, 1:100.000) of both precultures to a starting OD_{600} of 0.5. Cultivation was performed until an OD_{600} of 1.75 was reached and competent cells were prepared (as described in 2.5.4). Cells were electroporated with 100 ng of sgRNA:lacZ(+1) and spread on BHIS agar plates supplemented with spectinomycin, kanamycin and X-Gal (Figure 18). To verify that the ratio of both genotypes to be analyzed was still present after harvesting the main culture, prepared competent cells were spread on BHIS plates supplemented with spectinomycin and X-Gal and the strain ratio DM1132::PH36lacZ/pCL2-recET-cas9 to DM1132::PH36lacZ(+1)/pCL2-recET-cas9 was exemplarily determined for 1:10, 1:100 and 1:1000 suspensions.

As a control, both *C. glutamicum* strains were individually transformed with the targeting sgRNA:lacZ(+1), verifying that strain DM1132::PH36lacZ(+1) was efficiently targeted, but the strain without the mutation was not affected. The resulting 47 'escaper' cells of DM1132::PH36lacZ(+1) evaded targeting possibly due to mutations in the protospacer. Thus, strain DM1132::PH36lacZ was not targeted by the sgRNA due to the absence of the PAM motif, which resulted in 62,230 CFU. In the 1:2 and 1:10 mixtures of DM1132::PH36lacZ/ DM1132::PH36lacZ(+1) yellow cells from genotype *lacZ*(+1) were efficiently targeted resulting in much more blue-green cells (30,294/99 for 1:2; 805/123 for 1:10) of genotype *lacZ* than yellow cells *(lacZ*(+1)*)*. Looking at higher ratios (1:1000-1:100,000) the number of detected cells of genotype *lacZ* decreased, most likely because the small number of cells present in the suspension limits the uptake of plasmid DNA to generate kanamycin-resistant cells. However, if a cell suspension mixture of 1:100,000 cells was transformed with sgRNA:lacZ, at best 7 blue colonies among 139 yellow colonies could be detected. If all experiments are combined, approximately one blue/green colony among 167 yellow colonies could be detected, illustrating that the vast majority of cells of strain DM1132::PH36lacZ(+1) had been successfully killed.

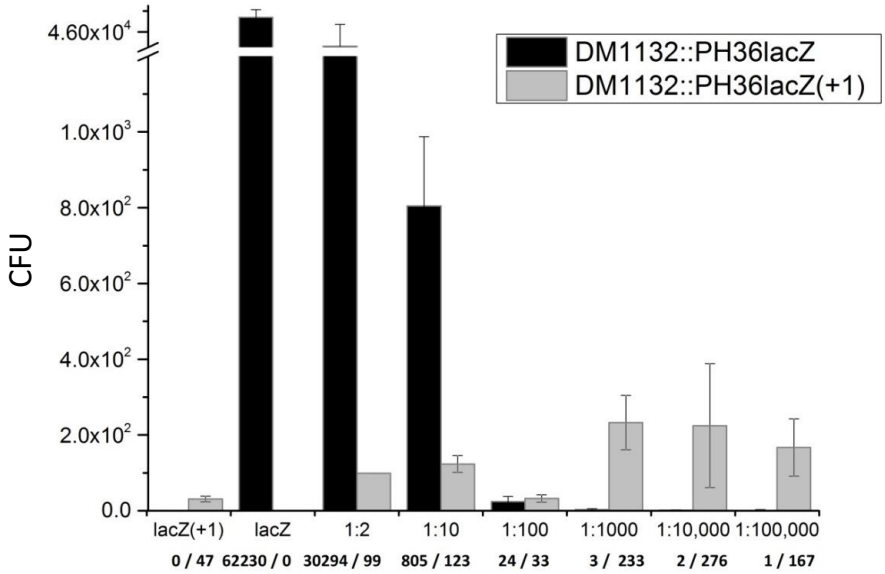

Fig. 18: CRISPR-Cas9 targeting with *C. glutamicum* strains DM1132::PH36lacZ/pCL2-recET-cas9 and DM1132::PH36lacZ(+1)/pCL2-recET-cas9 mixed in different ratios. Electroporation of the original strains (first two bars), as well as mixtures (with the ratios given below the respective bars) with 100 ng of pBHK18-sgRNA:lacZ(+1). Cells were spread on BHIS agar plates supplemented with spectinomycin, kanamycin and X-Gal. All cells of strain DM1132::PH36lacZ/pCL2-recET-cas9 show the blue-green phenotype, all cells of strain DM1132::PH36lacZ(+1)/pCL2-recET-cas9 show a yellow color.

This experiment was performed to simulate CRISPR-Cas9 targeting after recombineering. As determined, after dsDNA recombineering at best one out of 100,000 cells is recombinant. Since the simulation experiment shows that in the mixture of 1:100,000 CRISPR-Cas9 alters the ratio to 1:167, the application of dsDNA recombineering should in principle make it necessary to assay 167 clones to find the recombinant.

These results show that in principle CRISPR-Cas9 recombineering is possible and simplifies the screening procedure for recombinant clones, because fewer colonies (approximately 170 instead of 100,000) have to be tested to find one recombinant colony.

3.5.4 CRISPR-Cas9 recombineering in *C. glutamicum*

In this work two genome editing tools have been in principal established and characterized in *C. glutamicum* ATCC13032. For the integration of fragments of around 131 nt with dsDNA recombineering one cell out of 100,000 cells is recombinant. With CRISPR-Cas9, DNA sequences in *C. glutamicum* can be efficiently targeted and two genotypes can be separated. As described for *L. reuteri* and *E. coli*, the combination of both methods is functional and allows efficient genome editing (Jiang *et al.*, 2015; Oh and van Pijkeren, 2014). However the combination of all components in an effective system is rather complicated.

For the establishment of CRISPR-Cas9 recombineering in *C. glutamicum*, the two-step method was chosen with the β-galactosidase assay as test system. dsDNA recombineering of *C. glutamicum* strain DM1132::PH36lacZ(+1)/pCL2-recET-cas9 was performed with a 600 bp PCR fragment that repairs the frameshift in *lacZ*. After electroporation and 5 h regeneration, the suspension was used to inoculate a 50 ml preculture, which was grown overnight. The main culture was inoculated with the preculture and competent cells were prepared according to standard protocol. Electroporation was performed with 100 ng of plasmid DNA pBHK18-sgRNA:lacZ(+1) and cells were spread on BHIS plates supplemented with spectinomycin, kanamycin and X-Gal. However, after 3 days of incubation, a significantly higher number of CFU was detected than observed during the experiments described in 3.5.4. Due to the high amount of cells, no recombinant blue colony could be distinguished from wild-type cells, most likely because the X-Gal concentration was not sufficient to enable blue coloring at this high cell density.

Whereas for *E. coli* and *L. reuteri* the total number of cells after the procedure was 1.5 x 10^5 cells with recombinant numbers of 1.1x 10^5 and 1x10^3 respectively (Jiang *et al.*, 2015; Oh and van Pijkeren, 2014), the simulation experiments in 3.5.4 did not exhibit that high number of CFU after CRISPR-Cas9 targeting. Concluding from these results, the two-step method has to be optimized in order to achieve functional CRISPR-Cas9 recombineering with enrichment factors of up to 5000 in *C. glutamicum*.

3.6 Analysis of mutations leading to higher L-lysine production

Genome editing tools allow for improving microbial production strains by introducing favorable single nucleotide polymorphisms that ultimately lead to elevated production titers. Previously, by employing random chemical mutagenesis followed by a biosensor-based single cell screening approach for isolating L-lysine accumulating single-cells, the G81E substitution in UDP-N-acetylmuramoylalanyl-D-glutamate 2,6-diaminopimelate ligase (MurE) was identified in *C. glutamicum*. This amino acid substitution results in an increased accumulation of L-lysine (Binder *et al.*, 2012). The gene *murE* is essential in bacteria (Mengin-Lecreulx *et al.*, 1989), because MurE plays a key role in peptidoglycan synthesis by fusing *meso*-diaminopimelate to the dipeptide UDP-N-acetyl-α-D-muramoyl-L-alanyl-D-glutamate (UDP-MurNAc-L-Ala-D-Glu). The resulting tripeptide is further elongated by MurF until a pentapeptide is generated, which is finally incorporated into the growing peptidoglycan layer (Basavannacharya *et al.*, 2010). In addition to its pivotal role for peptidoglycan synthesis, *meso*-diaminopimelate also serves as

substrate for the diaminopimelate decarboxylase LysA, which catalyzes the final step in L-lysine synthesis (Yeh *et al.*, 1988).

The two mutations G81E and L121F in MurE were reported to increase L-lysine production titers (Binder *et al.*, 2012). Furthermore, with RecFACS, the combination of ssDNA recombineering and the biosensor-based FACS screening method, in a single approach mutants could be isolated that harbor one of 12 different amino acid substitutions in MurE G81 (Binder *et al.*, 2013).

By analyzing structure models of MurE from *M. tuberculosis* and *E. coli* a close proximity of G81 to the nucleoside binding site of UDP-MurNAc-L-Ala-D-Glu was detected (Basavannacharya *et al.*, 2010). In order to analyze the effect of MurE G81 mutations in more detail, 18 amino acid substitutions were introduced in the present work into *C. glutamicum* WT. The substitution of G81 by tyrosine could not be obtained. Strains were constructed by double homologous recombination using the non-replicative pK19mobsacB plasmid and cultivation was performed in the BioLector system. For each mutation, a minimum of two individually generated clones was analyzed regarding their L-lysine accumulation capabilities (Figure 19).

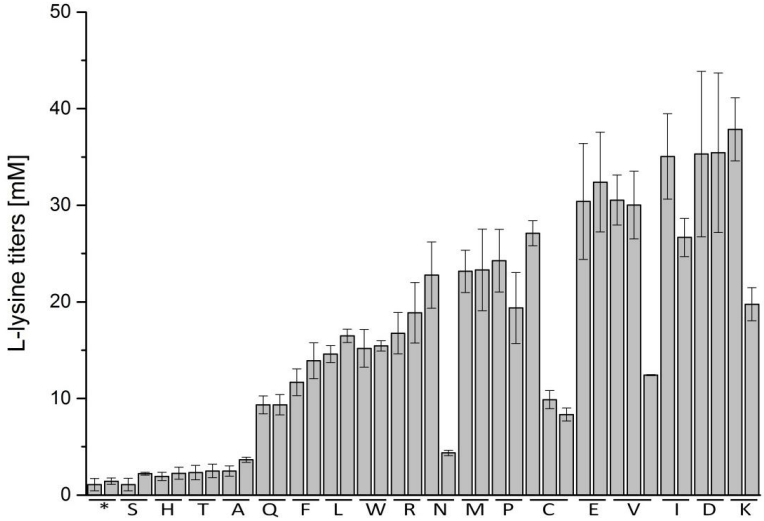

Fig. 19: Effect of amino acid substitution on L-lysine accumulation in *C. glutamicum* WT at position MurE G81. For each substitution (given as single letters, original amino acid glycine indicated with *) at least two individually derived clones were tested. Cultivation was performed in the BioLector system in CGXII medium with 4 % (w/v) glucose. Three independent cultivations were performed per clone.

The substitution of glycine to serine (S), histidine (H), threonine (T) or alanine (A) did not cause significant L-lysine accumulation. Substitution to glutamine (Q), phenylalanine (F), leucine (L), tryptophan (W) and arginine (R) increased L-lysine titers up to 19 mM. Interestingly, for all substitutions described above both clones with the same amino acid exchange accumulated comparable amounts of L-lysine. In contrast to that, mutants producing higher amounts of L-lysine exhibited partially larger clonal variabilities. Substituting glycine to asparagine (N) for

example, led to the accumulation of 23 mM and 4 mM L-lysine in two different clones. Similar effects could be observed for exchanges to cysteine (C), valine (V), isoleucine (I) or lysine (K). Highest coherent results in two clones could be obtained for G81E and G81D substitutions, most likely resulting in a stimulating effect due to negatively charged residues introduced in the UDP-N-acetylmuramoyl-tripeptide synthetase (Hochheim *et al.*, 2016). Amino acid substitutions resulting in large branched side chains or charged residues could affect the orientation of the helix, which might influence the UDP binding loop that plays a role in substrate binding.

Mutations in the UDP-N-acetylmuramoylalanyl-D-glutamate 2,6-diaminopimelate ligase led to increased levels of L-lysine production in *C. glutamicum* strains, which is most likely due to a reduced enzymatic activity of MurE and the resulting drain of *meso*-diaminopimelate towards L-lysine. This could affect the cell in two possible ways: the cell wall stability could be reduced, because less UDP-MurNAc-L-Ala-D-Glu-mDAP is formed by MurE or it could result in slower growth, because reduced MurE activity prolongs formation of the peptidoglycan layer. For clarification, a number of G81X mutant strains were analyzed for the minimal inhibitory concentration (MIC) of cell-wall targeting antibiotics in comparison to *C. glutamicum* WT. *C. glutamicum* strains ATCC13032 MurE-G81E, ATCC13032 MurE-G81K and ATCC13032 MurE-G81R as well as WT were spread on agar plates prior to application of an E-test stripe (Biomerieux, Nürtingen, Germany) containing a concentration gradient of benzylpenicillin, vancomycin or ethambutol. After 24 h incubation, the minimal inhibitory concentration was analyzed that determines the lowest antibiotic concentration in order to prevent visible bacterial growth (Table 10). No significant difference in MIC in response to cell wall targeting antibiotics could be observed between the *C. glutamicum* WT and the MurE variants, indicating that cell wall stability is not affected in the MurE variants. Furthermore, the obtained values corresponded to earlier reported MIC numbers for *C. glutamicum* (Möker *et al.*, 2004).

Tab. 10: Minimal inhibitory concentrations (MICs) of benzylpenicillin, vancomycin and ethambutol for growth of different *C. glutamicum* strains. Strains were cultivated in BHI medium to an OD_{600} = 1 and 1 ml of each cell suspension was spread on BHIS agar plates. E-test stripes with the respective antibiotic were applied and plates were incubated for 3 days at 25 °C.

		Minimal inhibitory concentration (µg /ml)		
Strain	**Antibiotic**	**Exp.1**	**Exp.2**	**Exp.3**
WT		0.5	0.25	0.38
G81E	Benzylpenicillin	0.5	0.25	0.38
G81K		0.5	0.25	0.38
G81R		0.5	0.25	0.38
WT		1.0, 2.0	0.38	0.38
G81E	Vancomycin	0.38	0.25-0.38	0.38
G81K		0.5	0.38	0.38
G81R		0.125, 1.5	0.38	0.125, 1.0
WT		2.0	1.5-1.7	2.0
G81E	Ethambutol	1.7-2.0	1.7-2.0	3.0
G81K		2.0	1.5-1.7	3.0
G81R		2.0	1.7-2.0	3.0

In the second test series, all mutant strains were cultivated in the BioLector system and growth rates were determined (Figure 20). The increase in L-lysine accumulation reduced the maximal specific growth rate, revealing a correlation between both parameters.

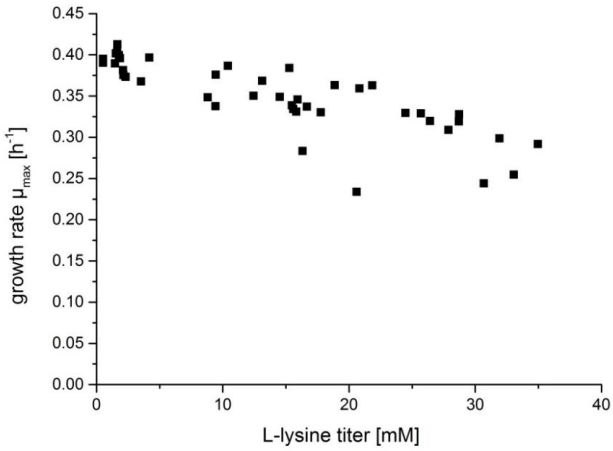

Fig. 20: Correlation of increased L-lysine production titers with reduced growth rates in *C. glutamicum* MurE G81 variants. Cultivation was performed in CGXII medium with 4 % (w/v) glucose.

The reduced growth rates as well as the unaltered response towards cell-wall targeting antibiotics support the hypothesis that reduced MurE-activity leads to a reduced peptidglycan formation rate, which in turn allows an increased flux of the intermediate *meso*-diaminopimelate towards L-lysine synthesis. However, when additional amino acid positions such as E484, R425 or the DPNR motif of MurE were targeted for site-saturation mutagenesis, the respective *C.*

glutamicum variants could not be obtained via RecFACS or with the pK19mobsacB method. Furthermore, the combination of the individually beneficial mutations G81E and L121F was not possible, most likely because both mutations combined abolish the activity of this essential enzyme. These findings support the fact that reduction of enzyme activity is limited and in order to further enhance production titers additional factors have to be considered, e.g. regarding L-lysine synthesis the slower growth rate could be repaired.

4 Discussion

4.1 dsDNA recombineering in *C. glutamicum*

For establishing a new genome editing technique such as dsDNA recombineering, many parameters have to be newly defined for each organism where this technique is supposed to be applied: the recombinases and their induction level, the DNA substrate and the size of its homology flanks.

For DNA recombineering various recombinases have been described, the most prominent being the λ Red system (Murphy, 1998) and the RecET system (Zhang *et al.*, 1998). Even though they possess the same function, they exhibit different activities in different organisms. Furthermore it appears not to be possible to uncouple the two enzyme activities encoded and to combine an exonuclease of one organism with the ssDNA annealing protein of another organism. For example, coupling RecE with Bet or RecT with Exo cannot catalyze a recombination reaction (Muyrers *et al.*, 2000), which is most likely due to the overlapping reading frame of *recE* and *recT* (Clark *et al.*, 1993). In *E. coli*, RecT showed a 40-fold reduced recombineering activity compared to Beta (Datta *et al.*, 2008), whereas in *C. glutamicum* Beta showed almost no activity (Binder *et al.*, 2013). In *Pantoea ananatis,* a bacterium recently introduced by Takumi and Nonaka for the production of L-glutamate and other amino acids (Takumi and Nonaka, 2016), λ Red genes or their gene products proved to be highly cytotoxic for the organism (Katashkina *et al.*, 2009). In some organisms like *Mycobacterium spec.* DNA recombineering can be performed with endogenous genes (*gp60* and *gp61)* (van Kessel and Hatfull, 2007), whereas in *C. glutamicum* enzymes from closely related species did not increase efficiencies. With Gp60 from the mycobacteriophage Che9c 40-fold reduced ssDNA recombineering levels were reported compared to RecT (Binder *et al.*, 2013). Furthermore, the RecT homologue RecTCau encoded by orf-1962 from the even closer related species *C. aurimucosum* showed higher ssDNA recombineering efficiencies than with Gp60, but these obtained DNA recombineering levels could be fourfold increased when RecT from *E. coli* was used (Binder *et al.*, 2013). Based on

these results, for dsDNA recombineering in *C. glutamicum* the exonuclease/recombinase pairs RecET from the Rac prophage and RecETCau from *C. aurimucosum* were tested, showing 2000-fold better recombineering efficiencies for RecET than for RecETCau. Even though BLAST alignments show that recombinases tend to be conserved and exonucleases seem to be more species-specific (Datta *et al.*, 2008; Zhang *et al.*, 1998), for each organism a variety of genes has to be experimentally tested to ensure high recombineering efficiencies.

Furthermore, the DNA substrate also influences recombineering efficiencies. Whereas homologous sequences of 50 bp are sufficient for dsDNA RecET recombineering in *E. coli* (Muyrers *et al.*, 2000), *Pseudomonas syringae* requires sequences of 80-100 bp (Swingle *et al.*, 2010). In case of *Mycobacterium spec.*, homology regions as large as 700 bp are necessary (van Kessel and Hatfull, 2007). Thus, the minimal length of the homology regions to ensure successful DNA recombineering varies strongly between the organisms. This was also observed for RecTE recombineering in *P. syringae* where a 250-fold increase was obtained when flanks were extended from 100 bp to 500 bp (Swingle *et al.*, 2010). It was also reported that the homology on either side of the substrate is indispensable since PCR products with only one homology arm failed to work (van Kessel and Hatfull, 2007; Zhang *et al.*, 1998).

For *C. glutamicum* it was not possible to integrate genes with a complete functional sequence via dsDNA recombineering at a specific location. Though in some experiments with the full-length *aph(3´)-IIa* gene kanamycin-resistant clones were obtained, their analysis revealed unspecific genomic integration. This apparently occurs due to the strong selection pressure at low frequencies. Neither the change of the integration locus nor the extension of flanking regions did lead to recombinant clones, even when flanking sequences of up to 875 bp were evaluated, which were previously successfully used to integrate genes via pK19mobsacB (Binder *et al.*, 2013).

In-depth analyses with the two *C. glutamicum* deletion strains DM1728kanR(-131) and DM1728kanR(-752) have shown that the use of dsDNA recombineering in *C. glutamicum* is limited to the integration of fragments smaller than 750 bp. Larger fragments are only integrated at very low efficiencies and can be often detected at incorrect genomic target locations. This correlation of the size of the fragment to be integrated with the recombineering efficiency has also been observed in *E. coli* before (Costantino, 2003; Ellis *et al.*, 2001; Swaminathan *et al.*, 2001). However, even though the insertion of larger fragments was performed with lower efficiencies than the engineering of small single-base changes, in contrast to *C. glutamicum* full-length genes can be integrated easily. Since dsDNA recombineering functions via a single-stranded intermediate (Mosberg *et al.*, 2010), the generated ssDNA fragment is integrated by oligo-directed repair that occurs at the DNA replication fork as the fork passes through the target region (Court *et al.*, 2002; Ellis *et al.*, 2001). A size of a fragment above

1 kb might limit the integration, because the typical size of an Okazaki fragment consists of 1 kb (Maresca *et al.*, 2010).

As described in this work, dsDNA recombineering in *C. glutamicum* is clearly limited to small sized fragments with rather long flanking regions. A 131 nt deletion can be repaired with efficiencies of about 2x 10^3 cells per 10^{10} cells when a dsDNA substrate with flanks of 900 bp is used. In order to increase recombineering efficiencies various approaches were applied modifying the DNA substrate, e.g. an ssDNA intermediate was generated *in vitro* (data not shown) or various 5'-modifications of the DNA substrate were tested. In *B. subtilis*, recombineering was successfully shown using an ssDNA intermediate, which was generated via a linear PCR amplification using only a single primer (Wang *et al.*, 2012). Since an ssDNA fragment could not be successfully generated via PCR in this work, an enzyme-based approach was performed, generating ssDNA *in vitro* by treatment with λ exonuclease (Murgha *et al.*, 2014). However, the successfully *in vitro* generated ssDNA was not able to increase recombineering efficiencies, but instead significantly lower numbers of recombinant CFU were obtained (data not shown).

The first step in dsDNA recombineering is the degradation of the dsDNA substrate into a full-length ssDNA intermediate (Mosberg *et al.*, 2010). This step is catalyzed by the exonuclease, degrading dsDNA in 5'-3' direction and preferring 5'-phosphorylated ends (Subramanian *et al.*, 2003). Furthermore, when ends are phosphorothioated or hydroxlated, degradation by the exonuclease is hampered (Liu and Liu, 2010; Mosberg *et al.*, 2010). In this work, with generated dsDNA substrates that contained phosphorylated 5'-ends of the template strand an increase in recombineering efficiencies could be observed in *C. glutamicum* compared to the unmodified fragment. 5'-Phosphorothioation of the template strand with 5'-phosphorylation of the non-template strand instead resulted in a decrease in recombineering efficiencies. The increase in recombineering efficiencies achieved through 5'-phosphorylation of the template strand was most likely due to the rapid degeneration of the more efficiently targeted phosphorylated strand (Maresca *et al.*, 2010), whereas the non-template strand was not as efficiently targeted, resulting in the single-strand DNA intermediate. 5'-Phosphorothioation of the template strand with 5'-phosphorylation of the non-template strand resulted in decreased efficiencies, most likely, because the generated single strand intermediate possesses a phophorothioated end that complicates the chromosomal integration of the fragment at the replication fork.

In order to compare the efficiency of ssDNA and dsDNA recombineering in *C. glutamicum* a variety of parameters have to be taken into account. Binder *et al*. reported highest efficiencies of 2x 10^5 recombinants per 10^8 cells, stating that every 1000^{th} cell is recombinant in ssDNA recombineering in *C. glutamicum* (Binder *et al.*, 2013). In contrast to that, with dsDNA

recombineering highest amounts of 1x 10^5 per 10^{10} cells were achieved, resulting in one recombinant out of 100,000 cells. In both experiments, one nucleotide was removed restoring the kanamycin resistance.

However, the efficiencies determined for ssDNA and dsDNA recombineering were obtained individually, since each method was performed under most optimal conditions. Therefore, for ssDNA recombineering an oligonucleotide of 100 nt was used, for dsDNA recombineering a PCR fragment of 600 bp was applied. In a more direct comparison, the length of the DNA substrate was adjusted, transforming with either 100 nt of an oligonucleotide or 100 bp of a PCR fragment. In this case for dsDNA recombineering higher recombineering efficiencies of 3.2 x 10^5 recombinants per 10^{10} cells could be observed than for ssDNA recombineering with 9.8 x 10^4 recombinants per 10^{10} cells, especially when it is taken into account that 10 µg of oligonucleotide were transformed in contrast to 1.2 µg PCR fragment. These results support the hypothesis that the oligonucleotides are most likely degraded when they enter the cell. In contrast to that, the interaction of RecE and RecT possibly ensures that RecT immediately binds to the nascent ssDNA while the active RecE generates the ssDNA fragment by degrading the dsDNA PCR fragment. Both, the interaction of RecE with RecT and the partial degradation of the oligonucleotide upon entering the cell could be supported by the observation that dsDNA recombineering with the 100 nt oligonucleotides led to significantly lower amounts of recombinant CFU than obtained with ssDNA recombineering.

4.2 CRISPR-Cas9 targeting in *C. glutamicum*

The CRISPR-Cas9 system has become one of the most promising genome editing tools over the last years, because it allows genome alteration in a precise site-specific manner (Doudna and Charpentier, 2014). It has been mainly applied in eukaryotes, as most eukaryotes possess the ability to repair DSB induced by CRISPR-Cas9 using endogenous repair systems like NHEJ or HDR, and thereby create deletions or insertions with the help of a heterologous template. In contrast to that, most prokaryotes lack these repair systems resulting in the inability to repair DSB independently. Thus, activation of CRISPR-Cas9 autoimmunity leads to cell death in many bacteria (Bikard *et al.*, 2013; Edgar and Qimron, 2010; Marraffini and Sontheimer, 2010) and archaea (Fischer *et al.*, 2012; Gudbergsdottir *et al.*, 2011). To overcome this challenge, the CRISPR-Cas9 system was used instead as a selection tool that targets and thereby eliminates strains with undesired genotypes (Jiang *et al.*, 2015; Li *et al.*, 2015; Oh and van Pijkeren, 2014; Pyne *et al.*, 2015). In combination with DNA recombineering this allows for efficient genome editing. When mixtures of edited and non-edited cells are transformed with Cas9 and the sgRNA corresponding to the genotype of non-edited cells, a functional CRISPR-Cas9 nucleoprotein

complex is formed, resulting in the specific targeting of non-edited cells, so that only edited cells survive.

To analyze the accessibility of the CRISPR-Cas9 system and the potential combination with DNA recombineering in *C. glutamicum*, the functionality of the CRISPR-Cas9 nucleoprotein complex was tested. As previously shown for other bacteria like *E. coli* and *Streptococcus* (Jiang *et al.*, 2013; Jiang *et al.*, 2015), clostridia (Wang *et al.*, 2015) or streptomycetes (Huang *et al.*, 2015), the CRISPR-Cas9 system renders the specific introduction of DSB in *C. glutamicum* that allows the separation of two genotypes. For a functional nucleoprotein complex, a few factors have to be considered. The activity of the nuclease Cas9 that introduces the DSB has to be tightly regulated, because it is reported to introduce DSB at off-target sites (Cho *et al.*, 2014). This might also be the reason for the multiple cloning difficulties during this study, e.g. the combination of sgRNA and *cas9* on one plasmid. Similar difficulties were reported for the construction of plasmids for *E. coli* (Jiang *et al.*, 2015). To regulate off-target effects, Cas9 toxicity was assessed by exchanging the start codon from ATG to GTG, TTG or 2xSTOP, showing that reduced activity increases living cell count after transformation in *C. glutamicum* strains. Furthermore, the observed heterogenous genotype of small and normal sized colonies was abolished. CRISPR-Cas9 targeting, however, could still be performed, even when TTG-Cas9 was used.

The other important component of the CRISPR-Cas9 system is the sgRNA. It consists of the 20 nt protospacer complementary to the chromosomal target region, which is controlled by the synthetic promoter PJ23119. Additional characteristics are the Cas9 binding handle and a terminator sequence (Jinek *et al.*, 2012). When the protospacer region anneals to the complementary chromosomal sequence and a chromosomal adjacent PAM motif is present, the nucleoprotein complex will bind and Cas9 can introduce the DSB. While a protospacer of 20 nt was reported as optimal size for targeting (Jinek *et al.*, 2012), Ran *et al.* stated that 17 nt are sufficient for correct DNA cleavage (Ran *et al.*, 2013). Furthermore, studies were performed analyzing the impact of the position of the point mutation in the protospacer as well as the effect of the distance of the point mutation to the PAM motif on targeting efficiencies. It was confirmed that only point mutations in 8-10 nt immediately after the PAM motif abolish targeting (Jinek *et al.*, 2012; Semenova *et al.*, 2011; Wiedenheft *et al.*, 2011). In *C. glutamicum* however, strains DM1728kanR(+1) and DM1728kanR(-131) were both efficiently targeted by an sgRNA with the same protospacer, even though only 8 nucleotides of the target protospacer were complementary to the sequence in the chromosome. Until now, in *C. glutamicum*, as well as in *L. reuteri* (Oh and van Pijkeren, 2014), only mutations destroying the present PAM motif led to successful differentiation between WT and mutant via CRISPR-Cas9 targeting. To allow editing other target sites within close proximity of the PAM site, additional studies would have to be

performed. These results show that the components of the CRISPR-Cas9 system have to be set-up for each organism and a number of parameters have to be defined individually to allow successful targeting.

In some prokaryotes, such as *B. subtilis,* the DSBs introduced by Cas9 can be endogenously repaired (Altenbuchner, 2016). In order to use the CRISPR-Cas9 system as an editing tool in *C. glutamicum*, the proteins Ku and Ligase D responsible for the minimal error-probe bacterial NHEJ system (Shuman and Glickman, 2007) could be heterologously expressed, which might lead to a functional CRISPR-Cas9 system. This was partially already demonstrated for *S. coelicolor* A3, where the heterologous expression of Ligase D was able to repair the incomplete NHEJ pathway (Brouns *et al.*, 2008).

4.3 CRISPR-Cas9 recombineering in *C. glutamicum*

Since *C. glutamicum* is not able to repair introduced DSBs by endogenous repair mechanisms, the CRISPR-Cas9 system can only be applied as a selection tool in combination with DNA recombineering and not directly as a genome editing tool. Even though both methods could be successfully established individually in *C. glutamicum*, the combination requires fine-tuning and the optimization of several parameters.

The assembly of the nuclease Cas9 and the recombinases on one plasmid already affects both recombineering and CRISPR-Cas9 targeting efficiency in *C. glutamicum*. With plasmid pCL2-recET-cas9, reduced numbers of recombinants were obtained, because the total number of viable cells was reduced due to Cas9 toxicity. In contrast to these results, Cas9 was shown to modestly induce recombineering efficiencies in *E. coli* (Jiang *et al.*, 2013), which could not be observed for *C. glutamicum*.

Besides the challenges regarding the construction of plasmids and the inducibility and toxicity of genes, also different procedures in the final execution of a CRISPR-Cas9 recombineering experiment have to be considered. This was shown both for *E. coli* and *L. reuteri*, the two bacteria in which CRISPR-Cas9 recombineering has been successfully established until now (Jiang *et al.*, 2015; Li *et al.*, 2015; Oh and van Pijkeren, 2014; Pyne *et al.*, 2015). In all three reported approaches for *E. coli*, the cells initially harbor a plasmid containing genes encoding for both Cas9 and the exonuclease/recombinase pair (Jiang *et al.*, 2015; Li *et al.*, 2015; Pyne *et al.*, 2015). In the following transformation step, the targeting RNA and the DNA recombineering substrate were simultaneously introduced. Whereas the targeting RNA is always provided on a plasmid, the homology template can either be introduced in form of an oligonucleotide or PCR fragment as well as plasmid-based. With this one-step procedure via co-transformation, high

efficiencies of single gene deletions of 69 ± 4 % could be generated (Jiang *et al.*, 2015). Even for large deletions up to 19.4 kb and insertions up to 3 kb efficiencies of 1 - 47 % could be reported (Pyne *et al.*, 2015). In contrast to that without the CRISPR-Cas9 system efficiencies of only 0 - 0.68 % were obtained.

In *L. reuteri* the co-transformation of DNA substrate and targeting RNA plasmid to perform editing and targeting in one step yielded only relatively low efficiencies (Oh and van Pijkeren, 2014). The authors suggested that co-transformation is only functional when conditions allowing for optimal ssDNA recombineering efficiencies are established, since lower numbers of recombinants would not be detected among many escaper cells. As DNA recombineering efficiencies in *C. glutamicum* are rather limited, the one-step procedure did not lead to recombinant clones as expected.
In a two-step approach, in the *L. reuteri* strain harboring plasmids encoding for Cas9, the tracrRNA and RecT, first recombineering was performed (by transformation with the oligonucleotide). After cultivation allowing for cells to regenerate, targeting was performed in a second transformation (by transformation with the targeting RNA), which led to high numbers of recombinants (Oh and van Pijkeren, 2014). This is most likely due to the fact that more replication cycles are allowed after transformation, leading to more efficient incorporation of the recombineering fragment, finally resulting in higher numbers of recombinants. Fortifying that, Binder *et al*. reported higher ssDNA recombineering frequencies in *C. glutamicum* when cells were regenerated for 5 h instead of 1 h after electroporation (Binder *et al.*, 2013) and van Pijkeren *et al*. stated a fivefold increase in recombinant numbers when *Lactobacillus* cells were grown in absence of an antibiotic selection marker after transformation, instead of direct plating on selective plates after recovery (Oh and van Pijkeren, 2014).

As described for dsDNA recombineering and also observed for CRISPR-Cas9 recombineering, the integration of point mutations can be performed with high efficiencies. However, the efficiency decreases when longer fragments are integrated, showing a correlation between the length of the homologous regions and numbers of recombinants (Jiang *et al.*, 2015). To overcome this problem, the template required for editing can also be provided plasmid-based. In fact, this procedure has been used during development of CRISPR-Cas9 recombineering for *E. coli* where template and sgRNA were provided on a single plasmid (Jiang *et al.*, 2015). Also, for applying CRISPR-Cas9 recombineering in *Streptomyces coelicolor* a plasmid providing *cas9* together with sgRNA was constructed (Tong *et al.*, 2015). With this system only the inactivation of genes without editing was possible. In another work with *S. coelicolor* a plasmid comprising a target-specific guide RNA, a codon-optimized *cas9* and two homology-directed repair templates was constructed enabling more elaborated genome modifications (Huang *et al.*, 2015). To assess

such methods for *C. glutamicum* similar attempts were undertaken to clone the gene for Cas9, the DNA-sequence for the sgRNA and the homology template on one single plasmid, but correct plasmids could never be obtained.

Experiments simulating CRISPR-Cas9 recombineering in *C. glutamicum* using the *lacZ* system and the plasmid pCL2-recET-cas9 showed that encountered DNA recombineering frequencies of 1 recombinant out of 100,000 non-edited cells can be enriched by an average factor of 500. Due to this enrichment, only 167 cells have to be tested to detect one recombinant after CRISPR-Cas9 recombineering instead of 100,000 cells. When plasmid pEKEx3-cas9 was used instead of pCL2-recET-cas9 for simulating CRISPR-Cas9 recombineering, at best, even an enrichment factor of 5000 could be reported (data not shown, because plasmid pEKEx3-cas9 does not enable previous DNA recombineering). However, the combination of both methods, DNA recombineering with CRISPR-Cas9 targeting, in the dual-step approach was not yet successful, because a larger number of escaper cells were generated, not enabling a visual detection of blue cells among the high number of yellow cells. In most cases these (yellow) escaper cells e.g. as observed in *E. coli,* were reported to contain mutations in the targeting spacer (Jiang *et al.*, 2013).

A functional CRISPR-Cas9 system without any repair system, however, may still be used in prokaryotes, e.g. for CRISPR-Cas9 mediated vaccination of biotechnologically interesting strains against bacteriophages by natural spacer acquisition (Barrangou *et al.*, 2007). Another application could be the specific knock-down of certain bacteria based on their genetic signatures reducing the dispersion of unwanted genes like antibiotic resistances or virulence loci. In a synthetic consortium of three phage-susceptible *E. coli* strains with different antibiotic resistances, CRISPR-Cas9 targeting of two strains resulted in a strong dominance of the third non-targeted strain (Citorik *et al.*, 2014).

4.4 The right test system to improve genome editing methods in *C. glutamicum*

For establishing genome editing methods such as DNA recombineering or CRISPR-Cas9, which enable integration, deletion or substitution of chromosomal fragments, a test system must be used, in which the overall editing efficiencies can be evaluated. It is crucial though, to find the appropriate test system not only for the genome editing method to be established, but also for the respective organism that is used.

In this work, many different approaches have been evaluated to find the best test system for DNA recombineering, the CRISPR-Cas9 system as well as CRISPR-Cas9 recombineering in *C. glutamicum*. Whereas the kanamycin resistance was successfully used as a test system for DNA recombineering, it was not suitable for establishing the CRISPR-Cas9 system in *C. glutamicum*.

Instead of only allowing for efficient targeting in *C. glutamicum* strain DM1728kanR(+1), both strains DM1728kanR(+1) and DM1728kanR(-131) were efficiently targeted by the same sgRNA. This sgRNA contained a protospacer with 8 nt complementary to chromosomal sequences of both strains, which sufficed for efficient targeting rendering efficient separation impossible.

Alternatively, in order to allow for fast detection of recombinant cells among large numbers of non-edited cells, visual differentiation test systems were analyzed. However, different colored cells due to inactivation of carotenoid expression as well as the expression of fluorescent proteins like E2-crimson only showed slight differences between strains, which did not suffice for efficient distinction.

In contrast to that, the integration of the *lacZ* gene in combination with the strong PH36 promoter led to *C. glutamicum* cells that exhibited a green phenotype when spread on X-gal. Since yellow *C. glutamicum* WT cells could be distinguished from green cells harboring *lacZ*, the system was chosen as the most suitable test system for CRISPR-Cas9 recombineering. However, the number of colonies growing on an agar plate influenced the phenotype. When too many cells expressing *lacZ* were spread on one plate, the green phenotype could no longer be observed. This is most likely due to the limited accessibility of X-gal because of overpopulation. A number of approximately 200 colonies per plate seemed suitable to allow precise distinction between both phenotypes, which is necessary for the establishment of CRISPR-Cas9 recombineering.

Furthermore, for the later removal of expression plasmids after genome editing, the expression plasmid pCL2-OriTS was constructed and analyzed, harboring a temperature-sensitive origin of replication according to Nakamura *et al*., (2006). Whereas stably maintained at 25 °C, during cultivation at high temperatures of 34 °C the expression plasmid is gradually lost. This valuable tool can therefore be used turning the genome-edited production strains into plasmid free production hosts.

4.5 MurE as target for L-lysine *C. glutamicum* production strain improvement

The mutation G81E in MurE was found to highly increase L-lysine production titers, whereas a few other amino acid substitutions at position G81 were less effective (Binder *et al.*, 2013). To

analyze the effect of amino acid exchanges at position G81 in MurE in more detail, *C. glutamicum* strains with all possible amino acid exchanges at this position (except G81Y) were generated and analyzed in this work. The fact that all mutants except G81Y could be obtained indicates that the respective enzyme variants are still catalytically active to form the essential peptide linkage during peptidoglycan synthesis. This can be explained by the fact that G81 is located in a second shell within a short helix, likely influencing access of the substrate UDP-MurNAc-L-Ala-D-Glu to the catalytic site. Besides activity also stability of MurE could be influenced, as reported for the mutant enzymes of *Staphylococcus aureus* (Ruane *et al.*, 2013), or *Mycobacterium leprae* (Shanmugam and Natarajan, 2014).

The analyzed mutant set of *C. glutamicum* illustrates a nice example for the existence of a clear correlation between L-lysine production and growth. Strains with highly increased L-lysine accumulation exhibited retarded growth, which could be previously observed in *C. glutamicum* mutants harboring decreased levels of specific citrate synthase activity (van Ooyen *et al.*, 2012). Furthermore, Becker *et al.* reported that an increased flux towards L-lysine by engineering the pentose phosphate pathway or the aspartate kinase was related with reduced growth (Becker *et al.*, 2011). Whereas the apparent limitations of the cell by the latter engineering approaches are unknown, those obtained by MurE mutagenesis are clearly due to a limited availability of *meso*-diaminopimelate for growth. Since *meso*-diaminopimelate is required for peptidoglycan synthesis as well as L-lysine synthesis, the increased flux towards L-lysine caused by the mutations will limit the flux via MurE towards the peptidoglycan. As verified by the unaltered MIC of the strains towards the cell wall targeting antibiotics vancomycin, benzylpenicillin and ethambutol, the cell wall integrity is retained. Thus, the cell balances the limited availability of the product of MurE by reducing the growth rate, rather than growing at a high rate at the cost of a weaker cell wall. In order to overcome the growth defect, the option to increase the total glycolytic flux in combination with increased NADPH availability via an increased sugar uptake could be considered. This has recently been obtained using increased expression of IolT1, a sugar facilitator of *C. glutamicum* (Ikeda *et al.*, 2011; Klaffl *et al.*, 2013). Also increased expression of the glucose-specific phosphotransferase system leads to increased glucose uptake (Pérez-García *et al.*, 2016). At an increased sugar uptake rate with a consequent increased overall flux towards L-lysine as well as the deactivation of regulatory mechanims, also more of *meso*-diaminopimelate could be available to even out a reduced MurE activity. Amongst others, analysis of the mutant strains showed that theoretically the MurE activity could be further reduced to 20 %, resulting in L-lysine titers of 137 mM (Hochheim *et al.*, 2016)

4.5 Summary and outlook

In this work, two genome editing methods were established for *C. glutamicum*: dsDNA recombineering and the CRISPR-Cas9 system. Both methods were functional in *C. glutamicum*, allowing for recombinant cells to be generated and genotypes to be separated. Since *C. glutamicum* lacks an endogenous repair system, the CRISPR-Cas9 system cannot be applied solely as a genome editing method. Since dsDNA recombineering in *C. glutamicum* is limited to the integration of smaller fragments and efficiencies are rather low, the establishment of a combined CRISPR-Cas9 recombineering method was attempted. This technique would allow for genome editing via recombineering with additional killing of all non-edited cells by CRISPR-Cas9, resulting in only edited cells that are able to survive in *C. glutamicum*. After evaluating many test systems to establish this technique, the β-galactosidase assay was identified as the most suitable test system for *C. glutamicum*. Even though simulations of CRISPR-Cas9 recombineering showed CRISPR-Cas9 targeting of different mixtures of edited and non-edited cells, conditions for combining CRISPR-Cas9 and recombinering could not be found yet. This is in part due to the difficulty of cloning the appropriate plasmids. Therefore, more parameters have to be verified and the overall procedure (one-step method vs. two-step method) has to be optimized to enable successful CRISPR-Cas9 recombineering in *C. glutamicum*.

References

Abbas, C. A., Sibirny, A. A., 2011. Genetic control of biosynthesis and transport of riboflavin and flavin nucleotides and construction of robust biotechnological producers. *Microbiology and Molecular Biology Reviews.* 75**,** 321-360.

Abe, S., Takayama, K.-I., Kinoshita, S., 1967. Taxonomical studies on glutamic acid-producing bacteria. *The Journal of General and Applied Microbiology.* 13**,** 279-301.

Adrio, J.-L., Demain, A. L., 2010. Recombinant organisms for production of industrial products. *Bioengineered bugs.* 1**,** 116-131.

Alcazar-Fuoli, L., Cairns, T., Lopez, J. F., Zonja, B., Pérez, S., Barceló, D., Igarashi, Y., Bowyer, P., Bignell, E., 2014. A modified recombineering protocol for the genetic manipulation of gene clusters in *Aspergillus fumigatus*. *PLoS One.* 9**,** e111875.

Altenbuchner, J., 2016. Editing of the *Bacillus subtilis* Genome by the CRISPR-Cas9 System. *Applied and Environmental Microbiology.* 82**,** 5421-5427.

Anders, C., Niewoehner, O., Duerst, A., Jinek, M., 2014. Structural basis of PAM-dependent target DNA recognition by the Cas9 endonuclease. *Nature.* 513**,** 569-573.

Bao, Z., Cartinhour, S., Swingle, B., 2012. Substrate and target sequence length influence RecTE(Psy) recombineering efficiency in *Pseudomonas syringae*. *PLoS One.* 7**,** e50617.

Barrangou, R., Fremaux, C., Deveau, H., Richards, M., Boyaval, P., Moineau, S., Romero, D. A., Horvath, P., 2007. CRISPR provides acquired resistance against viruses in prokaryotes. *Science.* 315**,** 1709-1712.

Basavannacharya, C., Robertson, G., Munshi, T., Keep, N. H., Bhakta, S., 2010. ATP-dependent MurE ligase in *Mycobacterium tuberculosis*: biochemical and structural characterisation. *Tuberculosis.* 90**,** 16-24.

Baumgart, M., Unthan, S., Rückert, C., Sivalingam, J., Grünberger, A., Kalinowski, J., Bott, M., Noack, S., Frunzke, J., 2013. Construction of a prophage-free variant of *Corynebacterium glutamicum* ATCC 13032 for use as a platform strain for basic research and industrial biotechnology. *Applied and environmental microbiology.* 79**,** 6006-6015.

Becker, J., Zelder, O., Häfner, S., Schröder, H., Wittmann, C., 2011. From zero to hero—Design-based systems metabolic engineering of *Corynebacterium glutamicum* for L-lysine production. *Metabolic engineering.* 13**,** 159-168.

Bikard, D., Jiang, W., Samai, P., Hochschild, A., Zhang, F., Marraffini, L. A., 2013. Programmable repression and activation of bacterial gene expression using an engineered CRISPR-Cas system. *Nucleic Acids Res.* 41**,** 7429-7437.

Bimboim, H., Doly, J., 1979. A rapid alkaline extraction procedure for screening recombinant plasmid DNA. *Nucleic Acids Res.* 7**,** 1513-1523.

Binder, S., Schendzielorz, G., Stäbler, N., Krumbach, K., Hoffmann, K., Bott, M., Eggeling, L., 2012. A high-throughput approach to identify genomic variants of bacterial metabolite producers at the single-cell level. *Genome biology.* 13**,** 1.

Binder, S., Siedler, S., Marienhagen, J., Bott, M., Eggeling, L., 2013. Recombineering in *Corynebacterium glutamicum* combined with optical nanosensors: a general strategy for fast producer strain generation. *Nucleic Acids Res.* 41**,** 6360-9.

Boeke, J. D., La Croute, F., Fink, G. R., 1984. A positive selection for mutants lacking orotidine-5′-phosphate decarboxylase activity in yeast: 5-fluoro-orotic acid resistance. *Molecular and General Genetics MGG.* 197**,** 345-346.

Bott, M., 2015. Need for speed–finding productive mutations using transcription factor-based biosensors, fluorescence-activated cell sorting and recombineering. *Microbial biotechnology.* 8**,** 8-10.

Bowater, R., Doherty, A. J., 2006. Making ends meet: repairing breaks in bacterial DNA by non-homologous end-joining. *PLoS Genet.* 2**,** e8.

Brouns, S. J., Jore, M. M., Lundgren, M., Westra, E. R., Slijkhuis, R. J., Snijders, A. P., Dickman, M. J., Makarova, K. S., Koonin, E. V., Van Der Oost, J., 2008. Small CRISPR RNAs guide antiviral defense in prokaryotes. *Science.* 321**,** 960-964.

Chen, L., Wang, W., Sun, W., Surette, M., Duan, K., 2010. Characterization of a cryptic plasmid from *Pseudomonas sp.* and utilization of its temperature-sensitive derivatives for genetic manipulation. *Plasmid.* 64**,** 110-117.

Cho, S. W., Kim, S., Kim, Y., Kweon, J., Kim, H. S., Bae, S., Kim, J.-S., 2014. Analysis of off-target effects of CRISPR/Cas-derived RNA-guided endonucleases and nickases. *Genome research.* 24**,** 132-141.

Citorik, R. J., Mimee, M., Lu, T. K., 2014. Sequence-specific antimicrobials using efficiently delivered RNA-guided nucleases. *Nature biotechnology.* 32**,** 1141-1145.

Clark, A., Sharma, V., Brenowitz, S., Chu, C., Sandler, S., Satin, L., Templin, A., Berger, I., Cohen, A., 1993. Genetic and molecular analyses of the C-terminal region of the *recE* gene from the Rac prophage of *Escherichia coli* K-12 reveal the *recT* gene. *Journal of bacteriology.* 175**,** 7673-7682.

Cleto, S., Jensen, J. V., Wendisch, V. F., Lu, T. K., 2016. *Corynebacterium glutamicum* metabolic engineering with CRISPR interference (CRISPRi). *ACS synthetic biology.*

Costantino, N., 2003. Enhanced levels of λ Red-mediated recombinants in mismatch repair mutants. *Proceedings of the National Academy of Sciences.* 100**,** 15748-15753.

Court, D. L., Sawitzke, J. A., Thomason, L. C., 2002. Genetic engineering using homologous recombination. *Annu Rev Genet.* 36**,** 361-88.

Datta, S., Costantino, N., Zhou, X., Court, D. L., 2008. Identification and analysis of recombineering functions from Gram-negative and Gram-positive bacteria and their phages. *Proc Natl Acad Sci U S A.* 105**,** 1626-31.

Deltcheva, E., Chylinski, K., Sharma, C. M., Gonzales, K., Chao, Y., Pirzada, Z. A., Eckert, M. R., Vogel, J., Charpentier, E., 2011. CRISPR RNA maturation by trans-encoded small RNA and host factor RNase III. *Nature.* 471**,** 602-607.

Demain, A. L., 2000. Microbial biotechnology. *Trends in biotechnology.* 18**,** 26-31.

Demain, A. L., Solomon, N. A., 1985. Biology of industrial organisms. Benjamin/Cummings Publishing Co., Inc.

DiCarlo, J. E., Norville, J. E., Mali, P., Rios, X., Aach, J., Church, G. M., 2013. Genome engineering in *Saccharomyces cerevisiae* using CRISPR-Cas systems. *Nucleic Acids Res.* gkt135.

Doudna, J. A., Charpentier, E., 2014. The new frontier of genome engineering with CRISPR-Cas9. *Science*. 346**,** 1258096.

Edgar, R., Qimron, U., 2010. The *Escherichia coli* CRISPR system protects from λ lysogenization, lysogens, and prophage induction. *Journal of bacteriology.* 192**,** 6291-6294.

Eggeling, L., Bott, M., 2015. A giant market and a powerful metabolism: L-lysine provided by *Corynebacterium glutamicum. Applied microbiology and biotechnology.* 99**,** 3387-3394.

Eggeling, L., Sahm, H., 1999. L-glutamate and L-lysine: traditional products with impetuous developments. *Applied Microbiology and Biotechnology.* 52**,** 146-153.

Eichenlaub, R., 1979. Mutants of the mini-F plasmid pML31 thermosensitive in replication. *Journal of bacteriology.* 138**,** 559-566.

Eikmanns, B. J., Kleinertz, E., Liebl, W., Sahm, H., 1991. A family of *Corynebacterium glutamicum/Escherichia coli* shuttle vectors for cloning, controlled gene expression, and promoter probing. *Gene.* 102**,** 93-98.

Elgamal, S., Artsimovitch, I., Ibba, M., 2016. Maintenance of Transcription-Translation Coupling by Elongation Factor P. *mBio.* 7**,** e01373-16.

Ellis, H. M., Yu, D., DiTizio, T., 2001. High efficiency mutagenesis, repair, and engineering of chromosomal DNA using single-stranded oligonucleotides. *Proceedings of the National Academy of Sciences.* 98**,** 6742-6746.

Feng, Z., Zhang, B., Ding, W., Liu, X., Yang, D.-L., Wei, P., Cao, F., Zhu, S., Zhang, F., Mao, Y., 2013. Efficient genome editing in plants using a CRISPR/Cas system.

Fischer, S., Maier, L.-K., Stoll, B., Brendel, J., Fischer, E., Pfeiffer, F., Dyall-Smith, M., Marchfelder, A., 2012. An archaeal immune system can detect multiple protospacer adjacent motifs (PAMs) to target invader DNA. *Journal of Biological Chemistry*. 287**,** 33351-33363.

Gao, B., Gupta, R. S., 2012. Phylogenetic framework and molecular signatures for the main clades of the phylum Actinobacteria. *Microbiology and Molecular Biology Reviews.* 76**,** 66-112.

Gasiunas, G., Barrangou, R., Horvath, P., Siksnys, V., 2012. Cas9–crRNA ribonucleoprotein complex mediates specific DNA cleavage for adaptive immunity in bacteria. *Proceedings of the National Academy of Sciences.* 109**,** E2579-E2586.

Georgi, T., Rittmann, D., Wendisch, V. F., 2005. Lysine and glutamate production by *Corynebacterium glutamicum* on glucose, fructose and sucrose: roles of malic enzyme and fructose-1, 6-bisphosphatase. *Metabolic engineering.* 7**,** 291-301.

Gilbert, L. A., Larson, M. H., Morsut, L., Liu, Z., Brar, G. A., Torres, S. E., Stern-Ginossar, N., Brandman, O., Whitehead, E. H., Doudna, J. A., 2013. CRISPR-mediated modular RNA-guided regulation of transcription in eukaryotes. *Cell.* 154**,** 442-451.

Grant, S. G., Jessee, J., Bloom, F. R., Hanahan, D., 1990. Differential plasmid rescue from transgenic mouse DNAs into *Escherichia coli* methylation-restriction mutants. *Proceedings of the National Academy of Sciences.* 87**,** 4645-4649.

Gratz, S. J., Ukken, F. P., Rubinstein, C. D., Thiede, G., Donohue, L. K., Cummings, A. M., O'Connor-Giles, K. M., 2014. Highly specific and efficient CRISPR/Cas9-catalyzed homology-directed repair in *Drosophila*. *Genetics.* 196**,** 961-971.

Grissa, I., Vergnaud, G., Pourcel, C., 2007. CRISPRFinder: a web tool to identify clustered regularly interspaced short palindromic repeats. *Nucleic Acids Res.* 35**,** W52-W57.

Groom, J., Chung, D., Young, J., Westpheling, J., 2014. Heterologous complementation of a *pyrF* deletion in *Caldicellulosiruptor hydrothermalis* generates a new host for the analysis of biomass deconstruction. *Biotechnology for biofuels.* 7**,** 1.

Gudbergsdottir, S., Deng, L., Chen, Z., Jensen, J. V., Jensen, L. R., She, Q., Garrett, R. A., 2011. Dynamic properties of the Sulfolobus CRISPR/Cas and CRISPR/Cmr systems when challenged with vector-borne viral and plasmid genes and protospacers. *Molecular microbiology.* 79**,** 35-49.

Hall, S. D., Kolodner, R. D., 1994. Homologous pairing and strand exchange promoted by the *Escherichia coli* RecT protein. *Proceedings of the National Academy of Sciences.* 91**,** 3205-3209.

Hanahan, D., 1983. Studies on transformation of *Escherichia coli* with plasmids. *Journal of molecular biology.* 166**,** 557-580.

Hanahan, D., 1985. Techniques for transformation of *E. coli. DNA cloning.* 1**,** 109-135.

Hashimoto-Gotoh, T., Yamaguchi, M., Yasojima, K., Tsujimura, A., Wakabayashi, Y., Watanabe, Y., 2000. A set of temperature sensitive-replication/-segregation and temperature resistant plasmid vectors with different copy numbers and in an isogenic background (chloramphenicol, kanamycin, lacZ, repA, par, polA). *Gene.* 241**,** 185-191.

Hayashi, H., Wada, H., Yoshimura, T., Esaki, N., Soda, K., 1990. Recent topics in pyridoxal 5'-phosphate enzyme studies. *Annual review of biochemistry.* 59**,** 87-110.

Hochheim, J., Kranz, A., Krumbach, K., Sokolowsky, S., Eggeling, L., Noack, S., Bocola, M., Bott, M., Marienhagen, J., 2016. Mutations in MurE, the essential UDP-N-acetylmuramoylalanyl-d-glutamate 2, 6-diaminopimelate ligase of *Corynebacterium glutamicum*: effect on l-lysine formation and analysis of systemic consequences. *Biotechnology Letters.* 1-6.

Hoffelder, M., Raasch, K., van Ooyen, J., Eggeling, L., 2010. The E2 domain of OdhA of *Corynebacterium glutamicum* has succinyltransferase activity dependent on lipoyl residues of the acetyltransferase AceF. *Journal of bacteriology.* 192**,** 5203-5211.

Huang, H., Zheng, G., Jiang, W., Hu, H., Lu, Y., 2015. One-step high-efficiency CRISPR/Cas9-mediated genome editing in *Streptomyces*. *Acta biochimica et biophysica Sinica.* 47**,** 231-243.

Hwang, W. Y., Fu, Y., Reyon, D., Maeder, M. L., Kaini, P., Sander, J. D., Joung, J. K., Peterson, R. T., Yeh, J.-R. J., 2013. Heritable and precise zebrafish genome editing using a CRISPR-Cas system. *PLoS One.* 8**,** e68708.

Ikeda, M., 2003. Amino acid production processes. Microbial production of l-amino acids. *Springer*, pp. 1-35.

Ikeda, M., Mizuno, Y., Awane, S.-i., Hayashi, M., Mitsuhashi, S., Takeno, S., 2011. Identification and application of a different glucose uptake system that functions as an alternative to the phosphotransferase system in *Corynebacterium glutamicum*. *Applied microbiology and biotechnology*. 90**,** 1443-1451.

Jäger, W., Schäfer, A., Pühler, A., Labes, G., Wohlleben, W., 1992. Expression of the *Bacillus subtilis sacB* gene leads to sucrose sensitivity in the gram-positive bacterium *Corynebacterium glutamicum* but not in *Streptomyces lividans*. *Journal of bacteriology.* 174**,** 5462-5465.

Jessen, J. R., Meng, A., McFarlane, R. J., Paw, B. H., Zon, L. I., Smith, G. R., Lin, S., 1998. Modification of bacterial artificial chromosomes through chi-stimulated homologous recombination and its application in zebrafish transgenesis. *Proceedings of the National Academy of Sciences.* 95**,** 5121-5126.

Jiang, W., Bikard, D., Cox, D., Zhang, F., Marraffini, L. A., 2013. RNA-guided editing of bacterial genomes using CRISPR-Cas systems. *Nature biotechnology.* 31**,** 233-239.

Jiang, W., Brueggeman, A. J., Horken, K. M., Plucinak, T. M., Weeks, D. P., 2014. Successful transient expression of Cas9 and single guide RNA genes in *Chlamydomonas reinhardtii*. *Eukaryotic cell.* 13**,** 1465-1469.

Jiang, Y., Chen, B., Duan, C., Sun, B., Yang, J., Yang, S., 2015. Multigene editing in the *Escherichia coli* genome via the CRISPR-Cas9 system. *Applied and environmental microbiology.* 81**,** 2506-2514.

Jinek, M., Chylinski, K., Fonfara, I., Hauer, M., Doudna, J. A., Charpentier, E., 2012. A programmable dual-RNA–guided DNA endonuclease in adaptive bacterial immunity. *Science.* 337**,** 816-821.

Kalinowski, J., Bathe, B., Bartels, D., Bischoff, N., Bott, M., Burkovski, A., Dusch, N., Eggeling, L., Eikmanns, B. J., Gaigalat, L., 2003. The complete *Corynebacterium glutamicum* ATCC 13032 genome sequence and its impact on the production of L-aspartate-derived amino acids and vitamins. *Journal of biotechnology.* 104**,** 5-25.

Kallscheuer, N., Vogt, M., Stenzel, A., Gätgens, J., Bott, M., Marienhagen, J., 2016. Construction of a *Corynebacterium glutamicum* platform strain for the production of stilbenes and (2S)-flavanones. *Metabolic Engineering.*

Karakousis, G., Ye, N., Li, Z., Chiu, S., Reddy, G., Radding, C., 1998. The beta protein of phage λ binds preferentially to an intermediate in DNA renaturation. *Journal of molecular biology.* 276**,** 721-731.

Katashkina, J. I., Hara, Y., Golubeva, L. I., Andreeva, I. G., Kuvaeva, T. M., Mashko, S. V., 2009. Use of the lambda Red-recombineering method for genetic engineering of *Pantoea ananatis*. *BMC Mol Biol.* 10**,** 34.

Keilhauer, C., Eggeling, L., Sahm, H., 1993. Isoleucine synthesis in *Corynebacterium glutamicum*: molecular analysis of the *ilvB-ilvN-ilvC* operon. *Journal of Bacteriology.* 175**,** 5595-5603.

Kim, I. K., Jeong, W. K., Lim, S. H., Hwang, I. K., Kim, Y. H., 2011. The small ribosomal protein S12P gene *rpsL* as an efficient positive selection marker in allelic exchange mutation systems for *Corynebacterium glutamicum*. *Journal of microbiological methods.* 84**,** 128-130.

Kim, J. M., Lee, K. H., Lee, S. Y., 2008. Development of a markerless gene knock-out system for *Mannheimia succiniciproducens* using a temperature-sensitive plasmid. *FEMS microbiology letters.* 278**,** 78-85.

Kind, S., Jeong, W. K., Schröder, H., Zelder, O., Wittmann, C., 2010. Identification and elimination of the competing N-acetyldiaminopentane pathway for improved production of diaminopentane by *Corynebacterium glutamicum*. *Applied and environmental microbiology*. 76**,** 5175-5180.

Kinoshita, S., Udaka, S., Shimono, M., 2004. Studies on the amino acid fermentation. Part 1. Production of L-glutamic acid by various microorganisms. *The Journal of general and applied microbiology*. 50**,** 331-343.

Kirchner, O., Tauch, A., 2003. Tools for genetic engineering in the amino acid-producing bacterium *Corynebacteriumglutamicum*. *Journal of biotechnology.* 104**,** 287-299.

Klaffl, S., Brocker, M., Kalinowski, J., Eikmanns, B. J., Bott, M., 2013. Complex regulation of the phosphoenolpyruvate carboxykinase gene *pck* and characterization of its GntR-type regulator IolR as a repressor of myo-inositol utilization genes in *Corynebacterium glutamicum*. *Journal of bacteriology*. 195**,** 4283-4296.

Koenen, M., Rüther, U., Müller-Hill, B., 1982. Immunoenzymatic detection of expressed gene fragments cloned in the *lac Z* gene of *E. coli*. *The EMBO journal*. 1**,** 509.

Krubasik, P., Takaichi, S., Maoka, T., Kobayashi, M., Masamoto, K., Sandmann, G., 2001. Detailed biosynthetic pathway to decaprenoxanthin diglucoside in *Corynebacterium glutamicum* and identification of novel intermediates. *Archives of microbiology.* 176**,** 217-223.

Krylov, A. A., Kolontaevsky, E. E., Mashko, S. V., 2014. Oligonucleotide recombination in corynebacteria without the expression of exogenous recombinases. *Journal of microbiological methods.* 105**,** 109-115.

Kuhlman, T. E., Cox, E. C., 2010. Site-specific chromosomal integration of large synthetic constructs. *Nucleic Acids Res.* gkp1193.

Larson, M. H., Gilbert, L. A., Wang, X., Lim, W. A., Weissman, J. S., Qi, L. S., 2013. CRISPR interference (CRISPRi) for sequence-specific control of gene expression. *Nature protocols.* 8**,** 2180-2196.

Lausberg, F., Chattopadhyay, A. R., Heyer, A., Eggeling, L., Freudl, R., 2012. A tetracycline inducible expression vector for *Corynebacterium glutamicum* allowing tightly regulable gene expression. *Plasmid.* 68**,** 142-147.

Li, Y., Lin, Z., Huang, C., Zhang, Y., Wang, Z., Tang, Y.-j., Chen, T., Zhao, X., 2015. Metabolic engineering of *Escherichia coli* using CRISPR–Cas9 meditated genome editing. *Metabolic engineering.* 31**,** 13-21.

Li, Z., Karakousis, G., Chiu, S., Reddy, G., Radding, C., 1998. The beta protein of phage λ promotes strand exchange. *Journal of molecular biology.* 276**,** 733-744.

Liang, F., Han, M., Romanienko, P. J., Jasin, M., 1998. Homology-directed repair is a major double-strand break repair pathway in mammalian cells. *Proceedings of the National Academy of Sciences.* 95**,** 5172-5177.

Litsanov, B., Kabus, A., Brocker, M., Bott, M., 2012. Efficient aerobic succinate production from glucose in minimal medium with *Corynebacterium glutamicum*. *Microbial biotechnology.* 5**,** 116-128.

Liu, H., Han, J., Liu, X., Zhou, J., Xiang, H., 2011. Development of *pyrF*-based gene knockout systems for genome-wide manipulation of the archaea *Haloferax mediterranei* and *Haloarcula hispanica*. *Journal of Genetics and Genomics.* 38**,** 261-269.

Liu, X. P., Liu, J. H., 2010. The terminal 5′ phosphate and proximate phosphorothioate promote ligation-independent cloning. *Protein Science.* 19**,** 967-973.

Makarova, K. S., Haft, D. H., Barrangou, R., Brouns, S. J., Charpentier, E., Horvath, P., Moineau, S., Mojica, F. J., Wolf, Y. I., Yakunin, A. F., 2011. Evolution and classification of the CRISPR–Cas systems. *Nature Reviews Microbiology*. 9**,** 467-477.

Mali, P., Aach, J., Stranges, P. B., Esvelt, K. M., Moosburner, M., Kosuri, S., Yang, L., Church, G. M., 2013. CAS9 transcriptional activators for target specificity screening and paired nickases for cooperative genome engineering. *Nature biotechnology.* 31**,** 833-838.

Maresca, M., Erler, A., Fu, J., Friedrich, A., Zhang, Y., Stewart, A. F., 2010. Single-stranded heteroduplex intermediates in lambda Red homologous recombination. *BMC Mol Biol.* 11**,** 54.

Marraffini, L. A., Sontheimer, E. J., 2010. CRISPR interference: RNA-directed adaptive immunity in bacteria and archaea. *Nature Reviews Genetics.* 11**,** 181-190.

Mashiko, D., Young, S. A., Muto, M., Kato, H., Nozawa, K., Ogawa, M., Noda, T., Kim, Y. J., Satouh, Y., Fujihara, Y., 2014. Feasibility for a large scale mouse mutagenesis by injecting CRISPR/Cas plasmid into zygotes. *Development, growth & differentiation*. 56**,** 122-129.

Mengin-Lecreulx, D., Parquet, C., Desviat, L. R., Plá, J., Flouret, B., Ayala, J. A., van Heijenoort, J., 1989. Organization of the *murE-murG* region of *Escherichia coli*: identification of the *murD* gene encoding the D-glutamic-acid-adding enzyme. *Journal of bacteriology.* 171**,** 6126-6134.

Möker, N., Brocker, M., Schaffer, S., Krämer, R., Morbach, S., Bott, M., 2004. Deletion of the genes encoding the MtrA–MtrB two-component system of *Corynebacterium glutamicum* has a strong influence on cell morphology, antibiotics susceptibility and expression of genes involved in osmoprotection. *Molecular microbiology.* 54**,** 420-438.

Mosberg, J. A., Lajoie, M. J., Church, G. M., 2010. Lambda red recombineering in *Escherichia coli* occurs through a fully single-stranded intermediate. *Genetics.* 186**,** 791-9.

Mullis, K. B., Faloona, F. A., 1987. [21] Specific synthesis of DNA in vitro via a polymerase-catalyzed chain reaction. *Methods in enzymology*. 155**,** 335-350.

Murgha, Y. E., Rouillard, J.-M., Gulari, E., 2014. Methods for the preparation of large quantities of complex single-stranded oligonucleotide libraries. *PLoS One.* 9**,** e94752.

Murphy, K. C., 1998. Use of bacteriophage λ recombination functions to promote gene replacement in *Escherichia coli*. *Journal of bacteriology*. 180**,** 2063-2071.

Murphy, K. C., Campellone, K. G., Poteete, A. R., 2000. PCR-mediated gene replacement in *Escherichia coli*. *Gene.* 246**,** 321-330.

Muyrers, J. P., Zhang, Y., Buchholz, F., Stewart, A. F., 2000. RecE/RecT and Redα/Redβ initiate double-stranded break repair by specifically interacting with their respective partners. *Genes & development.* 14**,** 1971-1982.

Nakamura, J., Kanno, S., Kimura, E., Matsui, K., Nakamatsu, T., Wachi, M., 2006. Temperature-sensitive cloning vector for *Corynebacterium glutamicum*. *Plasmid*. 56**,** 179-186.

Oh, J.-H., van Pijkeren, J.-P., 2014. CRISPR–Cas9-assisted recombineering in *Lactobacillus reuteri*. *Nucleic Acids Res.* gku623.

Okibe, N., Suzuki, N., Inui, M., Yukawa, H., 2011. Efficient markerless gene replacement in *Corynebacterium glutamicum* using a new temperature-sensitive plasmid. *Journal of microbiological methods.* 85**,** 155-163.

Okino, S., Suda, M., Fujikura, K., Inui, M., Yukawa, H., 2008. Production of D-lactic acid by *Corynebacterium glutamicum* under oxygen deprivation. *Applied microbiology and biotechnology*. 78**,** 449-454.

Otten, A., Brocker, M., Bott, M., 2015. Metabolic engineering of *Corynebacterium glutamicum* for the production of itaconate. *Metabolic engineering.* 30**,** 156-165.

Park, S. H., Kim, H. U., Kim, T. Y., Park, J. S., Kim, S.-S., Lee, S. Y., 2014. Metabolic engineering of *Corynebacterium glutamicum* for L-arginine production. *Nature communications.* 5.

Pascual, C., Lawson, P. A., Farrow, J. A., GIMENEZ, M. N., Collins, M. D., 1995. Phylogenetic analysis of the genus Corynebacterium based on 16S rRNA gene sequences. *International Journal of Systematic and Evolutionary Microbiology*. 45**,** 724-728.

Pátek, M., Nešvera, J., Hochmannová, J., 1989. Plasmid cloning vectors replicating in *Escherichia coli*, amino acid-producing coryneform bacteria and *Methylobacillus sp*. *Applied microbiology and biotechnology.* 31**,** 65-69.

Pérez-García, F., Peters-Wendisch, P., Wendisch, V. F., 2016. Engineering *Corynebacterium glutamicum* for fast production of L-lysine and L-pipecolic acid. *Applied microbiology and biotechnology.* 100**,** 8075-8090.

Pfeiffer, P., Thode, S., Hancke, J., Vielmetter, W., 1994. Mechanisms of overlap formation in nonhomologous DNA end joining. *Molecular and Cellular Biology.* 14**,** 888-895.

Pyne, M. E., Moo-Young, M., Chung, D. A., Chou, C. P., 2015. Coupling the CRISPR/Cas9 System with Lambda Red Recombineering Enables Simplified Chromosomal Gene Replacement in *Escherichia coli*. *Applied and environmental microbiology.* 81**,** 5103-5114.

Qi, L. S., Larson, M. H., Gilbert, L. A., Doudna, J. A., Weissman, J. S., Arkin, A. P., Lim, W. A., 2013. Repurposing CRISPR as an RNA-guided platform for sequence-specific control of gene expression. *Cell.* 152**,** 1173-1183.

Ran, F. A., Hsu, P. D., Lin, C.-Y., Gootenberg, J. S., Konermann, S., Trevino, A. E., Scott, D. A., Inoue, A., Matoba, S., Zhang, Y., 2013. Double nicking by RNA-guided CRISPR Cas9 for enhanced genome editing specificity. *Cell.* 154**,** 1380-1389.

Redder, P., Linder, P., 2012. A new range of vectors with a stringent 5-fluoro orotic acid-based counterselection system for generating mutants by allelic replacement in *Staphylococcus aureus*. *Applied and environmental microbiology. AEM.* 00202-12.

Riviere, K., Kieler-Ferguson, H. M., Jerger, K., Szoka, F. C., 2011. Anti-tumor activity of liposome encapsulated fluoroorotic acid as a single agent and in combination with liposome irinotecan. *Journal of controlled release.* 153**,** 288-296.

Ruane, K. M., Lloyd, A. J., Fülöp, V., Dowson, C. G., Barreteau, H., Boniface, A., Dementin, S., Blanot, D., Mengin-Lecreulx, D., Gobec, S., 2013. Specificity determinants for lysine incorporation in *Staphylococcus aureus* peptidoglycan as revealed by the structure of a MurE enzyme ternary complex. *Journal of Biological Chemistry*. 288**,** 33439-33448.

Sambrook, J., Fritsch, E. F., Maniatis, T., 1989. Molecular cloning. *Cold spring harbor laboratory press New York.*

Sander, J. D., Joung, J. K., 2014. CRISPR-Cas systems for editing, regulating and targeting genomes. *Nature biotechnology*. 32**,** 347-355.

Sanger, F., Nicklen, S., Coulson, A. R., 1977. DNA sequencing with chain-terminating inhibitors. *Proceedings of the National Academy of Sciences.* 74**,** 5463-5467.

Santamaria, R., Gil, J. A., Mesas, J. M., Martin, J. F., 1984. Characterization of an endogenous plasmid and development of cloning vectors and a transformation system in *Brevibacterium lactofermentum*. *Microbiology.* 130**,** 2237-2246.

Sapranauskas, R., Gasiunas, G., Fremaux, C., Barrangou, R., Horvath, P., Siksnys, V., 2011. The *Streptococcus thermophilus* CRISPR/Cas system provides immunity in *Escherichia coli*. *Nucleic Acids Res.* gkr606.

Sawitzke, J. A., Costantino, N., Li, X.-t., Thomason, L. C., Bubunenko, M., Court, C., Court, D. L., 2011. Probing cellular processes with oligo-mediated recombination and using the knowledge gained to optimize recombineering. *Journal of molecular biology.* 407**,** 45-59.

Schäfer, A., Tauch, A., Jäger, W., Kalinowski, J., Thierbach, G., Pühler, A., 1994. Small mobilizable multi-purpose cloning vectors derived from the *Escherichia coli* plasmids pK18 and pK19: selection of defined deletions in the chromosome of *Corynebacterium glutamicum*. *Gene.* 145**,** 69-73.

Schrumpf, B., Eggeling, L., Sahm, H., 1992. Isolation and prominent characteristics of an L-lysine hyperproducing strain of *Corynebacterium glutamicum*. *Applied microbiology and biotechnology.* 37**,** 566-571.

Schwarzer, A., Pühler, A., 1991. Manipuiation of *Corynebacterium glutamicum* by Gene Disruption and Replacement. *Nature Biotechnology.* 9**,** 84-87.

Semenova, E., Jore, M. M., Datsenko, K. A., Semenova, A., Westra, E. R., Wanner, B., van der Oost, J., Brouns, S. J., Severinov, K., 2011. Interference by clustered regularly interspaced short palindromic repeat (CRISPR) RNA is governed by a seed sequence. *Proceedings of the National Academy of Sciences.* 108**,** 10098-10103.

Shanmugam, A., Natarajan, J., 2014. Combination of site directed mutagenesis and secondary structure analysis predicts the amino acids essential for stability of *M. leprae* MurE. *Interdisciplinary Sciences: Computational Life Sciences.* 6**,** 40-47.

Sharan, S. K., Thomason, L. C., Kuznetsov, S. G., Court, D. L., 2009. Recombineering: a homologous recombination-based method of genetic engineering. *Nature protocols.* 4**,** 206-223.

Shenkerman, Y., Elharar, Y., Vishkautzan, M., Gur, E., 2014. Efficient and simple generation of unmarked gene deletions in *Mycobacterium smegmatis*. *Gene.* 533**,** 374-378.

Shuman, S., Glickman, M. S., 2007. Bacterial DNA repair by non-homologous end joining. *Nature Reviews Microbiology*. 5**,** 852-861.

Silo-Suh, L. A., Elmore, B., Ohman, D. E., Suh, S.-J., 2009. Isolation, characterization, and utilization of a temperature-sensitive allele of a Pseudomonas replicon. *Journal of microbiological methods*. 78**,** 319-324.

Smith, K. M., Cho, K.-M., Liao, J. C., 2010. Engineering *Corynebacterium glutamicum* for isobutanol production. *Applied microbiology and biotechnology.* 87**,** 1045-1055.

Stern, A., Keren, L., Wurtzel, O., Amitai, G., Sorek, R., 2010. Self-targeting by CRISPR: gene regulation or autoimmunity? *Trends in genetics.* 26**,** 335-340.

Subramanian, K., Rutvisuttinunt, W., Scott, W., Myers, R. S., 2003. The enzymatic basis of processivity in λ exonuclease. *Nucleic Acids Res.* 31**,** 1585-1596.

Suzuki, N., Inui, M., 2013. Genome engineering of *Corynebacterium glutamicum*. *Corynebacterium glutamicum. Springer,* pp. 89-105.

Swaminathan, S., Ellis, H. M., Waters, L. S., Yu, D., Lee, E.-C., Court, D. L., Sharan, S. K., 2001. Rapid engineering of bacterial artificial chromosomes using oligonucleotides. *genesis.* 29**,** 14-21.

Swingle, B., Bao, Z., Markel, E., Chambers, A., Cartinhour, S., 2010. Recombineering using RecTE from *Pseudomonas syringae*. *Applied and environmental microbiology.* 76**,** 4960-8.

Takumi, K., Nonaka, G., 2016. Bacterial cysteine-inducible cysteine resistance systems. *Journal of bacteriology*. 198**,** 1384-1392.

Tauch, A., Kirchner, O., Löffler, B., Götker, S., Pühler, A., Kalinowski, J., 2002. Efficient electrotransformation of *Corynebacterium diphtheriae* with a mini-replicon derived from the *Corynebacterium glutamicum* plasmid pGA1. *Current microbiology.* 45**,** 362-367.

Thiel, A., Michoud, G., Moalic, Y., Flament, D., Jebbar, M., 2014. Genetic manipulations of the hyperthermophilic piezophilic archaeon *Thermococcus barophilus*. *Applied and environmental microbiology.* 80**,** 2299-2306.

Tong, Y., Charusanti, P., Zhang, L., Weber, T., Lee, S. Y., 2015. CRISPR-Cas9 based engineering of actinomycetal genomes. *ACS synthetic biology*. 4**,** 1020-1029.

Trautwetter, A., Blanco, C., 1991. Structural organization of the *Corynebacterium glutamicum* plasmid pCG100. *Microbiology*. 137**,** 2093-2101.

Tripathi, S. A., Olson, D. G., Argyros, D. A., Miller, B. B., Barrett, T. F., Murphy, D. M., McCool, J. D., Warner, A. K., Rajgarhia, V. B., Lynd, L. R., 2010. Development of *pyrF*-based genetic system for targeted gene deletion in *Clostridium thermocellum* and creation of a pta mutant. *Applied and environmental microbiology*. 76**,** 6591-6599.

van Kessel, J. C., Hatfull, G. F., 2007. Recombineering in *Mycobacterium tuberculosis*. *Nat Methods.* 4**,** 147-52.

van Ooyen, J., Noack, S., Bott, M., Reth, A., & Eggeling, L., 2012. Improved L-lysine production with *Corynebacterium glutamicum* and systemic insight into citrate synthase flux and activity. *Biotechnology and bioengineering*. 109, 2070-2081.

Vertes, A. A., Inui, M., Yukawa, H., 2013. The biotechnological potential of *Corynebacterium glutamicum*, from Umami to Chemurgy. Corynebacterium glutamicum. *Springer,* pp. 1-49.

Wang, Y., Weng, J., Waseem, R., Yin, X., Zhang, R., Shen, Q., 2012. *Bacillus subtilis* genome editing using ssDNA with short homology regions. *Nucleic Acids Res.* gks248.

Wang, Y., Zhang, Z.-T., Seo, S.-O., Choi, K., Lu, T., Jin, Y.-S., Blaschek, H. P., 2015. Markerless chromosomal gene deletion in *Clostridium beijerinckii* using CRISPR/Cas9 system. *Journal of biotechnology*. 200**,** 1-5.

Wendisch, V. F., Jorge, J. M., Pérez-García, F., Sgobba, E., 2016. Updates on industrial production of amino acids using *Corynebacterium glutamicum*. *World Journal of Microbiology and Biotechnology*. 32**,** 1-10.

Wiedenheft, B., van Duijn, E., Bultema, J. B., Waghmare, S. P., Zhou, K., Barendregt, A., Westphal, W., Heck, A. J., Boekema, E. J., Dickman, M. J., 2011. RNA-guided complex from a bacterial immune system enhances target recognition through seed sequence interactions. *Proceedings of the National Academy of Sciences.* 108**,** 10092-10097.

Wieschalka, S., Blombach, B., Bott, M., Eikmanns, B. J., 2013. Bio-based production of organic acids with *Corynebacterium glutamicum*. *Microbial biotechnology*. 6**,** 87-102.

Witthoff, S., Schmitz, K., Niedenführ, S., Nöh, K., Noack, S., Bott, M., Marienhagen, J., 2015. Metabolic engineering of *Corynebacterium glutamicum* for methanol metabolism. *Applied and environmental microbiology*. 81**,** 2215-2225.

Yang, P., Wang, J., Qi, Q., 2015. Prophage recombinases-mediated genome engineering in *Lactobacillus plantarum*. *Microbial cell factories*. 14**,** 1.

Yeh, P., Sicard, A. M., Sinskey, A. J., 1988. General organization of the genes specifically involved in the diaminopimelate-lysine biosynthetic pathway of *Corynebacterium glutamicum. Molecular and General Genetics MGG.* 212**,** 105-111.

Yim, S. S., An, S. J., Kang, M., Lee, J., Jeong, K. J., 2013. Isolation of fully synthetic promoters for high-level gene expression in *Corynebacterium glutamicum*. *Biotechnology and bioengineering.* 110**,** 2959-2969.

Yu, D., Ellis, H. M., Lee, E. C., Jenkins, N. A., Copeland, N. G., Court, D. L., 2000. An efficient recombination system for chromosome engineering in *Escherichia coli*. *Proc Natl Acad Sci U S A.* 97**,** 5978-83.

Zahoor, A., Lindner, S. N., Wendisch, V. F., 2012. Metabolic engineering of *Corynebacterium glutamicum* aimed at alternative carbon sources and new products. *Computational and structural biotechnology journal.* 3**,** 1-11.

Zhang, X., Yan, J., Yu, L., Zhang, G., Zhang, Y., Chen, N., Wen, T., 2009. Construction of recombinant plasmids containing threonine operon and their effects on L-threonine accumulation. *Acta microbiologica Sinica.* 49**,** 591-596.

Zhang, Y., Buchholz, F., Muyrers, J. P., Stewart, A. F., 1998. A new logic for DNA engineering using recombination in *Escherichia coli*. *Nature genetics.* 20**,** 123-128.

Supplementary Data

Oligonucleotides

Tab. 11: Oligonucleotides for ssDNA recombineering

Name	Sequence (5'-3')	Characteristics
Kan80*_F	AGGAGTACGGATAAAATGCTTGATGGTCGGAAGAGGCATAAATTC CGTCAGCCAGTTTAGTCTGACCATCTCATCTGTA	
Oligo Kan80fw	AGGAGTACGGATAAAATGCTTGATGGTCGGAAGAGGCATAAATTC CGTCAGCCAGTTTAGTCTGACCATCTCATCTGTA	
Oligo Kan80*rv	AGGAGTACGGATAAAATGCTTGATGGTCGGAAGAGGCATAAATTC CGTCAGCCAGTTTAGTCTGACCATCTCATCTGTAA	
Oligo Kan80fw-PHO	PHO-TTACAGATGAGATGGTCAGACTAAACTGGCTGACGGAATTTATGC CTCTTCCGACCATCAAGCATTTTATCCGTACTCCT	5' PHO
Oligo Kan80*rv-PHO	PHO-AGGAGTACGGATAAAATGCTTGATGGTCGGAAGAGGCATAAATTC CGTCAGCCAGTTTAGTCTGACCATCTCATCTGTAA	5' PHO
Oligo Kan80fw-4PTO	aggaGTACGGATAAAATGCTTGATGGTCGGAAGAGGCATAAATTC CGTCAGCCAGTTTAGTCTGACCATCTCATCTGTA	5' PTO
Oligo Kan80rv-4PTO	ttacAGATGAGATGGTCAGACTAAACTGGCTGACGGAATTTATGCC TCTTCCGACCATCAAGCATTTTATCCGTACTCCT	5' PTO
murEG81E*	AACAACGATGACTGGGCGGGTCTCTCCTGCTTCGTTGAGCACCTC AAGTTCAGCGGCGTCAGTCAAAATGGCCACAGCTTTCGCAGCGTT ATCCGTACCT	
rpsL_rv	TCGATGCCGGAGGTAAGGCGCACACGAGCGACCTTACGAAGAGCA GAGTTAGGCTTGCGCGGGGTGGTGGTGTACACACGGGTGCATACG CCACGACGCT	
rpsL_wt	TCGATGCCGGAGGTAAGGCGCACACGAGCGACCTTACGAAGAGCA GAGTTAGGCTTCTTAGGGGTGGTGGTGTACACACGGGTGCATACG CCACGACGCT	
Olig_pyrF-fw*PHO	PHO-AGCCCTATGACATTCGGCGAGAAGCTTCTGAACGCCGCCTACCCGT GGCAGGCTATGCGTGGGCATTGATCCCCACGAAA	5' PHO
Oligo lacZ-fw	GAGCCGACACCACGGCCACCGATATTATTTGCCCGATGTACGCGC GCGTATGAAGACCAGCCCTTCCCGGCTGTGCCGAAATGGTCCATC AAAAAATGGC	
Oligo lacZ-rv	AAGCCATTTTTTGATGGACCATTTCGGCACAGCCGGGAAGGGCTG GTCTTCATACGCGCGCGTACATCGGGCAAATAATATCGGTGGCCG TGGTGTCGGC	
OliReplacZ(+1)f	ACCACGGCCACCGATATTATTTGCCCGATGTACGCGCGCGTGGAT GAAGACCAGCCCTTCCCGGCTGTGCCGAAATGGTCCATCAAAAAA TGGCTTTCGC	
OliReplacZ(+1)r	AGCGAAAGCCATTTTTTGATGGACCATTTCGGCACAGCCGGGAAG GGCTGGTCTTCATCCACGCGCGCGTACATCGGGCAAATAATATCG GTGGCCGTGG	

Tab. 12: Oligonucleotides for DNA substrate generation for dsDNA recombineering

Name	Sequence (5‘-3‘)	Characteristics
NCR(1)-F	TTGGCTCCGTTGTTCACGTCTAC	
NCR(2)-R	ATCTGCGGCAGTCACTTTGTTTACG	
NCR(a)-F	TGTTGTCTTCTCCTGGAGGC	
NCR(b)-R	CTTCTCAGAATCGCCTGTGG	
kan-ds-fw	AAGCCCGATGCGCCAGAGTTGTTTC	
kan-ds600-rv	CTCACCGAGGCAGTTCCATAGG	
Kan400HA_fw	CAAAGCCACGTTGTGTC	
Kan400HA_rv	TCTGCCAGTGTTACAACC	
Kan900HA_fw	GGAAAAACGGCTTTGCCGC	
Kan900HA_rv	CACCTTCCAAGATGGCATGGG	
KanR-HA845fw	TTGGCTCCGTTGTTCACGTC	
KanR-HA845rv	TCTGCGGCAGTCACTTTGAT	
Kan400fw-752	AACCGAAAGGCAGGAACAG	
Kan900fw-752	AAGGCCTAGTGTTCACTCAG	
Kan100_fw	GCCAATGATGTTACAGATG	
Kan100_rv	ATGCATCATCAGGAGTACGG	
KanHA900fw PHO	PHO-GGAAAAACGGCTTTGCCGC	5' PHO
KanHA900RV 4-PTO	caccTTCCAAGATGGCATG	5‘ PTO
pcr-lacZ(+1)-fw	GCCTGTATGTGGTGGATGAAG	
pcr-lacZ(+1)-rv	TCGGCAAAGACCAGACCGTTC	
pcr-lacZ(+1)-PHO	PHO-GCCTGTATGTGGTGGATGAAG	5' PHO
ds-murEG91E-for	GTGCCGCGTCCGAATTATTAACACC	
ds-murEG91E-rv	GCGCATTCGAGCAAACAATGCC	

Tab. 13: Oligonucleotides for construction of plasmids

Name	Sequence (5'-3')	Characteristics
SalI-recET-F	CGCTGCAGGTCGACAAGGAGATATAC	*Sal*I
SacI-recET-R	CCGAGCTCTGAATTATTCCTCTGAATTATCGATTAC	*Sac*I
SalI-1963-fw	GCCGTCGACAAGGAGATATAGATATGAATAATACCAC	*Sal*I
1963-rv	CCCATTGTTAGTTCTCCTTTACAGGGTTGATGC	
1962-fw	GTAAAGGAGAACTAACAATGGGAAACAATCTAGAG	
SacI-1962-rv	GTGAGCTCCAGGCTGAATTATTCCTCTG	*Sac*I
SOE-revE-rv	GGTGGTTGCTTAGTCATTTGCATATTCCTTAG	
SOE-recT-fw	TGCAAATGACTAAGCAACCACCAATCG	
kan(-131)fw	CGCGTATTTCGTCTCGCTCAGG	
kan(-50)rv	ATCGCAGTGGTGAGTAAC	
NCR1fw	GGATCTAGATTGGCTCCGTTGTTCAC	*Xba*I
NCR2rv	GCATATGCCCGGGAGTACTGGATCCCTCATGGACACAATTTAAACTTC	
NCR3fw	GGATCCAGTACTCCCGGGCATATGCTTCGCGTATGGCAATGAC	
NCR4rv	CGTCCGAATTCATCTGCGGCAGTCACTTTGA	*EcoR*I
pcas9-XhoI-fw	GGCTCGAGGAAGTCACTTTGATGTTTACTTAAACG	*Xho*I
pcas-XhoI-rv	CTCGAGAACGTCAGTCACCTCCTAGC	XhoI
cas-ptac-xhoI-	ATCTCGAGATTCGGAATCTTGCACGC	XhoI

fw		
cas-ptac-xhoIrv	ATCTCGAGGAATTCGAGCTCGGTAC	*Xho*I
sgRNA_murE-fw-XhoI	CCTCGAGCGAATTCTCGTTGACAGC	*Xho*I
sgRNA_murE-rv-XhoI	GCCTCGAGGGATCCAGTAATGCCAAC	*Xho*I
spec-fw	TCCGATCGCGTAACGTGACTGGCAAG	*Pvu*I
spec-rv	GCGATCGCGATATCATATGCAAGGG	*Pvu*I
sgRNA_fw-SalI	CGTCGACCGAATTCTCGTTGACAGC	*Sal*I
sgRNA_rv-SalI	GCGTCGACGGATCCAGTAATGCCAAC	*Sal*I
cas9-ptac-XmaI	ATCCCGGGTATTCGGAATCTTGCACGC	*Xma*I
cas9-xbaI-fw	CGGTCTAGAAAAGGAGCGCATAATGGATAAGAAATACTCAATAGGC	*Xba*I
lacZ-sgRNA-fw	GTCCTAGGTATAATGCTAGCTTGCCCGATGTACGCGCGCGGTTTTAGAGCTAGA AATAGC	*Avr*II, *Nhe*I
pCterm_pyrF_fw	TGTTTAAGTTTAGTGGATGGGTTTCCTGGTTTCCCCAGGTCATAG	
pCterm_pyrF_rv	TATTCTAGAGAAGTGCGCGACGCTG	
pNterm_pyrF_fw	ATAGTCGACGAAGGAAGCAGTG	
pNterm_pyrF_rv	CCCATCCACTAAACTTAAACACTTCTCGCCGAATGTCATAGG	

Restriction map for constructed plasmids

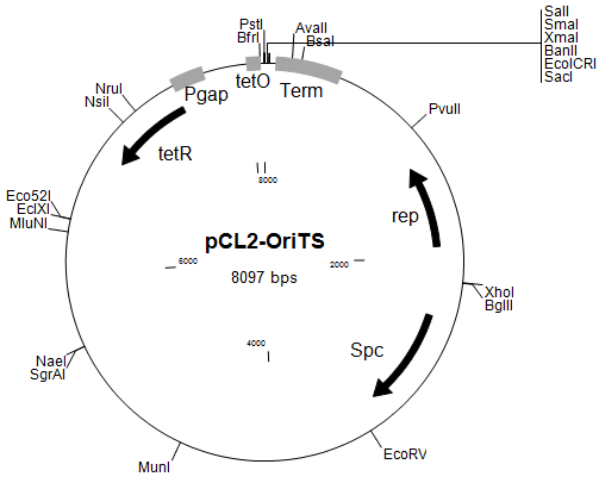

Fig. 21: pCL2-OriTS. Temperature sensitive expression plasmid pCLTON2

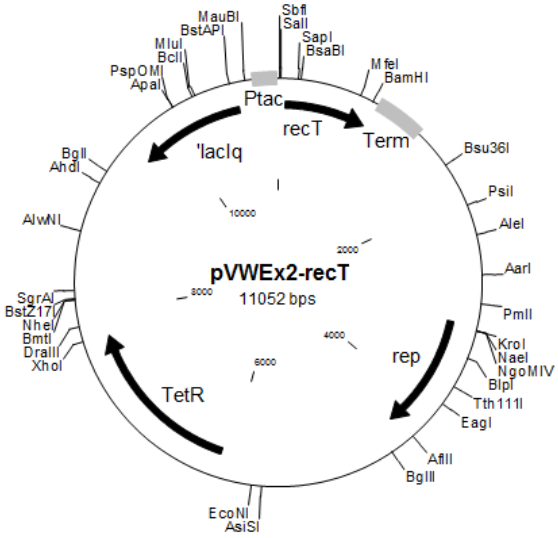

Fig. 22: pVWEX2-recT. Expression plasmid pVWEx2 with *recT* from prophage Rac

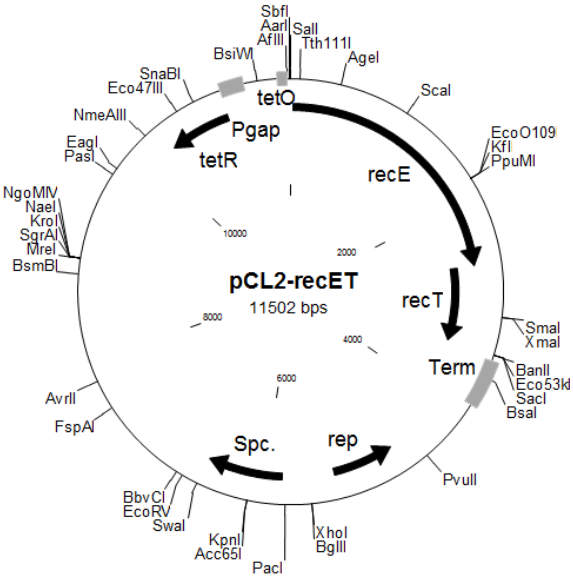

Fig. 23: pCL2-recET. Expression vector plasmid with *recE* and *recT* from prophage Rac

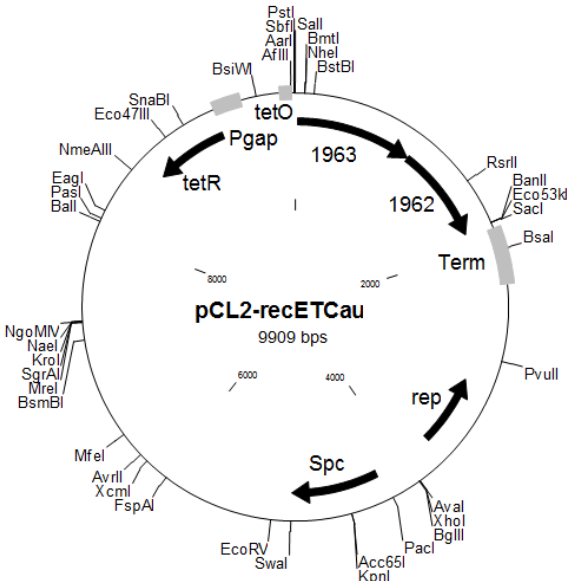

Fig. 24: pCL2-recETCau. Expression plasmid pCLTON2 with RecET homologues *1962* and *1963* from *C. aurimucosum*

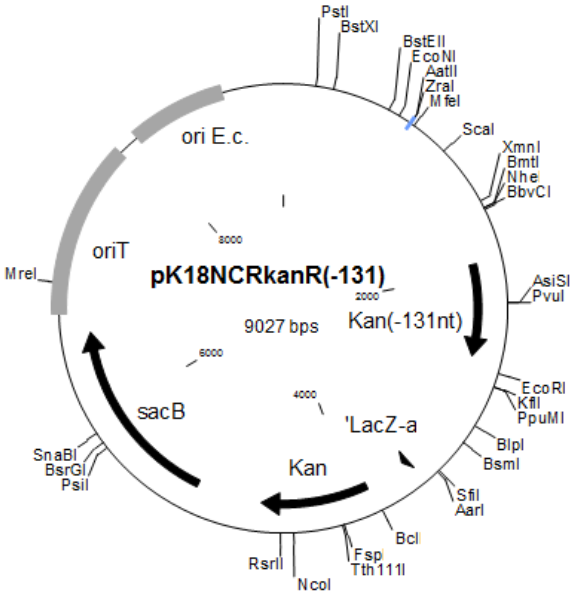

Fig. 25: pK18NCRkanR(-131). Integration plasmid pK18mobsacB with Kan(-131nt) and flanking regions of lysOP7 region

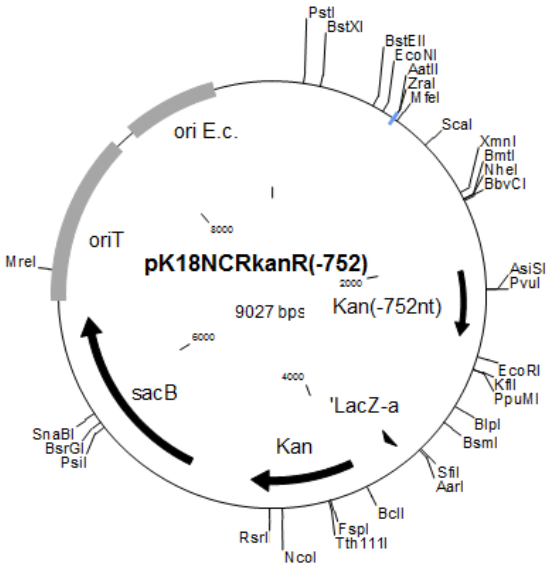

Fig. 26: pK18NCRkanR(-752). Integration plasmid pK18mobsacB with Kan(-752nt) and flanking regions of lysOP7 region

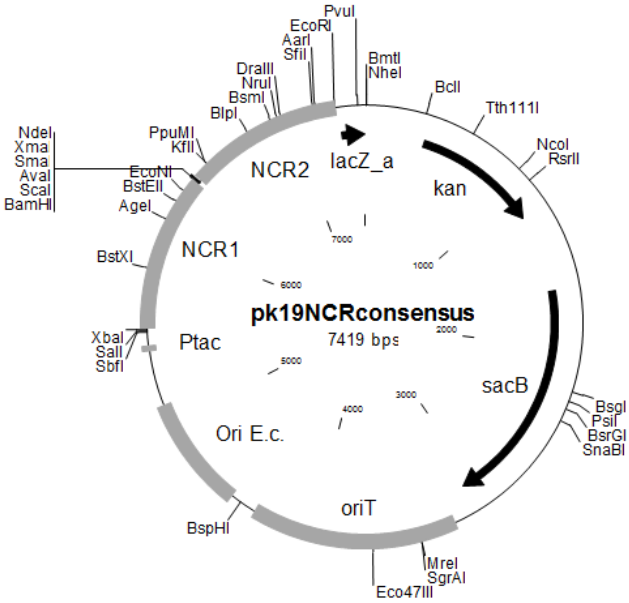

Fig. 27: pK19NCRconsensus. Integration plasmid pK19mobsacB with MCS flanked by lysOP7 regions

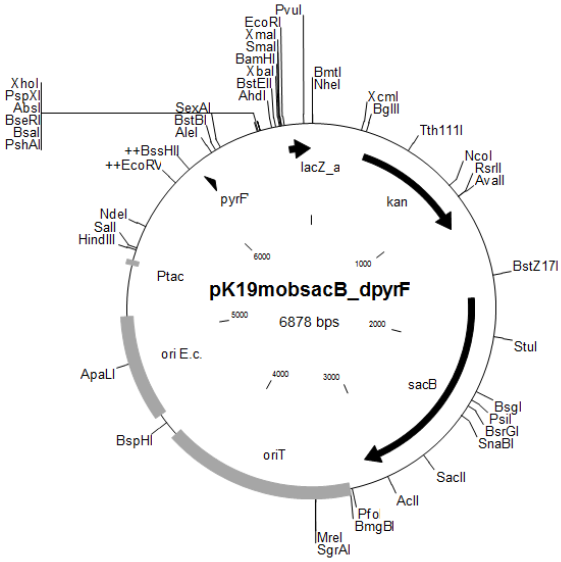

Fig. 28: pK19mobsacB_ΔpyrF. Integration plasmid pK19mobsacB with in frame deletion of *pyrF*

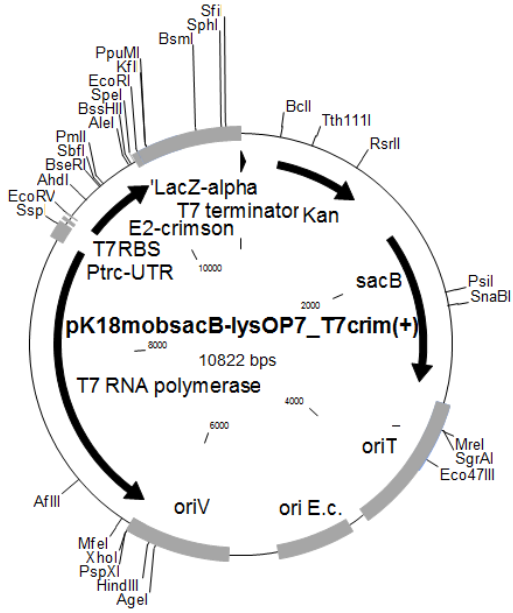

Fig. 29: pK19mobsacB_lysOP7_T7crim(+). Integration plasmid pK19mobsacB with *e2-crimson* under control of T7 expression system

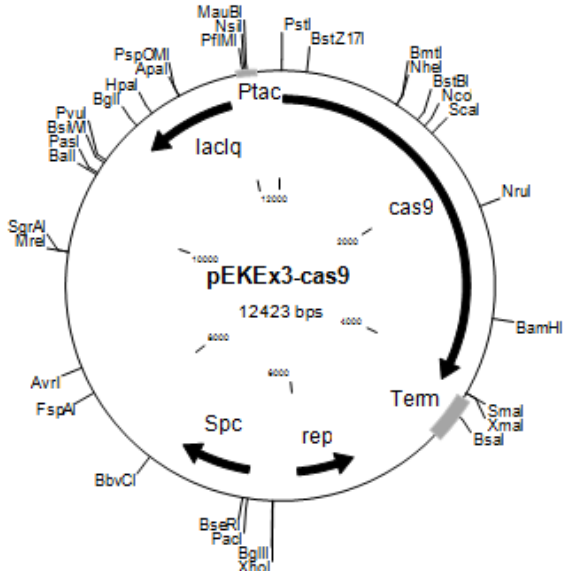

Fig. 30: pEKEx3-cas9. Expression plasmid pEKEx3 with Cas9

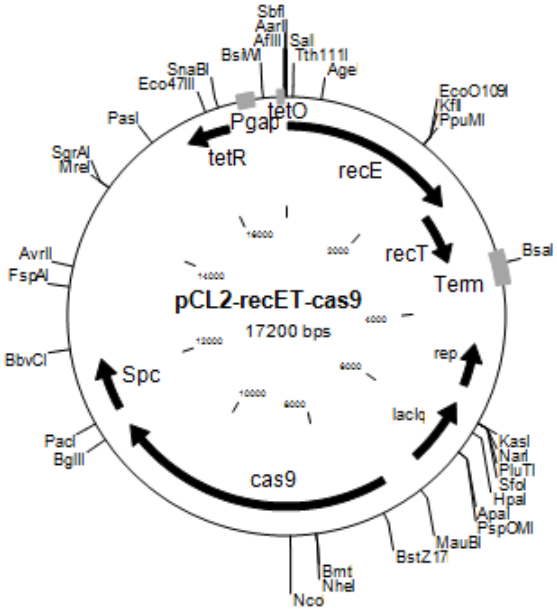

Fig. 31: pCL2-recET-cas9. Expression plasmid pCL2-recET with Cas9 under control of Ptac

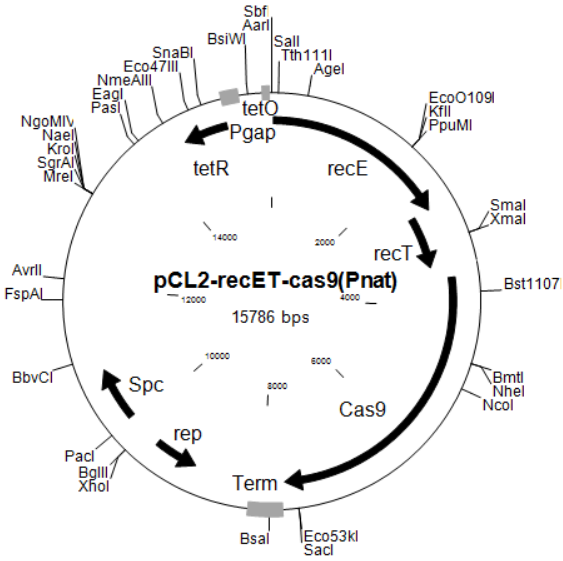

Fig. 32: pCL2-recET-cas9(Pnat). Expression plasmid pCL2-recET with *cas9* under control of native *S. pyogenes* promoter

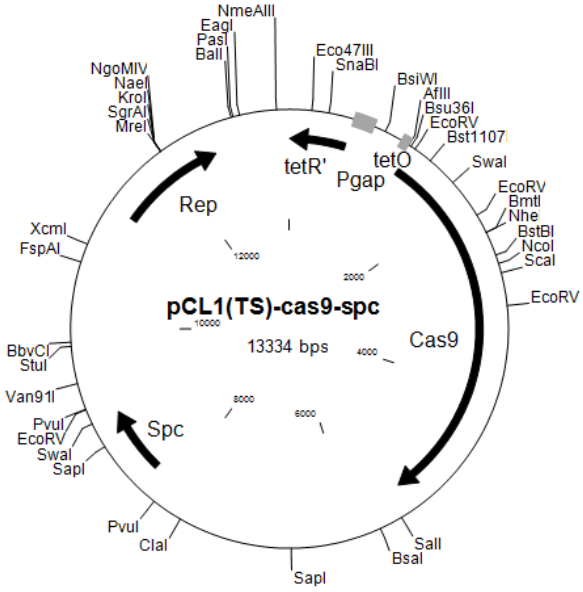

Fig. 33: pCL1(TS)-cas9-spc. Expression plasmid pCL1(TS) with *cas9*

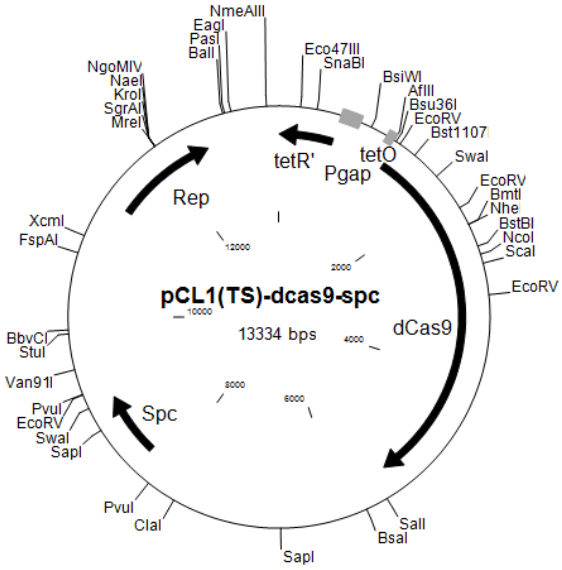

Fig. 34: pCL1(TS)-dcas9-spc. Expression plasmid pCL1(TS) with *dcas9*

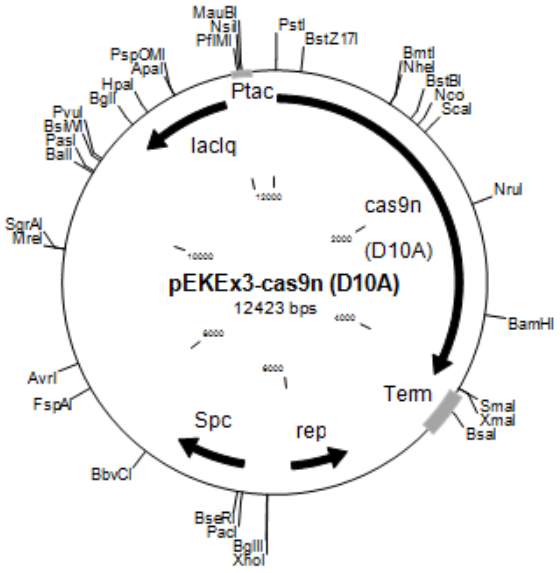

Fig. 35: pEKEx3-cas9n (D10A). Expression plasmid pEKEx3 with *cas9n* (D10A)

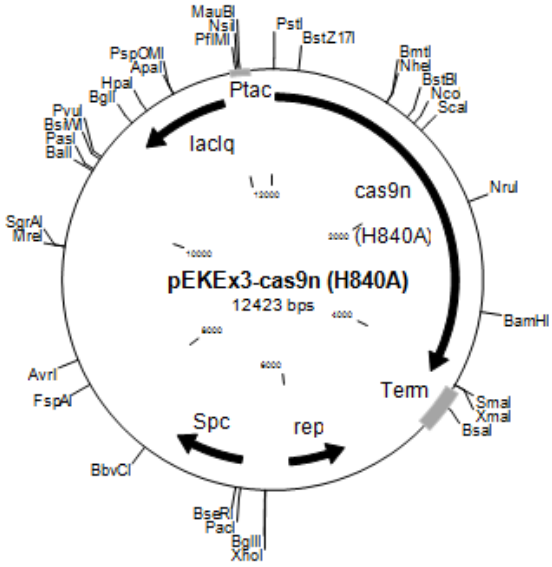

Fig. 36: pEKEx3-cas9n (H840A). Expression plasmid pEKEx3 with *cas9n* (H840A)

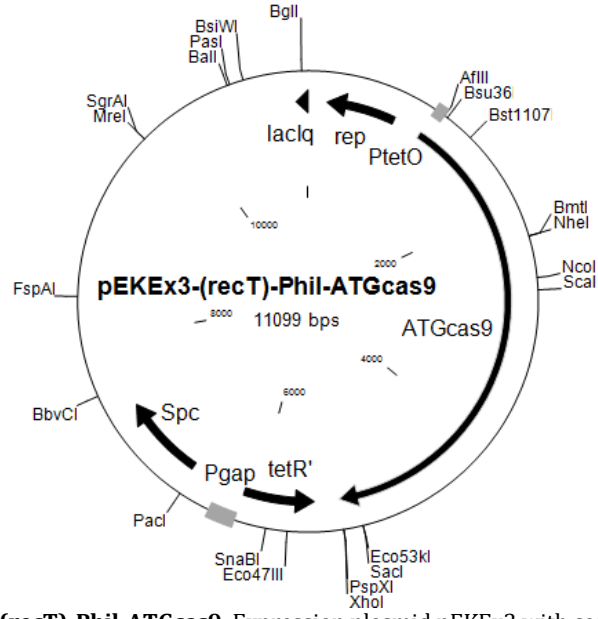

Fig. 37: pEKEx3-(recT)-PhiI-ATGcas9. Expression plasmid pEKEx3 with cas9 under control of TetR expression system

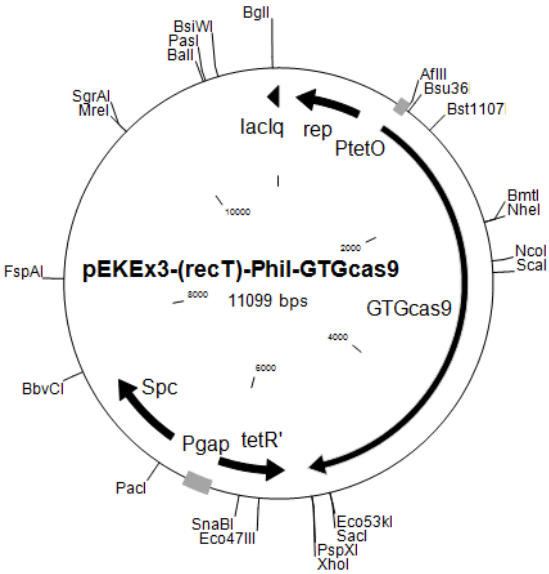

Fig. 38: pEKEx3-(recT)-Phil-GTGcas9. Expression plasmid pEKEx3 with GTGcas9 under control of TetR expression system

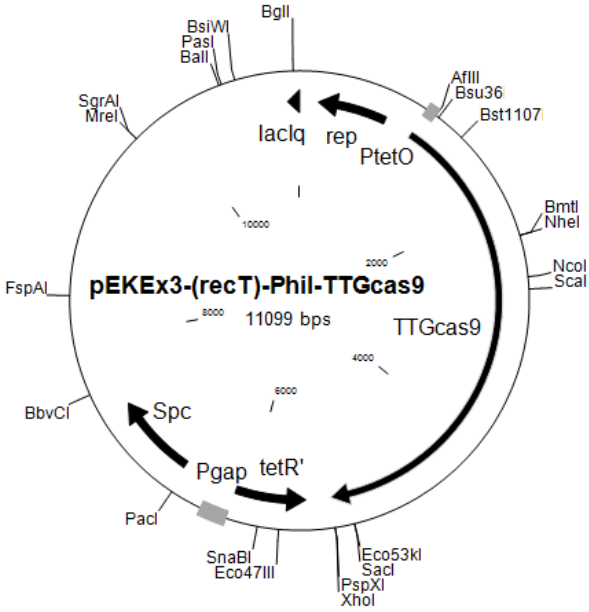

Fig. 39: pEKEx3-(recT)-Phil-TTGcas9. Expression plasmid pEKEx3 with TTGcas9 under control of TetR expression system

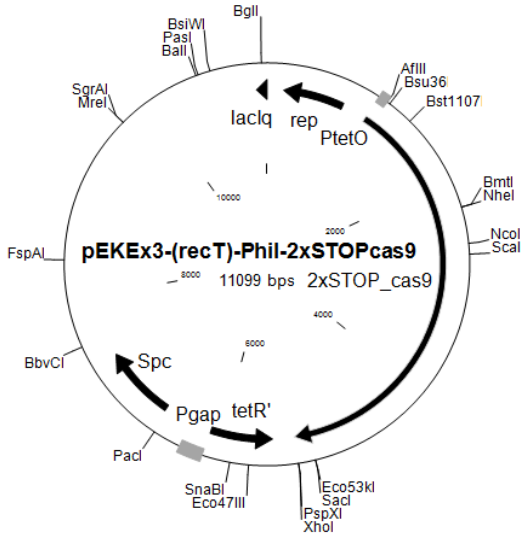

Fig. 40: pEKEx3-(recT)-Phil-2xSTOPcas9. Expression plasmid pEKEx3 with ATGcas9_2xSTOP under control of TetR expression system

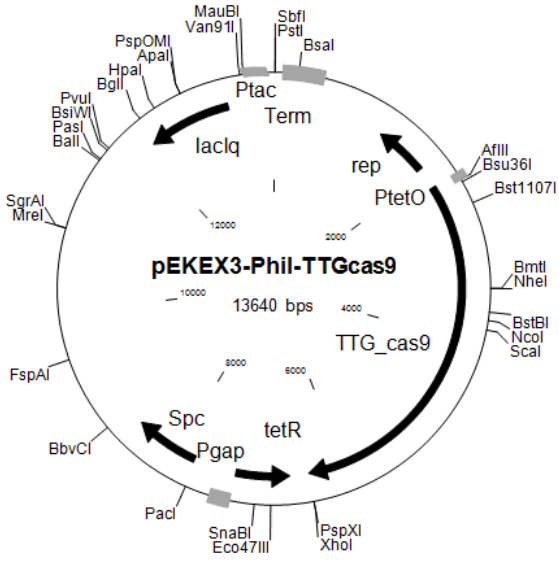

Fig. 41: pEKEx3 –Phil-TTGcas9. Expression plasmid pEKEx3 with ATGcas9_2xSTOP under control of TetR expression system

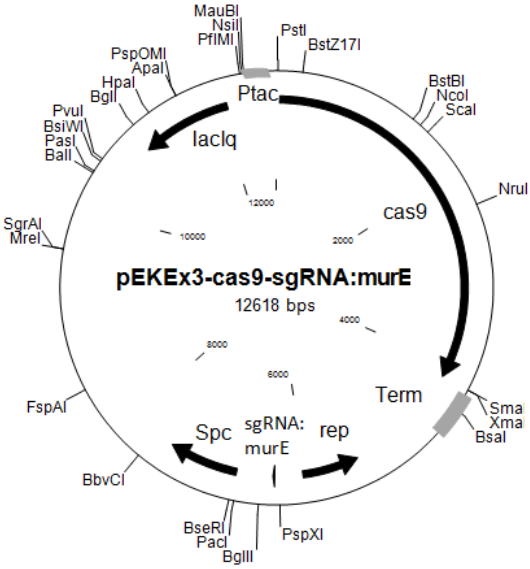

Fig. 42: pEKEx3-cas9-sgRNA:murE. Expression plasmid pEKEx3-cas9 with sgRNA targeting *murE G818*

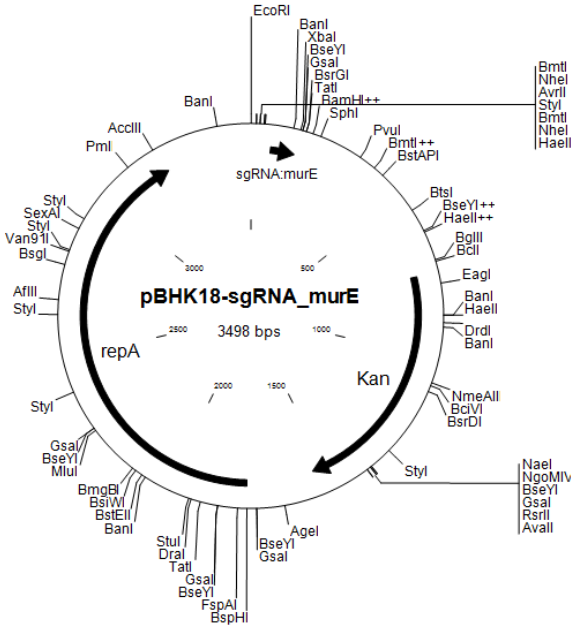

Fig. 43: pBHK18-sgRNA:murE. Low copy plasmid pBHK18 with sgRNA targeting *murE G818*

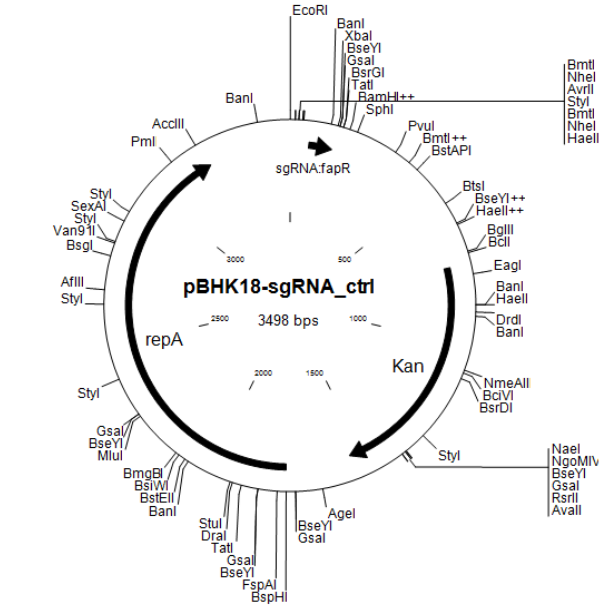

Fig. 44: pBHK18-sgRNA:ctrl. Low copy plasmid pBHK18 with sgRNA targeting *fapR* from *E.coli*

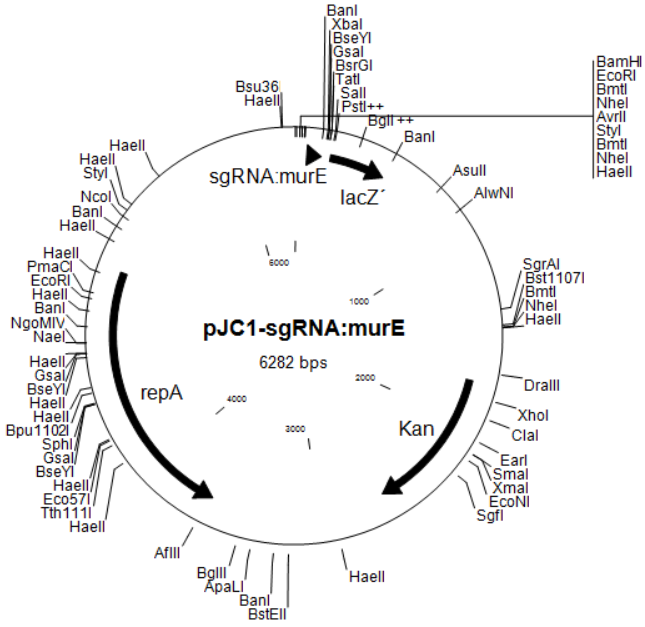

Fig. 45: pJC1-sgRNA:murE. Expression plasmid pJC1 with sgRNA targeting *murE G81*

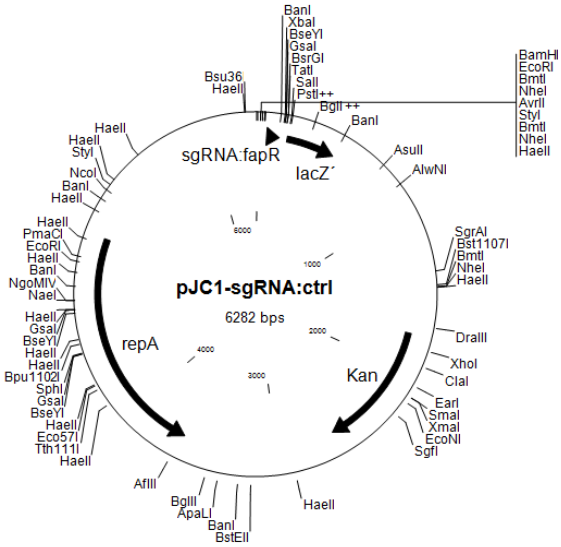

Fig. 45: pJC1-sgRNA:ctrl. Expression plasmid pJC1 with sgRNA targeting *fapR* from *E.coli*

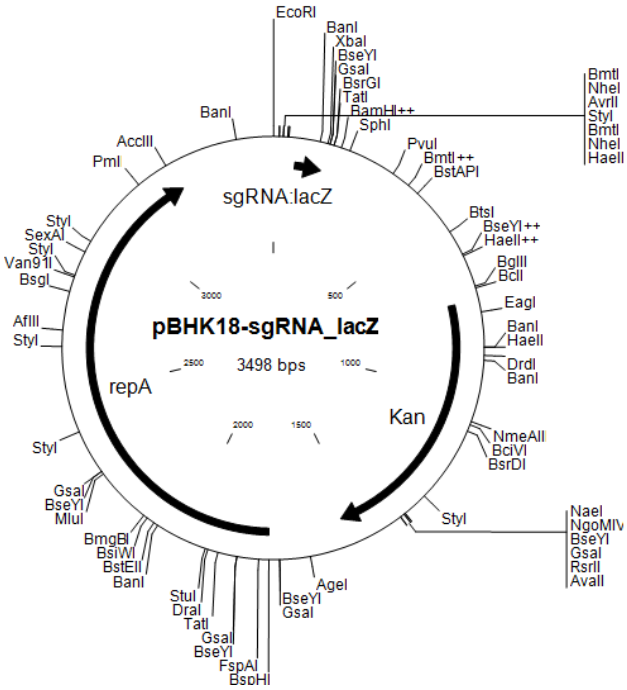

Fig. 46: pBHK18-sgRNA:lacZ. Low copy plasmid pBHK18 with sgRNA targeting *lacZ*

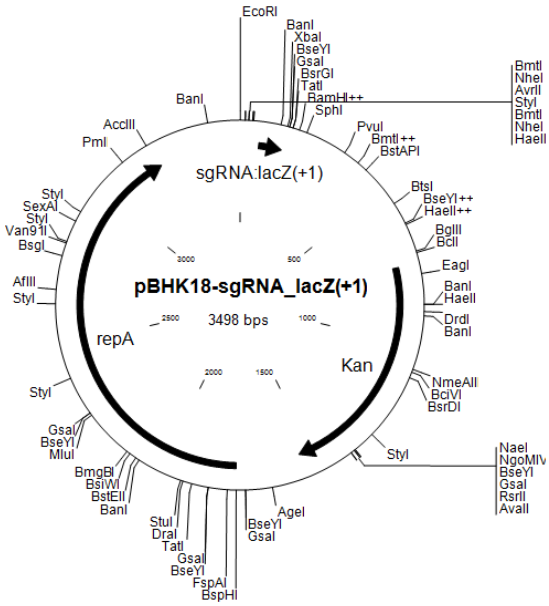

Fig. 46: pBHK18-sgRNA:lacZ(+1). Low copy plasmid pBHK18 with sgRNA targeting *lacZ(+1)*

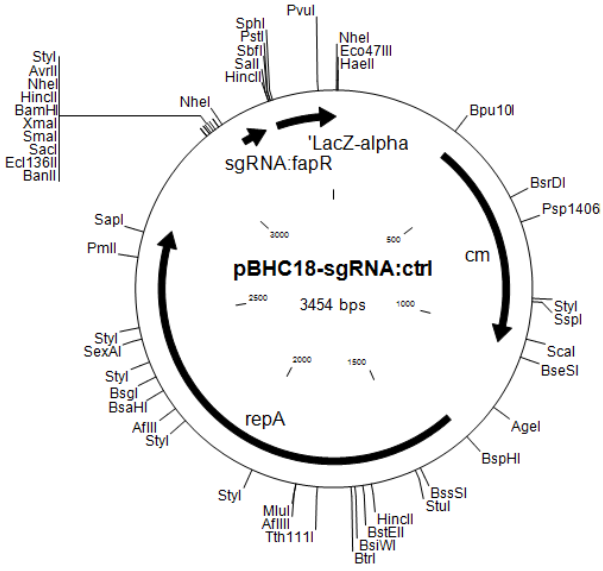

Fig. 47: pBHC18-sgRNA:ctrl. Low copy plasmid pBHC18 with sgRNA targeting *fapR* from *E.coli*

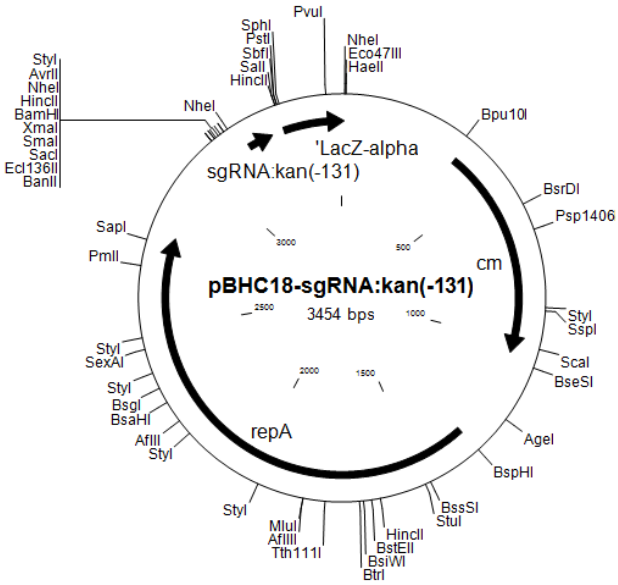

Fig. 48: pBHC18-sgRNA:kan(-131). Low copy plasmid pBHC18 with sgRNA targeting *kan(-131)*

Tab. 14: Comparison of dsDNA recombineering efficiencies in three different strains: *C. glutamicum* DM1728kanR(+1)/pCL2-recET, DM1728kanR(-131)/pCL2-recET and DM1728kanR(-752)/pCL2-recET with DNA fragments with flanking regions of of 1500 nt (upper table), 900 nt (middle table) and 400 nt (lower table).

Strain	Plasmid	Fragment with 1500 nt HA	KanR CFU	SD
DM1728kanR(+1)	pCL2-recET	2157HA-::-1-1499HA	1.30×10^4	1.54×10^4
DM1728kanR(-131)	pCL2-recET	2225HA-::131-1301HA	3.63×10^3	2.43×10^3
DM1728kanR(-752)	pCL2-recET	1596HA-::752-1298HA	9.84×10^2	5.34×10^2

Strain	Plasmid	Fragment with 900 nt HA	KanR CFU	SD
DM1728kanR(+1)	pCL2-recET	832HA-::-1-1099HA	2.89×10^4	2.82×10^4
DM1728kanR(-131)	pCL2-recET	900HA-::131-900HA	3.43×10^3	4.70×10^3
DM1728kanR(-752)	pCL2-recET	900HA-::752-900HA	2.31×10^2	2.16×10^2

Strain	Plasmid	Fragment with 400 nt HA	KanR CFU	SD
DM1728kanR(+1)	pCL2-recET	344HA-::-1-617HA	1.43×10^4	1.28×10^4
DM1728kanR(-131)	pCL2-recET	400Ha-::131-400HA	2.15×10^2	2.36×10^2
DM1728kanR(-752)	pCL2-recET	400HA-::752-400HA	0.00	0.00

Danksagung

Zunächst möchte ich meinem Doktorvater Prof. Dr. Michael Bott für die Übernahme der Betreuung meiner Dissertation danken, sowie für ein sehr ergiebiges CLIB Follow-up meeting und die Möglichkeit diese Arbeit im IBG-1 durchführen zu können.

Herrn Prof. Dr. Michael Feldbrügge danke ich für die freundliche Unterstützung durch Übernahme des Zweitgutachtens und erfolgreiches „Brainstorming" während des CLIB Follow-up meetings.

Desweiteren möchte ich Dr. Jan Marienhagen danken für die Betreuung meines Projektes und die daraus entstandenen vielen herausfordernden Diskussionsrunden („Beerdigungen diverser Klassen").

Mein ganz besonder Dank gilt Dr. Lothar Eggeling, der mir während meiner gesamten Zeit immer mit voller Begeisterung zur Seite stand, ständiges Interesse für die Entwicklung meines Projektes gezeigt hat und mir in so manchen schwierigen Situationen mit seinen vielen Anregungen, Ratschlägen und seiner Expertise in enttäuschenden Situationen weiter geholfen hat. Vielen Dank dafür, Lothar!

Dem Graduiertencluster „CLIB-GC" danke ich für das Stipendium, die vielen lehrreichen Veranstaltungen, sowie die Unterstützung von Seite der Verantwortlichen.

Desweiteren möchte ich ganz herzlich Karin und Sascha danken für die tatkräftige Unterstützung und mühevolle Arbeit während der gesamten Zeit.

Ich danke allen aktuellen und ehemaligen Mitgliedern der AG Eggeling/Marienhagen, unter anderem bestehend aus Nicolai, Micha, Chris, Lion, Jennifer, Hugo, Sabrina und Philana, für die vielen schönen und lustigen gemeinsamen Momente (z.B. auf dem Barbecue-Boot oder auf dem legendären Oktoberfest in Bretzenheim), sowie eure Hilfsbereitschaft und Unterstützung im, sowie außerhalb des Labors.

Zuletzt danke ich meiner Familie, Martin und meiner Freundin Steffi dafür, dass sie während dieser Zeit immer für mich da waren und mich stets unterstützt und aufgemuntert haben. Eure Wertschätzung und Zuneigung hat es mir erst ermöglicht, diese intensive Zeit erfolgreich abzuschließen.

Band / Volume 69
L-Cystein-Bildung mit *Corynebacterium glutamicum* und optische Sensoren zur zellulären Metabolitanalyse
K. Hoffmann (2014),vi, 83 pp
ISBN: 978-3-89336-939-3

Band / Volume 70
Metabolic engineering of Corynebacterium glutamicum for production of the adipate precursor 2-oxoadipate
M. Spelberg (2014), 118 pp
ISBN: 978-3-89336-954-6

Band / Volume 71
Design and application of metabolite sensors for the FACS-based isolation of feedback-resistant enzyme variants
G. Schendzielorz (2014), 129 pp
ISBN: 978-3-89336-955-3

Band / Volume 72
The development and application of a single cell biosensor for the detection of L-methionine and branched-chain amino acids
N. Mustafi (2014), 137 pp
ISBN: 978-3-89336-956-0

Band / Volume 73
Metabolic engineering of *Corynebacterium glutamicum* for production of L-leucine and 2-ketoisocaproate
M. Vogt (2014), VI, 92 pp
ISBN: 978-3-89336-968-3

Band / Volume 74
Pupylierung in *Corynebacterium glutamicum*
A. Küberl (2014), VI, 163 pp
ISBN: 978-3-89336-969-0

Band / Volume 75
Tat-translocase composition in *Corynebacterium glutamicum* and the effect of TorD coexpression
D. Oertel (2014), v, 117 pp
ISBN: 978-3-89336-996-6

Band / Volume 76
The 6C RNA of *Corynebacterium glutamicum*
J. Pahlke (2014), II, 144 pp
ISBN: 978-3-95806-003-6

Band / Volume 77
Anaerobes Wachstum von *Corynebacterium glutamicum* durch gemischte Säurefermentation
A. Michel (2014), 145 pp
ISBN: 978-3-95806-010-4

Band / Volume 78
Engineering of *Corynebacterium glutamicum* towards utilization of methanol as carbon and energy source
S. Witthoff (2015), V, 113 pp
ISBN: 978-3-95806-029-6

Band / Volume 79
Interaction of the two-component systems HrrSA and ChrSA in *Corynebacterium glutamicum*
E. Hentschel (2015), V, 118 pp
ISBN: 978-3-95806-053-1

Band / Volume 80
Strukturelle und funktionelle Untersuchungen zur Kupfer-Homöostase in *Corynebacterium glutamicum*
X. Schuplezow (2015), 114 pp
ISBN: 978-3-95806-085-2

Band / Volume 81
Development and application of single cell biosensors for the improvement of amino acid production in *Escherichia coli* and *Corynebacterium glutamicum*
R. Mahr (2016), IV, 179
ISBN: 978-3-95806-145-3

Band / Volume 82
Strain development of *Gluconobacter oxydans*: Complementation of non-functional metabolic pathways and increase of carbon flux
I. Kiefler (2016), III, 103 pp
ISBN: 978-3-95806-158-3

Band / Volume 83
Novel genetic tools for production strain development of *Corynebacterium glutamicum*
J. Hochheim (2017), VII, 63, XXXVII pp
ISBN: 978-3-95806-212-2

Weitere ***Schriften des Verlags im Forschungszentrum Jülich*** unter
http://wwwzb1.fz-juelich.de/verlagextern1/index.asp

Gesundheit / Health
Band / Volume 83
ISBN 978-3-95806-212-2